Supplementary Information

Tailored Supramolecular Soft Robotics by Intermolecular Interactions Defined Aspect-Ratio of Nanoassemblies for Photocontrolled Cell-Material Interfaces

Ka-Lung Hung,[1,2,5] Wai-Ki Wong,[1,2,3,5] Leong-Hung Cheung,[1,2,5] Ming-Hin Chau,[1,2] Takashi Kajitani,[4] and Franco King-Chi Leung*[1,2,3]

[1] The Hong Kong Polytechnic University Shenzhen Research Institute, Shenzhen, 518057, People's Republic of China.
[2] Department of Applied Biology and Chemical Technology, Research Institute of Future Food, The Hong Kong Polytechnic University, Hong Kong, China.
[3] Centre for Eye and Vision Research, 17W Hong Kong Science Park, Hong Kong, China.
[4] Core Facility Center, Research Infrastructure Management Center, Institute of Science Tokyo 4259 Nagatsuta, Midori-ku, Yokohama 226-8501, Japan.
[5] These authors contributed equally to this work.
*Corresponding Author: kingchifranco.leung@polyu.edu.hk (F.K.-C. Leung)

Table of Contents

1. Materials and Method.

All commercial reagents are purchased from Dieckmann, Macklin, Sigma Aldrich and Tokyo Chemical Industry Co. Ltd, and were used as received unless otherwise specified. All reactions were performed under nitrogen unless otherwise specified. Analytical thin layer chromatography (TLC) was performed with Macherey-Nagel Silica gel 60 UV254 aluminum plates and visualization was accomplished by UV light (254 / 365 nm) or staining with phosphomolybdic acid followed by heating. Flash column chromatography was performed using Macherey-Nagel Silica gel 60 (230–400 mesh). Deuterated solvents were purchased from Cambridge Isotope Laboratories Inc.

General.

NMR spectra were recorded at 25 °C on Bruker Avance III Ultrashield 400 Plus NMR spectrometer (^{1}H: 400 MHz, ^{13}C: 101 MHz) and Bruker Avance III Ultrashield 600 Plus NMR spectrometer (^{1}H: 600 MHz, ^{13}C: 151 MHz). Chemical shifts (δ) are expressed relative to the resonances of the residual non-deuterated solvent for ^{1}H [tetramethylsilane (TMS) in $CDCl_3$: ^{1}H(δ) = 7.26 ppm or ^{1}H(δ) = 0 ppm, CD_3OD: ^{1}H(δ) = 3.31 ppm and ^{13}C [$CDCl_3$: ^{13}C(δ) = 77.16 ppm, CD_3OD: ^{13}C(δ) = 49.00 ppm]**[1]**. Absolute values of the coupling constants are given in Hertz (Hz), regardless of their sign. Multiplicities are abbreviated as singlet (s), double doublet (dd), doublet (d), triplet (t), quartet (q), p = pentet and multiplet (m). High-resolution mass spectrometry (HR-MS) was performed on an Agilent 6540 Q-TOF Mass Spectrometer with ESI ionization.

Fourier-Transform Infrared Spectroscopy (FTIR)

The FTIR measurement was performed on Thermo Scientific Nicolet iS50 Fourier Transform Infrared Spectrometer in a range of 650–4000 cm^{-1}, where data were selected in a range of 1800–1500 cm^{-1} for observing hydrogen bonding. The corresponding solvent blank was acquired before sample measurement. The THF and D_2O of $\mathbf{DA_A}$ (8.0 wt.% and 8.0 wt.%, respectively) were directly dropped on a CaF_2 window with a 0.2 mm spacer.

Circular Dichroism (CD)

CD spectra were recorded on Jasco J-1500 Circular Dichroism Spectrophotometer. A quartz cuvette with an optical pathlength of 4.0 mm was used for the CD spectroscopy measurements.

Transmission Electron Microscopy (TEM)

The TEM was performed on a ThermoFisher Talos L120C Transmission Electron Microscope with a LaB6 filament operating at 120 kV equipped with a Ceta 16M CCD camera. TEM samples were prepared by depositing sample solutions (5.0 μL) onto a carbon grid (Micro to Nano, EMR Carbon support film on copper, 400 square mesh) for 60 s and removed by blotting. Subsequently, the UranyLess EM stain solution (Electron Microscopy Science, 5.0 μL) was directly deposited onto the grid for 15 s and the stain was removed by blotting.

Pyrene Fluorescence Assay[2]

The critical aggregation concentration (CAC) of **DA_A** was analysed by incorporation of the hydrophobic fluorescence probe of pyrene, which the I_1/I_3 ratio will be decreased when there are more aggregates formation. Pyrene was dissolved at 0.5 mM in ethanol and diluted into sample stock solutions, with a final concentration of 1.2 μM. As a result, all samples contain 0.25% ethanol, which is expected to not interfere with the supramolecular assembly behavior. Using an Agilent G9800AA Cary Eclipse fluorescence spectrophotometer, the aqueous solutions of **DA_A** (concentration: 1.0 x 10^{-4} to 1.0 mM) and Pyrene (1.2 μM) were excited at 335 nm and the spectra were recorded over a wavelength range of 360–500 nm. The I_1/I_3 ratio were calculated by fluorescence intensity of I_{373}/I_{393} wavelength of pyrene in MilliQ water from the emission wavelength of the sample. The I_1/I_3 ratio were plotted against sample concentrations to determine CAC.

Polarized Optical Microscopy Analysis and Scanning Electron Microscopy (SEM)

Polarized optical microscopy (POM) was performed on a Leica DM2700-P optical polarizing microscope. When an aqueous solution of **DA_A** (5.0 wt.%) was manually drawn from a pipette into an aqueous solution of $CaCl_2$ (150 mM) on a glass substrate, a noodle-like soft scaffold with an arbitrary length was formed. The arbitrary length of the macroscopic soft scaffold of **DA_A** was directly subjected to perform and observe under POM on a Leica DM2700-P optical polarizing microscope. The SEM was performed on a Tescan VEGA3 Scanning Electron Microscope. An aqueous solution of **DA_A** (5.0 wt.%) was manually drawn into an aqueous solution of $CaCl_2$ (150 mM) on a stage with conductive carbon adhesive tape from a pipette, a string with arbitrary length was formed. After removal the solution of metal chloride, the string of **DA_A** was washed with MilliQ water for three times and dried in air for 48 hours before measurement. The air-dried samples were subject to gold sputtering for 20 min prior to SEM measurement.

Preparation of Fluorescence Microsphere Loaded Macroscopic Soft Scaffold of DA_A

An annealed aqueous solution of 5.0 wt.% **DA_{LPhe}** (68.6 mM) was mixed with FluoSpheres™ Polystyrene Microspheres (Invitrogen™, thermofisher: F8836) at 3:2 volume ratio to obtain a 3.0 wt.% **DA_{LPhe}** aqueous mixture solution. The solution mixture was then manually drawn from a pipette into an aqueous solution of $CaCl_2$ (150 mM) in a quartz container, forming a noodle-like with arbitrary length of macroscopic soft scaffold **DA_{LPhe}** composing microspheres. After that, the microsphere was observed using Leica DM 2700P microscope equipped with Leica I3 filter and excited with 470 nm light source (M470L4-C2, 1.0 A). The actuation motion was induced by a red-laser (0.2W, 650 nm).

Photoirradiation Induced Volume Changes

The macroscopic soft scaffolds of **DA_A** (3.0 wt.%) were fabricated in a small petri dish containing $CaCl_2$ solution (150 mM). The $CaCl_2$ solution was removed and washed with MilliQ water for 3 times, followed by removing excessive water around the macroscopic soft scaffolds of **DA_A** and refilling *n*-dodecane solution into petri dish. The macroscopic soft scaffolds of **DA_A** were irradiated with red-laser (0.2 W, 650 nm) for 60 min to reveal volume reduction and recorded by Leica DM2700-P optical polarizing microscope.

2. Description of Supplementary Movies.
Photoirradiation studies were performed with red-light laser (0.2W, 650 nm). The movies are recorded directly with an iPhone Camera or Lumenera INFINITY3-6URC 6.0 Megapixel USB 3 Microscopy Camera for actuation studies under Leica DM2700-P optical polarizing microscope.

Movie S1: Photoactuation of a macroscopic soft scaffold DA_{LPhe} (3.0 wt.%) in $CaCl_2$ Solution. A macroscopic soft scaffold composed of **DA_{LPhe}** (3.0 wt.%) in an aqueous solution was fabricated by manually drawing from a pipette into an aqueous solution of $CaCl_2$ (150 mM) in a quartz container, a noodle-like soft scaffold with an arbitrary length was formed. Upon red laser (0.2W, 650 nm) irradiation for 60 min at a distance of 5 cm, the macroscopic soft scaffold of **DA_{LPhe}** was bent toward the red laser-light source.

Movie S2: Photoactuation of a macroscopic soft scaffold DA_{LVal} (3.0 wt.%) in $CaCl_2$ Solution. A macroscopic soft scaffold composed of **DA_{LVal}** (3.0 wt.%) in an aqueous solution was fabricated by manually drawing from a pipette into an aqueous solution of $CaCl_2$ (150 mM) in a quartz container, a noodle-like soft scaffold with an arbitrary length was formed. Upon red laser (0.2W, 650 nm) irradiation for 60 min at a distance of 5 cm, the macroscopic soft scaffold of **DA_{LVal}** was bent toward the red-laser light source.

Movie S3: Photoactuation of a macroscopic soft scaffold DA_{LAla} (3.0 wt.%) in $CaCl_2$ Solution. A macroscopic soft scaffold composed of **DA_{LAla}** (3.0 wt.%) in an aqueous solution was fabricated by manually drawing from a pipette into an aqueous solution of $CaCl_2$ (150 mM) in a quartz container, a noodle-like soft scaffold with an arbitrary length was formed. Upon red laser (0.2W, 650 nm) irradiation for 60 min at a distance of 5 cm, the macroscopic soft scaffold of **DA_{LAla}** was bent toward the red laser-light source.

Movie S4: Photoactuation of a macroscopic soft scaffold DA_{DPhe} (3.0 wt.%) in $CaCl_2$ Solution. A macroscopic soft scaffold composed of **DA_{DPhe}** (3.0 wt.%) in an aqueous solution was fabricated by manually drawing from a pipette into an aqueous solution of $CaCl_2$ (150 mM) in a quartz container, a noodle-like soft scaffold with an arbitrary length was formed. Upon red laser (0.2W, 650 nm) irradiation for 60 min at a distance of 5 cm, the macroscopic soft scaffold of **DA_{DPhe}** was bent toward the red laser-light source.

Movie S5: Photoactuation of FluoSpheres™ Polystyrene Microspheres encapsulated macroscopic soft scaffold DA_{LPhe} (3.0 wt.%) in $CaCl_2$ Solution. A FluoSpheres™ Polystyrene Microspheres encapsulated macroscopic soft scaffold **DA_{LPhe}** (3.0 wt.%) in an aqueous solution was fabricated by manually drawing from a pipette into an aqueous solution of $CaCl_2$ (150 mM) in a quartz container, a noodle-like soft scaffold with an arbitrary length was formed. The photoactuation was observed under microscope with 470 nm excitation. Upon photoirradiation

with red laser (0.2W, 650 nm) for 70 s, the microspheres encapsulated macroscopic soft scaffold **DA$_{LPhe}$** were bent toward the red laser light source, accompany by the movement of microspheres.

Movie S6: Photoirradiation induced volume change of a macroscopic soft scaffold DA$_{LPhe}$ (3.0 wt.%) immersed in *n*-dodecane solution. A macroscopic soft scaffold composed of **DA$_{LPhe}$** (3.0 wt.%) in an aqueous solution was fabricated by manually drawing from a pipette into an aqueous solution of $CaCl_2$ (150 mM) in a quartz container, a noodle-like soft scaffold with an arbitrary length was formed. The excessive aqueous solution of $CaCl_2$ was removed and refilled with *n*-dodecane solution. Under optical microscope, the macroscopic soft scaffold **DA$_{LPhe}$** was slightly shrunk upon red laser irradiation (0.2W, 650 nm) for 60 min.

Movie S7: Photoirradiation induced volume change of a macroscopic soft scaffold DA$_{LVal}$ (3.0 wt.%) immersed in *n*-dodecane solution. A macroscopic soft scaffold composed of **DA$_{LVal}$** (3.0 wt.%) in an aqueous solution was fabricated by manually drawing from a pipette into an aqueous solution of $CaCl_2$ (150 mM) in a quartz container, a noodle-like soft scaffold with an arbitrary length was formed. The excessive aqueous solution of $CaCl_2$ was removed and refilled with *n*-dodecane solution. Under optical microscope, the macroscopic soft scaffold **DA$_{LVal}$** was significantly shrunk upon red laser irradiation (0.2W, 650 nm) for 60 min.

Movie S8: Photoirradiation induced volume change of a macroscopic soft scaffold DA$_{LAla}$ (3.0 wt.%) immersed in *n*-dodecane solution. A macroscopic soft scaffold composed of **DA$_{LAla}$** (3.0 wt.%) in an aqueous solution was fabricated by manually drawing from a pipette into an aqueous solution of $CaCl_2$ (150 mM) in a quartz container, a noodle-like soft scaffold with an arbitrary length was formed. The excessive aqueous solution of $CaCl_2$ was removed and refilled with *n*-dodecane solution. Under optical microscope, the macroscopic soft scaffold **DA$_{LAla}$** was significantly shrunk upon red laser irradiation (0.2W, 650 nm) for 60 min.

Movie S9: Photoirradiation of a cell cultured macroscopic soft scaffold DA$_{LPhe}$ (3.0 wt.%) after 2 % FBS medium incubation for 1 day. A macroscopic soft scaffold of **DA$_{LPhe}$** (3.0 wt.%) in an aqueous solution was fabricated by manually drawn from a pipette into an aqueous solution of $CaCl_2$ (150 mM) in a bioinert culture dish, a noodle-like soft scaffold with an arbitrary length was formed. The macroscopic soft scaffold was cultured with hMSCs in 2% FBS medium over 1 day incubation. The actuation motion of cell cultured macroscopic soft scaffold **DA$_{LPhe}$** was performed and irradiated with red-laser (0.2 W, 650 nm) for 30 min.

3. Synthesis

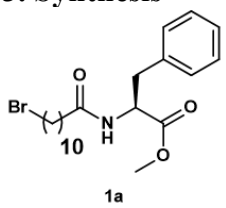

1a

Compound 1a

A mixture of 11-Bromoundecanoic Acid (2.0 g, 7.54 mmol, 1.0 equiv.), HBTU (3.21 g, 8.29 mmol, 1.1 equiv.) and DIPEA (5.36 mL, 30.16 mmol, 4.0 equiv.) in DMF (20 mL) was stirred at 20 °C for 1 h. After that, the mixture was added with *L*-Phenylalanine Methyl Ester Hydrochloride (1.82 g, 7.54 mmol, 1.1 equiv.) and stirred at 20 °C for 1 h. The reaction mixture was diluted with ethyl acetate (20 mL), washed with brine (1 x 20 mL), water (2 x 20 mL) and Na_2CO_3 (1 x 20 mL) and brine (1 x 20 mL), sequentially. The organic layer was dried over Na_2SO_4 and the filtrate was concentrated under reduced pressure. The residue was purified by flash column chromatography on SiO_2 (*n*-hexane/ethyl acetate = 5/1, R_f = 0.6) to afford **Compound 1a** (1.55 g, 3.63 mmol, 48% yield) as a white solid.

^{1}H NMR (600 MHz, $CDCl_3$) δ 7.31 – 7.22 (m, 3H), 7.11 – 7.07 (m, 2H), 5.88 (d, *J* = 7.8 Hz, 1H), 4.94 – 4.87 (m, 1H), 3.73 (s, 3H), 3.41 (t, *J* = 6.9 Hz, 2H), 3.18 – 3.07 (m, 2H), 2.17 (m, 2H), 1.85 (m, 2H), 1.58 (m, 2H), 1.42 (m, 2H), 1.31 – 1.27 (s, 10H).

^{13}C NMR (151 MHz, $CDCl_3$) δ 172.76, 172.32, 136.01, 129.38, 128.68, 127.24, 53.01, 52.44, 38.04, 36.66, 34.18, 32.94, 29.51, 29.48, 29.43, 29.38, 29.28, 28.97, 28.85, 28.27, 25.63.

HR-MS (ESI) calculated for $C_{21}H_{32}BrNO_3$ $[M+H]^+$ m/z 426.1644, found 426.1642.

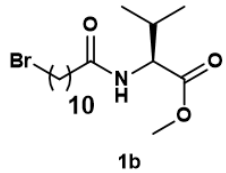

1b

Compound 1b

A mixture of 11-Bromoundecanoic Acid (3.10 g, 11.7 mmol, 1.0 equiv.), HBTU (4.87 g, 12.8 mmol, 1.1 equiv.) and DIPEA (8.1 mL, 46.5 mmol, 4.0 equiv.) in DMF (20 mL) was stirred at 20 °C for 1 h. After that, the mixture was added with *L*-valine Methyl Ester Hydrochloride (2.15 g, 12.8 mmol, 1.1 equiv.) and stirred at 20 °C for 1 h. The reaction mixture was diluted with ethyl acetate (20 mL), washed with brine (1 x 20 mL), water (2 x 20 mL) and Na_2CO_3 (1 x 20 mL) and brine (1 x 20 mL), sequentially. The organic layer was dried over Na_2SO_4 and the filtrate was concentrated under reduced pressure. The residue was purified by flash column chromatography on SiO_2 (*n*-hexane/ethyl acetate = 5/1, R_f = 0.6) to afford **Compound 1b** (2.26 g, 5.97 mmol, 51% yield) as a white solid.

^{1}H NMR (600 MHz, $CDCl_3$) δ 6.02 (d, J = 9.5 Hz, 1H), 4.54 (m, 1H), 3.69 (s, 3H), 3.37 – 3.34 (m, 2H), 2.22 – 2.17 (m, 2H), 1.83 – 1.78 (m, 2H), 1.63 – 1.58 (m, 2H), 1.39 – 1.36 (m, 2H), 1.29 – 1.24 (m, 10H), 0.90 – 0.85 (m, 6H).

^{13}C NMR (151 MHz, $CDCl_3$) δ 173.10, 172.81, 56.85, 52.15, 36.69, 34.08, 32.84, 31.32, 29.38, 29.36, 29.30, 29.24, 28.75, 28.17, 25.71, 18.99, 17.88.

HR-MS (ESI) calculated for $C_{17}H_{32}BrNO_3$ $[M+H]^+$ m/z 378.1644, found 378.1642.

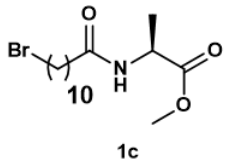

1c

Compound 1c

A mixture of 11-Bromoundecanoic Acid (4.98 g, 18.78 mmol, 1.0 equiv.), HBTU (7.83 g, 20.66 mmol, 1.1 equiv.) and DIPEA (13.1 mL, 75.12 mmol, 4.0 equiv.) in DMF (40 mL) was stirred at 20 °C for 1 h. After that, the mixture was added with *L*-alanine Methyl Ester Hydrochloride (2.88 g, 20.66 mmol, 1.1 equiv.) and stirred at 20 °C for 1 h. The reaction mixture was diluted with ethyl acetate (20 mL), washed with brine (1 x 20 mL), water (2 x 20 mL) and Na_2CO_3 (1 x 20 mL) and brine (1 x 20 mL), sequentially. The organic layer was dried over Na_2SO_4 and the filtrate was concentrated under reduced pressure. The residue was purified by flash column chromatography on SiO_2 (*n*-hexane/ethyl acetate = 5/1, R_f = 0.6) to afford **Compound 1c** (4.28 g, 12.22 mmol, 65% yield) as a white solid.

^{1}H NMR (600 MHz, $CDCl_3$) δ 6.00 (d, J = 7.4 Hz, 1H), 4.63 – 4.58(m, 1H), 3.75 (s, 3H), 3.40 (t, J = 6.9 Hz, 2H), 2.20 (t, J = 7.6 Hz, 2H), 1.86 – 1.82 (m, 2H), 1.65 – 1.62 (m, 2H), 1.43 – 1.40 (m, 5H), 1.32 – 1.27 (m, 10H).

^{13}C NMR (151 MHz, $CDCl_3$) δ 173.90, 172.75, 52.62, 47.99, 36.70, 34.24, 32.95, 29.49, 29.46, 29.40, 29.31, 28.86, 28.28, 25.67, 18.77.

HR-MS (ESI) calculated for $C_{15}H_{28}BrNO_3$ $[M+H]^+$ m/z 350.1331, found 350.1330.

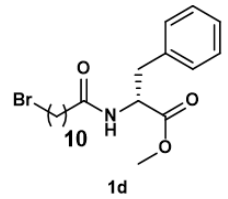

1d

Compound 1d

A mixture of 11-Bromoundecanoic Acid (2.02 g, 7.62 mmol, 1.0 equiv.), HBTU (3.18 g, 8.39 mmol, 1.1 equiv.) and DIPEA (5.3 mL, 33.5 mmol, 4.0 equiv.) in DMF (20 mL) was stirred at 20 °C for 1 h. After that, the mixture was added with *D*-Phenylalanine Methyl Ester Hydrochloride (1.81 g, 8.39 mmol, 1.1 equiv.) and stirred at 20 °C for 1 h. The reaction mixture was diluted with

ethyl acetate (20 mL), washed with brine (1 x 20 mL), water (2 x 20 mL) and Na_2CO_3 (1 x 20 mL) and brine (1 x 20 mL), sequentially. The organic layer was dried over Na_2SO_4 and the filtrate was concentrated under reduced pressure. The residue was purified by flash column chromatography on SiO_2 (*n*-hexane/ethyl acetate = 5/1, R_f = 0.6) to afford **Compound 1d** (2.33 g, 5.46 mmol, 72% yield) as a white solid.

^{1}H NMR (600 MHz, $CDCl_3$) δ 7.30 – 7.23 (m, 3H), 7.10 – 7.08 (m, 2H), 5.87 (d, *J* = 7.8 Hz, 1H), 4.92 – 4.89 (m, 1H), 3.73 (s, 3H), 3.41 (t, *J* = 6.9 Hz, 2H), 3.17 – 3.08 (m, 2H), 2.18 – 2.15 (m, 2H), 1.87 – 1.83 (m, 2H), 1.61 – 1.56 (m, 2H), 1.44 – 1.39 (m, 2H), 1.31 – 1.26 (m, 10H).

^{13}C NMR (151 MHz, $CDCl_3$) δ 172.75, 172.31, 136.00, 129.38, 128.68, 127.25, 53.00, 52.46, 38.03, 36.67, 34.21, 32.94, 29.49, 29.44, 29.39, 29.28, 28.85, 28.28, 25.64.

HR-MS (ESI) calculated for $C_{21}H_{32}BrNO_3$ $[M+H]^+$ m/z 426.1644, found 426.1643.

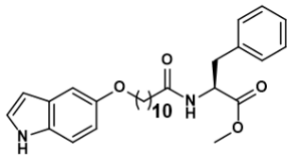

2a

Compound 2a

A mixture of Compound **1a** (1.43 g, 3.36 mmol, 1.0 equiv.), 5-hydroxyindole (0.49 g, 3.70 mmol, 1.1 equiv.) and potassium carbonate (1.16 g, 8.40 mmol, 2.5 equiv.) in DMF (10 mL) was heated at 85 °C for 16 h. After cooling to room temperature, the reaction mixture was diluted with ethyl acetate (20 mL), washed with brine (1 x 20 mL), water (2 x 20 mL) and brine (1 x 20 mL) sequentially. The organic layer was dried over Na_2SO_4 and the filtrate was concentrated under reduced pressure. The residue was purified by flash column chromatography on SiO_2 (*n*-hexane/ethyl acetate = 3/1, R_f = 0.30) to afford **Compound 2a** (0.783 g, 1.64 mmol, 49% yield) as a white solid.

^{1}H NMR (600 MHz, $CDCl_3$) δ 8.13 (s, 1H), 7.30 – 7.23 (m, 4H), 7.16 (t, *J* = 2.8 Hz, 1H), 7.10 – 7.08 (m, 3H), 6.85 (dd, *J* = 8.8, 2.4 Hz, 1H), 6.46 (t, *J* = 3.1 Hz, 1H), 5.85 (d, *J* = 7.8 Hz, 1H), 4.92 – 4.89 (m, 1H), 3.99 (t, *J* = 6.6 Hz, 2H), 3.72 (s, 3H), 3.17 – 3.07 (m, 2H), 2.19 – 2.11 (m, 2H), 1.82 – 1.77 (m, 2H), 1.60 –1.55 (m, 2H), 1.49 – 1.44 (m, 2H), 1.37 – 1.32 (m, 2H), 1.31 – 1.26 (m, 10H).

^{13}C NMR (151 MHz, CDCl3) δ 172.84, 172.34, 153.79, 136.02, 131.12, 129.39, 128.70, 128.46, 127.26, 124.89, 113.09, 111.72, 103.67, 102.46, 68.96, 53.04, 52.44, 38.06, 36.69, 29.65, 29.61, 29.51, 29.42, 29.32, 26.24, 25.68.

HR-MS (ESI) calculated for $C_{29}H_{38}N_2O_4$ $[M+H]^+$ m/z 479.2910, found 479.2908.

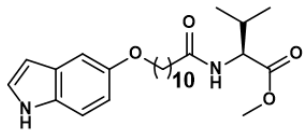

2b

Compound 2b

A mixture of Compound **1b** (1.89 g, 4.99 mmol, 1.0 equiv.), 5-hydroxyindole (0.73 g, 5.49 mmol, 1.1 equiv.) and potassium carbonate (1.72 g, 12.47 mmol, 2.5 equiv.) in DMF (10 mL) was heated at 85 °C for 20 h. After cooling to room temperature, the reaction mixture was diluted with ethyl acetate (20 mL), washed with brine (1 x 20 mL), water (2 x 20 mL) and brine (1 x 20 mL) sequentially. The organic layer was dried over Na_2SO_4 and the filtrate was concentrated under reduced pressure. The residue was purified by flash column chromatography on SiO_2 (*n*-hexane/ethyl acetate = 2/1, R_f = 0.30) to afford **Compound 2b** (1.05 g, 2.44 mmol, 49% yield) as a white solid.

^{1}H NMR (600 MHz, $CDCl_3$) δ 8.32 (s, 1H), 7.25 (d, *J* = 8.1 Hz, 1H), 7.15 (s, 1H),7.10 (s, 1H), 6.85 (d, *J* = 8.8 Hz, 1H), 6.45 (s, 1H), 5.97 (d, *J* = 8.8 Hz, 1H), 4.59 (dd, *J* = 9.1, 4.9 Hz, 1H), 3.99 (t, *J* = 6.6 Hz, 2H), 3.73 (s, 3H), 2.22 (t, *J* = 7.6 Hz, 2H), 2.14 (p, *J* = 6.8 Hz, 1H), 1.79 (t, *J* = 7.1 Hz, 2H), 1.63 (t, *J* = 7.5 Hz, 2H), 1.46 (t, *J* = 7.6 Hz, 2H), 1.34 – 1.29 (m, 10H), 0.92 (dd, *J* = 22.23, 6.9 Hz, 6H).

^{13}C NMR (151 MHz, $CDCl_3$) δ 173.28, 172.87, 153.65, 131.10, 128.38, 124.94, 112.95, 111.75, 103.53, 102.26, 68.90, 56.94, 52.24, 36.82, 31.39, 29.60, 29.56, 29.50, 29.48, 29.39, 29.32, 26.20, 25.80, 19.05, 17.94.

HR-MS (ESI) calculated for $C_{25}H_{38}N_2O_4$ $[M+H]^+$ m/z 431.2910, found 431.2908.

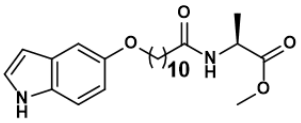

2c

Compound 2c

A mixture of Compound **1b** (1.82 g, 5.20 mmol, 1.0 equiv.), 5-hydroxyindole (0.76 g, 5.72 mmol, 1.1 equiv.) and potassium carbonate (1.16 g, 12.99 mmol, 2.5 equiv.) in DMF (10 mL) was heated at 85 °C for 16 h. After cooling to room temperature, the reaction mixture was diluted with ethyl acetate (20 mL), washed with brine (1 x 20 mL), water (2 x 20 mL) and brine (1 x 20 mL) sequentially. The organic layer was dried over Na_2SO_4 and the filtrate was concentrated under reduced pressure. The residue was purified by flash column chromatography on SiO_2 (*n*-hexane/ethyl acetate = 3/1, R_f = 0.30) to afford **Compound 2c** (1.29 g, 3.20 mmol, 62% yield) as a white solid.

^{1}H NMR (600 MHz, $CDCl_3$) δ 8.11 (s, 1H), 7.28 (d, *J* = 8.6 Hz, 1H), 7.18 (s, 1H), 7.10 (s, 1H), 6.86 (d, *J* = 8.8, 2.1 Hz, 1H), 6.47 (s, 1H), 5.99 (d, *J* = 7.4 Hz, 1H), 4.64 – 4.59 (m, 1H), 3.99 (t,

J = 6.6 Hz, 2H), 3.75 (s, 3H), 2.20 (t, *J* = 7.7 Hz, 2H), 1.82 – 1.77 (m, 2H), 1.65 – 1.63 (m, 2H), 1.49 – 1.44 (m, 2H), 1.40 (d, *J* = 7.1 Hz, 3H), 1.33 – 1.29 (m, 10H).

^{13}C NMR (151 MHz, $CDCl_3$) δ 173.90, 172.81, 153.77, 131.06, 128.43, 124.89, 113.09, 111.73, 103.59, 102.48, 68.93, 52.62, 48.00, 36.72, 29.65, 29.60, 29.52, 29.44, 29.34, 26.24, 25.71, 18.76.

HR-MS (ESI) calculated for $C_{23}H_{34}N_2O_4$ $[M+H]^+$ m/z 403.2597, found 403.2595.

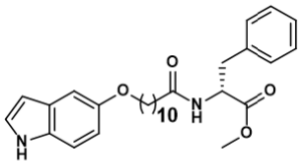

2d

Compound 2d

A mixture of Compound **1d** (1.19 g, 2.79 mmol, 1.0 equiv.), 5-hydroxyindole (0.41 g, 2.79 mmol, 1.1 equiv.) and potassium carbonate (1.16 g, 6.98 mmol, 2.5 equiv.) in DMF (10 mL) was heated at 85 °C for 16 h. After cooling to room temperature, the reaction mixture was diluted with ethyl acetate (20 mL), washed with brine (1 x 20 mL), water (2 x 20 mL) and brine (1 x 20 mL) sequentially. The organic layer was dried over Na_2SO_4 and the filtrate was concentrated under reduced pressure. The residue was purified by flash column chromatography on SiO_2 (*n*-hexane/ethyl acetate = 3/1, R_f = 0.30) to afford **Compound 2d** (0.64 g, 1.34 mmol, 48% yield) as a white solid.

^{1}H NMR (600 MHz, $CDCl_3$) δ 8.15 (s, 1H), 7.32 – 7.22 (m, 4H), 7.17 (t, *J* = 2.8 Hz, 1H), 7.12 – 7.06 (m, 3H), 6.86 (dd, *J* = 8.8, 2.4 Hz, 1H), 6.46(t, *J* = 2.5 Hz, 1H), 5.87 (d, *J* = 7.8 Hz, 1H), 4.92 – 4.89(m, 1H), 3.99 (t, *J* = 6.6 Hz, 2H), 3.73 (s, 3H), 3.15 (m, 1H), 3.09 (dd, *J* = 13.9, 5.8 Hz, 1H), 2.18 – 2.12 (m, 2H), 1.82 – 1.77 (m, 2H), 1.59 – 1.55 (m, 2H), 1.49 – 1.44 (m, 2H), 1.37 – 1.25 (m, 10H)

^{13}C NMR (151 MHz, $CDCl_3$) δ 172.87, 172.33, 153.73, 135.98, 131.06, 129.38, 128.70, 128.41, 127.26, 124.90, 113.05, 111.73, 103.55, 102.42, 68.90, 53.01, 52.47, 38.02, 36.68, 29.64, 29.59, 29.51, 29.42, 29.31, 26.23, 25.67.

HR-MS (ESI) calculated for $C_{29}H_{38}N_2O_4$ $[M+H]^+$ m/z 479.2910, found 479.2910.

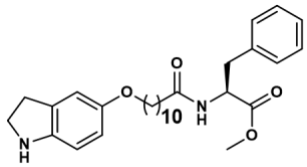

3a

Compound 3a

To a solution of Compound **2a** (0.7680 g, 1.60 mmol, 1.0 equiv.) in acetic acid (8 mL), sodium cyanoborohydride (0.3025 g, 4.81 mmol, 3.0 equiv.) was added in one portion. The reaction

mixture was stirred at 20 °C for 3 h. The reaction was cooled to 0 °C and quenched by adding H_2O (5 mL). The pH of reaction mixture was adjusted to ~7 by adding 4 M NaOH solution. The reaction mixture was extracted with ethyl acetate (3 x 15 mL). The combined organic layer was washed with brine (1 x 15 mL). The organic layer was dried over Na_2SO_4 and the filtrate was concentrated under reduced pressure. The residue was purified by flash column chromatography on SiO_2 (*n*-hexane/ethyl acetate = 2/1, R_f = 0.15) to afford **Compound 3a** (0.61 g, 1.27 mmol, 79% yield) as white solid.

1H NMR (600 MHz, CDCl3) δ 7.31 – 7.25 (m, 5H), 7.10 (d, *J* = 7.2 Hz, 2H), 6.77 (s, 1H), 6.60 (s, 2H), 5.89 (d, *J* = 7.8 Hz, 1H), 4.92 (q, *J* = 6.8, 5.8 Hz, 1H), 3.89 (td, *J* = 6.6, 2.0 Hz, 2H), 3.75 (s, 3H), 3.54 (t, *J* = 8.2 Hz, 2H), 3.19 – 3.09 (m, 2H), 3.01 (t, *J* = 8.3 Hz, 2H), 2.18 (t, *J* = 7.7 Hz, 2H), 1.77 – 1.72(m, 2H), 1.62 – 1.57 (m, 2H), 1.46 – 1.41 (m, 2H), 1.35 – 1.28 (m, 10H).

^{13}C NMR (151 MHz, $CDCl_3$) δ 172.80, 172.33, 153.18, 145.32, 136.01, 131.22, 129.40, 128.70, 127.26, 113.22, 112.50, 110.29, 69.07, 53.02, 52.47, 47.93, 38.05, 36.70, 30.61, 29.65, 29.59, 29.51, 29.43, 29.32, 26.19, 25.68.

HR-MS (ESI) calculated for $C_{29}H_{40}N_2O_4$ $[M+H]^+$ m/z 481.3066, found 481.3065.

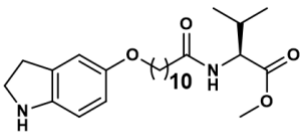

3b

Compound 3b

To a solution of Compound **2b** (0.99 g, 2.30 mmol, 1.0 equiv.) in acetic acid (7 mL), sodium cyanoborohydride (0.43 g, 6.90 mmol, 3.0 equiv.) was added in one portion. The reaction mixture was stirred at 20 °C for 3 h. The reaction was cooled to 0 °C and quenched by adding H_2O (5 mL). The pH of reaction mixture was adjusted to ~7 by adding 4 M NaOH solution. The reaction mixture was extracted with ethyl acetate (3 x 15 mL). The combined organic layer was washed with brine (1 x 15 mL). The organic layer was dried over Na_2SO_4 and the filtrate was concentrated under reduced pressure. The residue was purified by flash column chromatography on SiO_2 (*n*-hexane/ethyl acetate = 2/1, R_f = 0.15) to afford **Compound 3b** (0.77 g, 1.78 mmol, 78% yield) as white solid.

^{1}H NMR (600 MHz, $CDCl_3$) δ 6.76 (s, 1H), 6.58 (s, 2H), 5.92 (d, *J* = 8.9 Hz, 1H), 4.60 – 4.58 (m, 1H), 3.87 (t, *J* = 6.7 Hz, 2H), 3.74 (s, 3H), 3.53 (t, *J* = 8.3 Hz, 2H), 3.00 (t, *J* = 8.3 Hz, 2H), 2.23 (t, *J* = 7.8 Hz, 2H), 2.18 – 2.13 (m, 1H), 1.75 – 1.70 (m, 2H), 1.66– 1.61(m, 2H), 1.45 – 1.40(m, 2H), 1.34 – 1.29 (m, 10H), 0.94 (dd, *J* = 6.8, 1.9 Hz, 3H), 0.90 (dd, *J* = 6.9, 1.9 Hz, 3H).

^{13}C NMR (151 MHz, $CDCl_3$) δ 173.17, 172.90, 153.18, 145.33, 131.22, 113.23, 112.51, 110.29, 69.09, 56.92, 52.27, 47.93, 36.89, 31.47, 30.61, 29.64, 29.59, 29.53, 29.50, 29.44, 29.37, 26.19, 25.83, 19.08, 17.97.

HR-MS (ESI) calculated for $C_{25}H_{40}N_2O_4$ $[M+H]^+$ m/z 433.3066, found 433.3065.

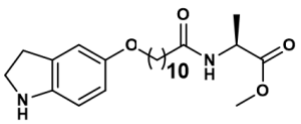

3c

Compound 3c

To a solution of Compound **2c** (1.28 g, 3.17 mmol, 1.0 equiv.) in acetic acid (8 mL), sodium cyanoborohydride (0.60 g, 9.52 mmol, 3.0 equiv.) was added in one portion. The reaction mixture was stirred at 20 °C for 3 h. The reaction was cooled to 0 °C and quenched by adding H_2O (5 mL). The pH of reaction mixture was adjusted to ~7 by adding 4 M NaOH solution. The reaction mixture was extracted with ethyl acetate (3 x 15 mL). The combined organic layer was washed with brine (1 x 15 mL). The organic layer was dried over Na_2SO_4 and the filtrate was concentrated under reduced pressure. The residue was purified by flash column chromatography on SiO_2 (*n*-hexane/ethyl acetate = 2/1, R_f = 0.15) to afford **Compound 3c** (0.82 g, 2.02 mmol, 64 % yield) as white solid.

^{1}H NMR (600 MHz, $CDCl_3$) δ 6.76 (s, 1H), 6.58 (s, 2H), 6.00 (d, *J* = 7.3 Hz, 1H), 4.64 – 4.59 (m, 1H), 3.87 (t, *J* = 6.6 Hz, 2H), 3.75 (s, 3H), 3.53 (t, *J* = 8.3 Hz, 2H), 3.00 (t, *J* = 8.3 Hz, 2H), 2.20 (t, *J* = 7.6 Hz, 2H), 1.75 – 1.70 (m 2H), 1.65 – 1.61 (m, 3H), 1.45 – 1.40 (m, 5H), 1.34 – 1.28 (m, 10H).

^{13}C NMR (151 MHz, $CDCl_3$) δ 173.90, 172.77, 153.17, 145.36, 131.22, 113.22, 112.51, 110.27, 69.09, 52.61, 48.00, 47.94, 36.73, 30.62, 29.64, 29.60, 29.53, 29.51, 29.44, 29.34, 26.19, 25.71, 18.78.

HR-MS (ESI) calculated for $C_{23}H_{36}N_2O_4$ $[M+H]^+$ m/z 405.2753, found 405.2752.

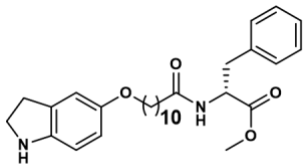

3d

Compound 3d

To a solution of Compound **2d** (0.63 g, 1.32 mmol, 1.0 equiv.) in acetic acid (7 mL), sodium cyanoborohydride (0.25 g, 3.96 mmol, 3.0 equiv.) was added in one portion. The reaction mixture was stirred at 20 °C for 3 h. The reaction was cooled to 0 °C and quenched by adding H_2O (5 mL). The pH of reaction mixture was adjusted to ~7 by adding 4 M NaOH solution. The reaction mixture was extracted with ethyl acetate (3 x 15 mL). The combined organic layer was washed with brine (1 x 15 mL). The organic layer was dried over Na_2SO_4 and the filtrate was concentrated under reduced pressure. The residue was purified by flash column chromatography on SiO_2 (*n*-hexane/ethyl acetate = 2/1, R_f = 0.15) to afford **Compound 3d** (0.32 g, 0.66 mmol, 50% yield) as white solid.

^{1}H NMR (600 MHz, $CDCl_3$) δ 7.30 – 7.23 (m, 5H), 7.09 (d, *J* = 7.2, 2H), 6.76 (s, 1H), 6.58 (s, 1H), 5.90 (d, *J* = 7.9 Hz, 1H), 4.91 (q, *J* = 6.8 Hz, 1H), 3.87 (t, *J* = 6.6 Hz, 2H), 3.73 (s, 3H), 3.52

(t, *J* = 8.3 Hz, 2H), 3.17 – 3.08 (m, 2H), 3.00 (t, *J* = 8.3 Hz, 2H), 2.16 (t, *J* = 7.8 Hz, 2H), 1.75 – 1.73 (p, J = 6.7 Hz, 2H), 1.58 (p, *J* = 7.2 Hz, 2H), 1.42 (p, *J* = 7.8 Hz, 2H), 1.35 – 1.26 (m, 10H).

^{13}C NMR (151 MHz, $CDCl_3$) δ 172.81, 172.33, 153.16, 145.34, 136.01, 131.22, 129.40, 128.70, 127.26, 113.21, 112.50, 110.28, 69.07, 53.01, 52.47, 47.94, 38.05, 36.70, 30.61, 29.65, 29.59, 29.51, 29.43, 29.32, 26.19, 25.68.

HR-MS (ESI) calculated for $C_{29}H_{40}N_2O_4$ $[M+H]^+$ m/z 481.3066, found 481.3065.

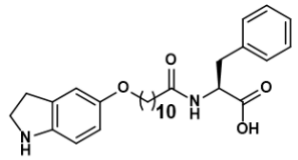

4a

Compound 4a

To a solution of Compound **3a** (186.5 mg, 0.39 mmol, 1.0 equiv.) in methanol (2 mL) and THF (2 mL), an aqueous solution of NaOH (4M, 1 mL) was added the reaction mixture and then heated at 80 °C for 1 h. After cooling to room temperature, volatile solvents were removed under reduced pressure. The pH of reaction mixture was adjusted to ~7 by adding 1 M HCl solution that off-white precipitate formed. The filtered precipitate was washed with H_2O (0.5 mL) to afford **Compound 4a** as an off-white solid (116.9 mg, 0.25 mmol, 65% yield).

^{1}H NMR (600 MHz, DMSO) δ 8.01 (d, *J* = 8.2 Hz, 1H), 7.25 – 7.16 (m, 5H), 6.68 (s, 1H), 6.48 (d, *J* = 8.4 Hz, 1H), 6.40 (d, *J* = 8.3 Hz, 1H), 4.37 (q, *J* = 8.2 Hz, 1H), 3.80 (t, *J* = 6.6 Hz, 2H), 3.04 (dd, *J* = 13.8, 4.7 Hz, 1H), 2.86 – 2.78 (m, 3H), 2.01 (t, *J* = 7.3 Hz, 2H), 1.63 (p, *J* = 6.9 Hz, 2H), 1.39 – 1.16 (m, 12H), 1.10 – 1.08 (m, 2H).

^{13}C NMR (151 MHz, DMSO) δ 173.24, 172.01, 151.36, 146.39, 138.01, 130.31, 129.13, 128.04, 126.24, 112.76, 112.02, 108.89, 68.09, 53.49, 46.94, 36.83, 35.16, 29.89, 29.02, 28.95, 28.91, 28.84, 28.82, 28.47, 25.61, 25.23.

HR-MS (ESI) calculated for $C_{28}H_{38}N_2O_4$ [M+H]+ m/z 467.2910, found 467.2909.

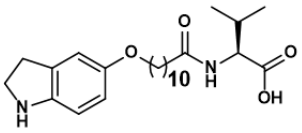

4b

Compound 4b

To a solution of Compound **3b** (150 mg, 0.35 mmol, 1.0 equiv.) in methanol (2 mL) and THF (2 mL), an aqueous solution of NaOH (4M, 1 mL) was added the reaction mixture and then heated at 80 °C for 1 h. After cooling to room temperature, volatile solvents were removed under reduced pressure. The pH of reaction mixture was adjusted to ~7 by adding 1 M HCl solution that off-white

precipitate formed. The filtered precipitate was washed with H_2O (0.5 mL) to afford **Compound 4b** as an off-white solid (114 mg, 0.27 mmol, 78% yield).

^{1}H NMR (600 MHz, DMSO) δ 7.91 (d, *J* = 8.6 Hz, 1H), 6.67 (s, 1H), 6.48 (d, *J* = 8.4 Hz, 1H), 6.40 (d, *J* = 8.3 Hz, 1H), 4.13 (t, *J* = 7.2 Hz, 1H), 3.80 (t, *J* = 6.6 Hz, 2H), 2.84 (t, *J* = 8.4 Hz, 2H), 2.20 – 2.09 (m, 2H), 2.05 – 1.99 (m, 1H), 1.65 – 1.60 (m, 2H), 1.50 – 1.44 (m, 2H), 1.38 – 1.34 (m, 2H), 1.30 – 1.24(m, 10H), 0.86 (d, *J* = 6.8 Hz, 6H).

^{13}C NMR (151 MHz, DMSO) δ 173.29, 172.51, 151.37, 146.38, 130.32, 112.77, 112.02, 108.89, 68.10, 57.04, 46.93, 34.97, 29.89, 29.77, 29.00, 28.94, 28.81, 28.78, 28.61, 25.60, 25.40, 19.20, 18.07.

HR-MS (ESI) calculated for $C_{24}H_{39}N_2O_4$ $[M+H]^+$ m/z 419.2190, found 419.2189.

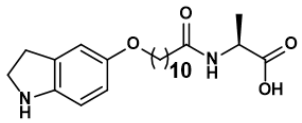

4c

Compound 4c

To a solution of Compound **3c** (0.14 g, 0.34 mmol, 1.0 equiv.) in methanol (2 mL) and THF (2 mL), an aqueous solution of NaOH (4M, 1 mL) was added the reaction mixture and then heated at 80 °C for 1 h. After cooling to room temperature, volatile solvents were removed under reduced pressure. The pH of reaction mixture was adjusted to ~7 by adding 1 M HCl solution that off-white precipitate formed. The filtered precipitate was washed with H_2O (0.5 mL) to afford **Compound 4c** as an off-white solid (0.11 g, 0.28 mmol, 84 % yield).

^{1}H NMR (400 MHz, 9 : 1 $CDCl_3$ with 0.03% v/v TMS : CD_3OD) δ 6.70 (s, 1H), 6.66 – 6.62 (m, 1H), 6.57 – 6.54 (m, 1H), 4.39 – 4.33 (m, 1H), 3.82 (t, *J* = 6.3 Hz, 2H), 3.46 (t, *J* = 8.2 Hz, 2H), 2.98 – 2.32 (m, 2H), 2.14 – 2.09 (m, 2H), 1.69 – 1.62 (m, 2H), 1.54 – 1.50 (m, 2H), 1.38 – 1.30 (m, 5H), 1.26 – 1.20 (d, *J* = 11.6 Hz, 10H).

^{13}C NMR (101 MHz, 9 : 1 $CDCl_3$ with 0.03% v/v TMS : CD_3OD) δ 175.61, 173.76, 154.26, 142.77, 132.17, 113.45, 112.19, 112.10, 68.97, 47.33, 36.36, 30.38, 29.41, 29.31, 29.29, 29.24, 29.22, 29.17, 25.92, 25.61, 18.12.

HR-MS (ESI) calculated for $C_{22}H_{34}N_2O_4$ $[M+H]^+$ m/z 391.2597, found 391.2598.

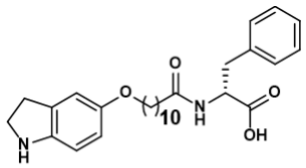

4d

Compound 4d

To a solution of Compound **3d** (114 mg, 0.24 mmol, 1.0 equiv.) in methanol (2 mL) and THF (2 mL), an aqueous solution of NaOH (4M, 1 mL) was added the reaction mixture and then heated at 80 °C for 1 h. After cooling to room temperature, volatile solvents were removed under reduced pressure. The pH of reaction mixture was adjusted to ~7 by adding 1 M HCl solution that off-white precipitate formed. The filtered precipitate was washed with H_2O (0.5 mL) to afford **Compound 4d** as an off-white solid (83 mg, 0.18 mmol, 75% yield).

^{1}H NMR (600 MHz, DMSO) δ 8.02 (d, *J* = 8.1 Hz, 1H), 7.25 – 7.16 (m, 5H), 6.67 (s, 1H), 6.48 (dd, *J* = 8.3, 2.5 Hz, 1H), 6.39 (d, *J* = 8.3 Hz, 1H), 4.38 – 4.35 (m, 1H), 3.80 (t, *J* = 6.5 Hz, 2H), 3.04 (dd, *J* = 13.8, 4.7 Hz, 1H), 2.85 – 2.80 (m, 3H), 2.01 (t, *J* = 7.3 Hz, 2H), 1.63 (p, *J* = 6.7 Hz, 2H), 1.39 – 1.16 (m, 12H), 1.12 – 1.08 (m, 2H).

^{13}C NMR (151 MHz, DMSO) δ 173.24, 172.01, 151.36, 146.39, 138.01, 130.31, 129.13, 128.04, 126.24, 112.76, 112.02, 108.89, 68.09, 53.49, 46.94, 36.83, 35.16, 29.89, 29.02, 28.95, 28.91, 28.84, 28.82, 28.47, 25.61, 25.23.

HR-MS (ESI) calculated for $C_{28}H_{38}N_2O_4$ $[M+H]^+$ m/z 467.2910, found 465.2911.

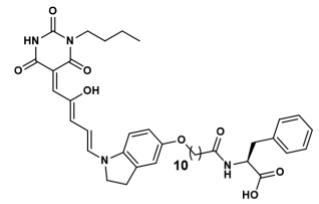

6a (DA_{LPhe})

Compound 6a (DA_{LPhe})

Compound **4a (**89.63 mg, 0.192 mmol, 1.0 equiv.**)** and Compound **5** (50.41 mg, 0.192 mmol, 1.0 equiv.) were suspended in dichloromethane (0.8 mL). After hexafluoro-2-propanol (0.2 mL) was added, the reaction mixture was stirred at 20 °C for 24 h under air. Undissolved solid was filtered off and washed with THF solution. The filtrate was concentrated under reduced pressure. The residue was dissolved in THF (1 mL). After introducing *n*-hexane (10 mL), the recrystallized **Compound 6a (DA_{LPhe})** (112 mg, 0.154 mmol, 80 % yield) was collected as a black solid.

^{1}H NMR (400 MHz, THF) δ 12.49 – 12.31 (m, 0.4 H), 10.84 – 10.58 (m, 0.6 H), 10.11 – 9.94 (m, 0.5 H), 7.96 (d, J = 12.4 Hz, 1H), 7.65 (dd, J = 6.0, 2.1 Hz, 1H), 7.22 – 7.12 (m, 5H), 7.03 (d, J = 8.0 Hz, 0.83H), 6.87 (s, 0.42H), 6.81 (d, J = 11.3 Hz, 0.85H), 6.69 (s, 0.22H), 6.63 (d, J = 7.6 Hz, 0.23H), 6.52 – 6.48 (m, 0.39H), 6.41 (t, J = 7.7 Hz, 0.27H), 6.32 – 6.30 (m, 0.24H), 6.13 (t, J = 12.2 Hz, 0.5H), 5.29 (d, J = 27.5 Hz, 0.35H), 4.77 – 4.72 (m, 1H), 4.13 (t, J = 8.0 Hz, 1H), 3.94 (t,

J = 6.4 Hz, 1H), 3.88 – 3.72 (m, 2H), 3.27 – 3.11 (m, 3H), 2.98 – 2.92 (m, 2H), 2.07 (t, J = 7.4 Hz, 2H), 1.54 – 1.44 (m, 6H), 1.36 – 1.22 (m, 12H), 0.95 – 0.85 (m, 3H).

HR-MS (ESI-) calculated for $C_{41}H_{51}N_4O_8$ $[M-H]^-$ m/z 727.3707, found 727.3705.

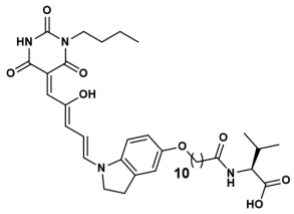

6b (DA_{LVal})

Compound 6b (DA_{LVal})

Compound **4b (**50.2 mg, 0.120 mmol, 1.0 equiv.**)** and Compound **5** (31.4 mg, 0.120 mmol, 1.0 equiv.) were suspended in dichloromethane (0.8 mL). After hexafluoro-2-propanol (0.2 mL) was added, the reaction mixture was stirred at 20 °C for 24 h under air. Undissolved solid was filtered off and washed with THF solution. The filtrate was concentrated under reduced pressure. The residue was dissolved in THF (1 mL). After introducing *n*-hexane (10 mL), the recrystallized **Compound 6b (DA_{LVal})** (73.2 mg, 0.11 mmol, 90 % yield) was collected as a black solid.

^{1}H NMR (400 MHz, THF) δ 12.49 – 12.31(m, 0.9H), 10.85 – 10.58 (m, 1.1H), 10.11 – 9.95 (m, 0.8H), 7.96 (d, J = 12.4 Hz, 0.59H), 7.65 (dd, J = 5.9, 2.0 Hz, 0.26H), 7.18 (t, J = 7.7 Hz, 0.93H), 6.98 (d, J = 9.0 Hz, 0.88H), 6.87 (d, J = 2.4 Hz, 0.51H), 6.84 – 6.77 (m, 0.97H), 6.69 (s, 0.26H), 6.52 – 6.48 (m, 0.42H), 6.41 (t, J = 7.8 Hz, 0.34H), 6.32 – 6.30 (m, 0.25H), 6.16 – 6.10 (t, J = 12.2 Hz, 0.59H), 5.29 (d, J = 26.5 Hz, 0.5H), 4.73 (s, 1H), 4.48 (m, 1H), 4.13 (t, J = 7.9 Hz, 1H), 3.86 – 3.80 (m, 2H), 3.26 (t, J = 8.1 Hz, 2H), 2.93 – 2.82 (m, 1H), 2.15 (t, J = 7.4 Hz, 2H), 1.62 – 1.51 (m, 6H), 1.38 – 1.28 (m, 12H), 0.95 – 0.87 (m, 9H).

HR-MS (ESI-) calculated for $C_{41}H_{51}N_4O_8$ $[M-H]^-$ m/z 679.3707, found 679.3710.

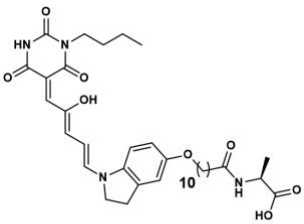

6c (DA_{LAla})

Compound 6c (DA_{LAla})

Compound **4c (**77.8 mg, 0.20 mmol, 1.0 equiv.**)** and Compound **5** (52.2 mg, 0.20 mmol, 1.0 equiv.) were suspended in dichloromethane (0.8 mL). After hexafluoro-2-propanol (0.2 mL) was added, the reaction mixture was stirred at 20 °C for 24 h under air. Undissolved solid was filtered off and washed with THF solution. The filtrate was concentrated under reduced pressure. The residue was

dissolved in THF (1 mL). After introducing *n*-hexane (10 mL), the recrystallized **Compound 6c (DA_{LAla})** (78.3 mg, 0.12 mmol, 60 % yield) was collected as a black solid.

^{1}H NMR (400 MHz, THF) δ 12.49 – 12.31(m, 0.56H), 10.85 – 10.58 (m, 0.91H), 10.11 – 9.95 (m, 0.75H), 7.97 (d, J = 12.2 Hz, 0.43H), 7.65 (dd, J = 5.9, 2.0 Hz, 0.2H), 7.20 – 7.10 (m, 2H), 6.87 (s, 0.44H), 6.83 –6.80 (m, 0.91H), 6.69 – 6.62 (m, 0.5H), 6.52 – 6.48 (m, 0.39H), 6.41 (t, J = 7.7 Hz, 0.3H), 6.32 – 6.30 (m, 0.22H), 6.13 (t, J = 12.2 Hz, 0.51H), 5.32 – 5.26 (m, 0.44H), 4.73 (s, 0.29H), 4.45 (p, J = 7.3 Hz, 1H), 4.15 – 4.10 (m, 1H), 3.94 (t, J = 6.5 Hz, 1H), 3.86 – 3.79 (m, 2H), 3.28 – 3.21 (m, 2H), 2.10 (t, J = 7.4 Hz, 2H), 1.61 – 1.44 (m, 6H), 1.36 – 1.28 (m, 15H), 0.95 – 0.85 (m, 3H).

HR-MS (ESI-) calculated for $C_{41}H_{51}N_4O_8$ $[M-H]^-$ m/z 651.3394, found 651.3397.

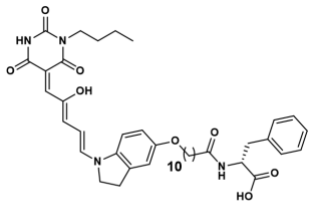

6d (DA_{DPhe})

Compound 6d (DA_{DPhe})

Compound **4d (**73 mg, 0.16 mmol, 1.0 equiv.**)** and Compound **5** (41 mg, 0.16 mmol, 1.0 equiv.) were suspended in dichloromethane (0.8 mL). After hexafluoro-2-propanol (0.2 mL) was added, the reaction mixture was stirred at 20 °C for 24 h under air. Undissolved solid was filtered off and washed with THF solution. The filtrate was concentrated under reduced pressure. The residue was dissolved in THF (1 mL). After introducing *n*-hexane (10 mL), the recrystallized **Compound 6d (DA_{DPhe})** (93 mg, 0.13 mmol, 82 % yield) was collected as a black solid.

^{1}H NMR (600 MHz, DMSO) δ 12.72 – 12.46 (m, 0.98H), 10.93 – 10.80 (m, 0.39H), 8.56 – 8.50 (m, 0.43H), 8.11 (d, J = 8.2 Hz, 0.92H), 7.48 – 7.45 (m, 0.48H), 7.27 – 7.17 (m, 5H), 7.09 (d, J = 12.8 Hz, 0.48H), 6.99 (s, 0.49H), 6.94 (d, J = 9.0 Hz, 0.50H), 6.82 (s, 0.49H), 6.70 (d, J = 34.3 Hz, 0.34H), 6.51 (d, J = 64.2 Hz, 0.36H), 6.38 – 6.21 (m, 0.29H), 6.16 – 6.13 (m, 0.48H), 5.08 – 4.95 (m, 0.20), 4.43 – 4.39 (m, 1H), 4.25 (t, J = 7.7 Hz, 1H), 3.97 (t, J = 6.6 Hz, 1H), 3.80 – 3.70 (m, 2H), 3.25 (t, *J* = 7.8 Hz, 1H), 3.04 (dd, J = 13.8, 4.6 Hz, 1H), 2.84 – 2.80 (m, 1H), 2.02 (t, J = 7.4 Hz, 2H), 1.72 – 1.63 (m, 2H), 1.50 – 1.44 (m, 2H), 1.42 – 1.05 (m, 16H), 0.90 – 0.82 (m, 3H).

HR-MS (ESI-) calculated for $C_{41}H_{51}N_4O_8$ $[M-H]^-$ m/z 727.3707, found 727.3710.

4. Supporting Figures

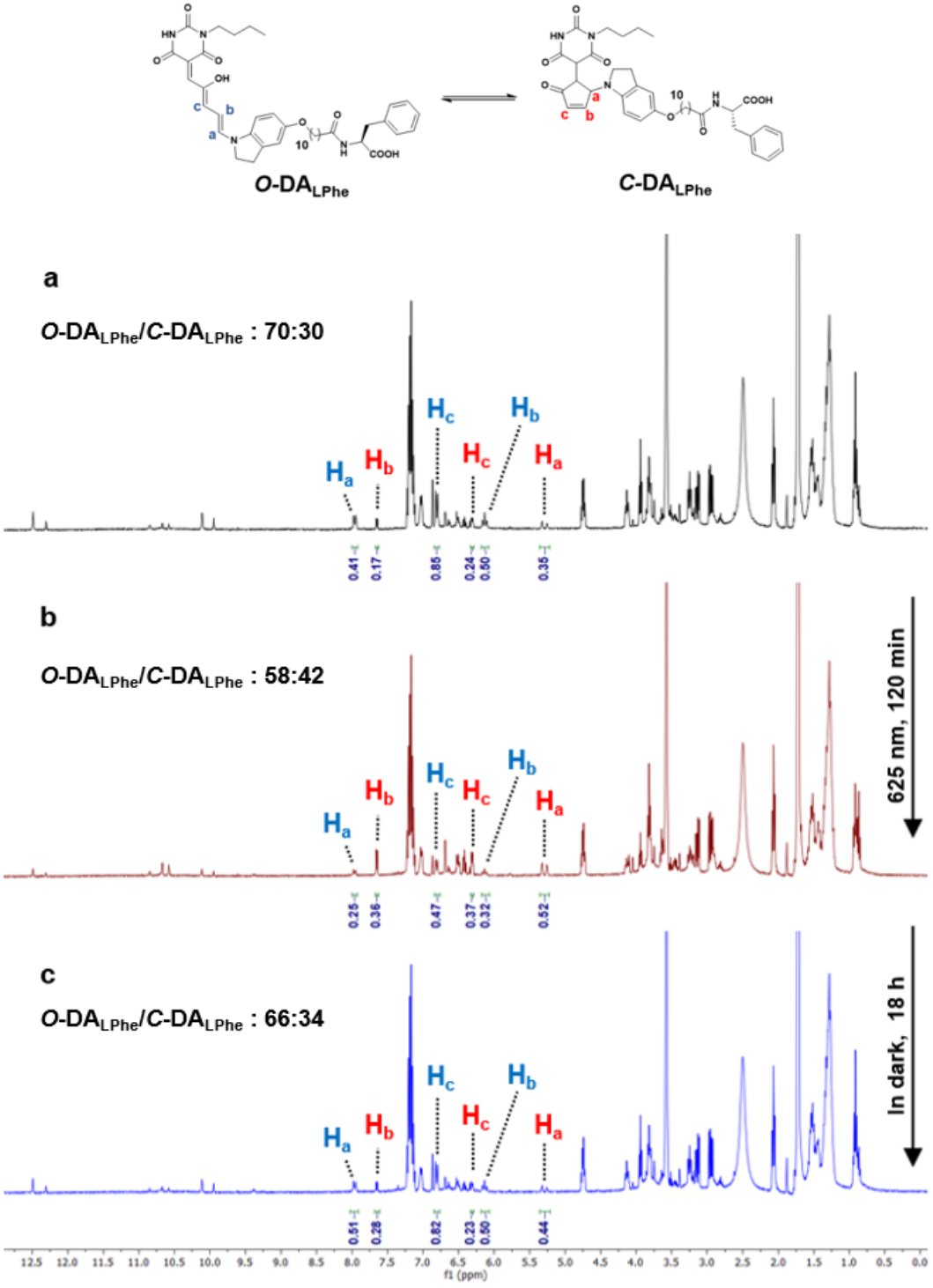

Supplementary Fig. 1 | Stacked ^{1}H NMR spectra of photoisomerisation and thermal recovery of DA$_{LPhe}$. A THF-*d*$_8$ solution of synthetically prepared **DA$_{LPhe}$** (5.65 mM, 400 MHz, 25 °C) **a** before irradiation (black), **b** after irradiation with 625 nm light for 120 min (red), and **c** thermal recovery at 20 °C in dark for 18 h (blue) were recorded.

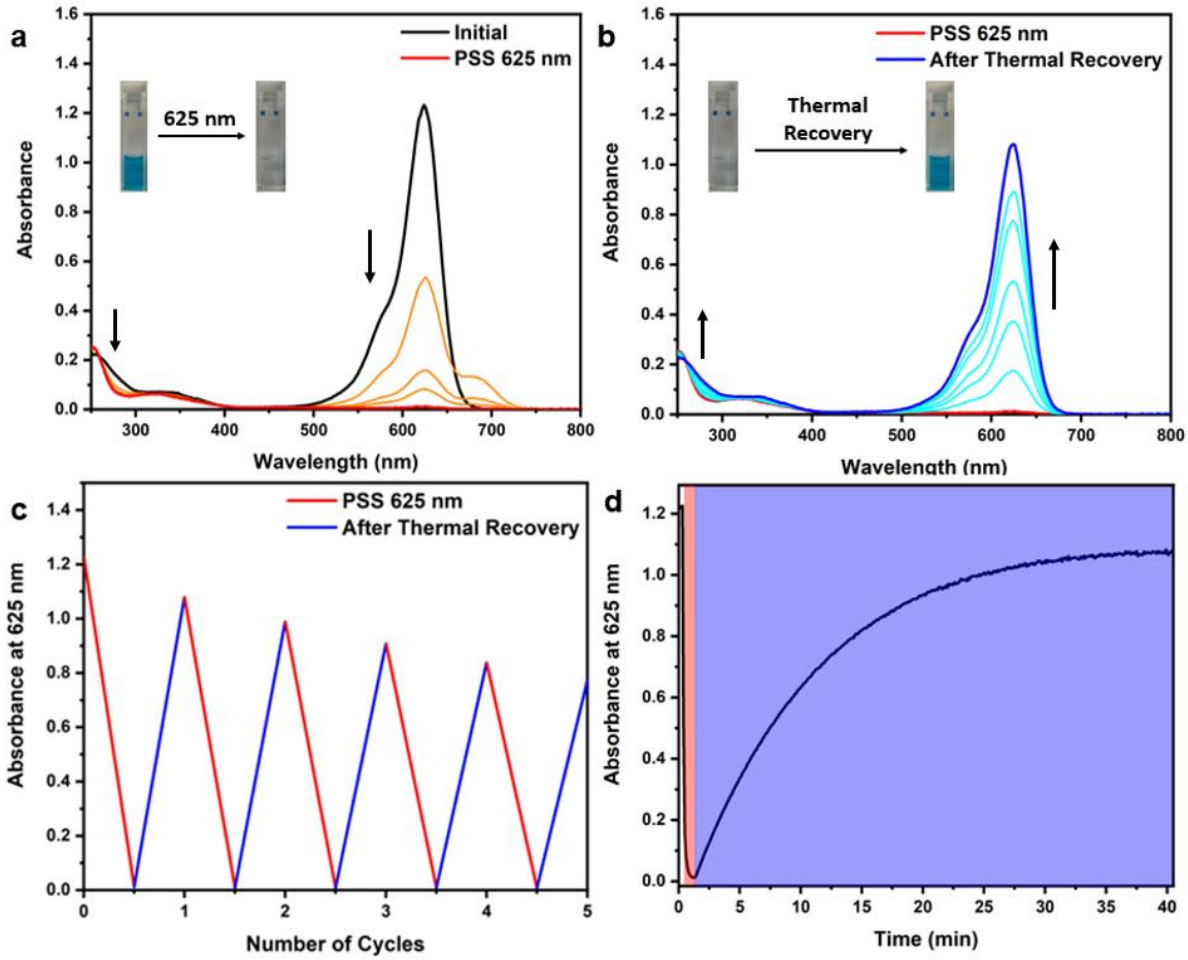

Supplementary Fig. 2 | Photoisomerisation and thermal recovery of DA_{LVal} in THF solution. UV-vis absorption spectra of DA_{LVal} in THF (20 μM). **a** Absorption spectra of DA_{LVal} at initial (black-line), photoirradiation of 625 nm over 1 min (orange-line) and after reached PSS 625 nm for 1 min (red-line). **b** Absorption spectra of DA_{LVal} at PSS 625 nm (red-line), thermal recovery over 40 min (cyan-line) and after thermal recovery for 40 min (blue-line). **c** Multiple photoswitching cycles of DA_{LVal} in THF (20 μM), alternative photoirradiation at 625 nm (red-line) for 1.0 min and thermal recovery for 40 min (blue-line). **d** Time-course of the photoisomerisation process of DA_{LVal} in THF, monitored at λ_{max} 625 nm of DA_{LVal} (red area: photoirradiation period and blue area: thermal recovery process).

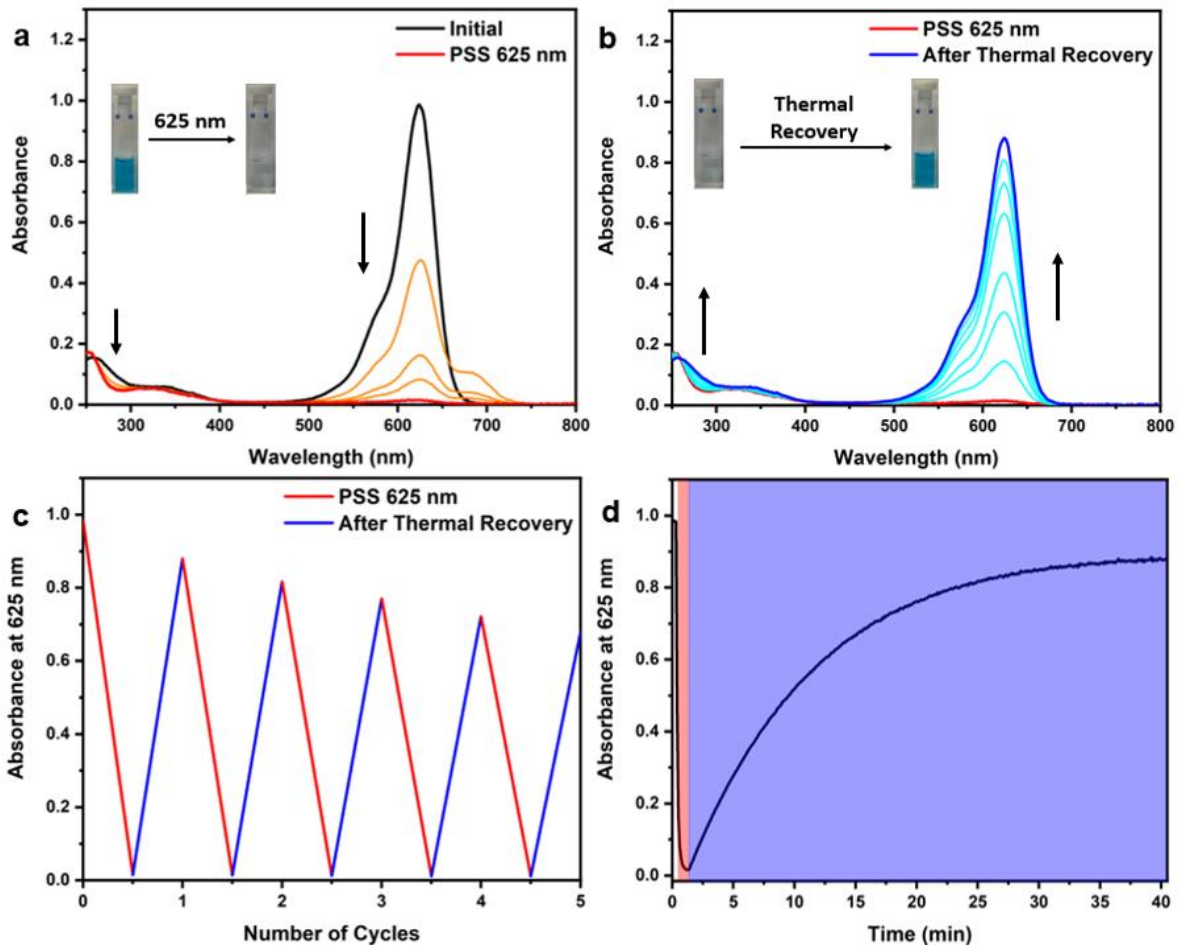

Supplementary Fig. 3 | Photoisomerisation and thermal recovery of DA_{LAla} in THF solution. UV-vis absorption spectra of DA_{LAla} in THF (20 μM). **a** Absorption spectra of DA_{LAla} at initial (black-line), photoirradiation of 625 nm over 1 min (orange-line) and after reached PSS 625 nm for 1 min (red-line). **b** Absorption spectra of DA_{LAla} at PSS 625 nm (red-line), thermal recovery over 40 min (cyan-line) and after thermal recovery for 40 min (blue-line). **c** Multiple photoswitching cycles of DA_{LAla} in THF (20 μM), alternative photoirradiation at 625 nm (red-line) for 1.0 min and thermal recovery for 40 min (blue-line). **d** Time-course of the photoisomerisation process of DA_{LAla} in THF, monitored at λ_{max} 625 nm of DA_{LAla} (red area: photoirradiation period and blue area: thermal recovery period)

.

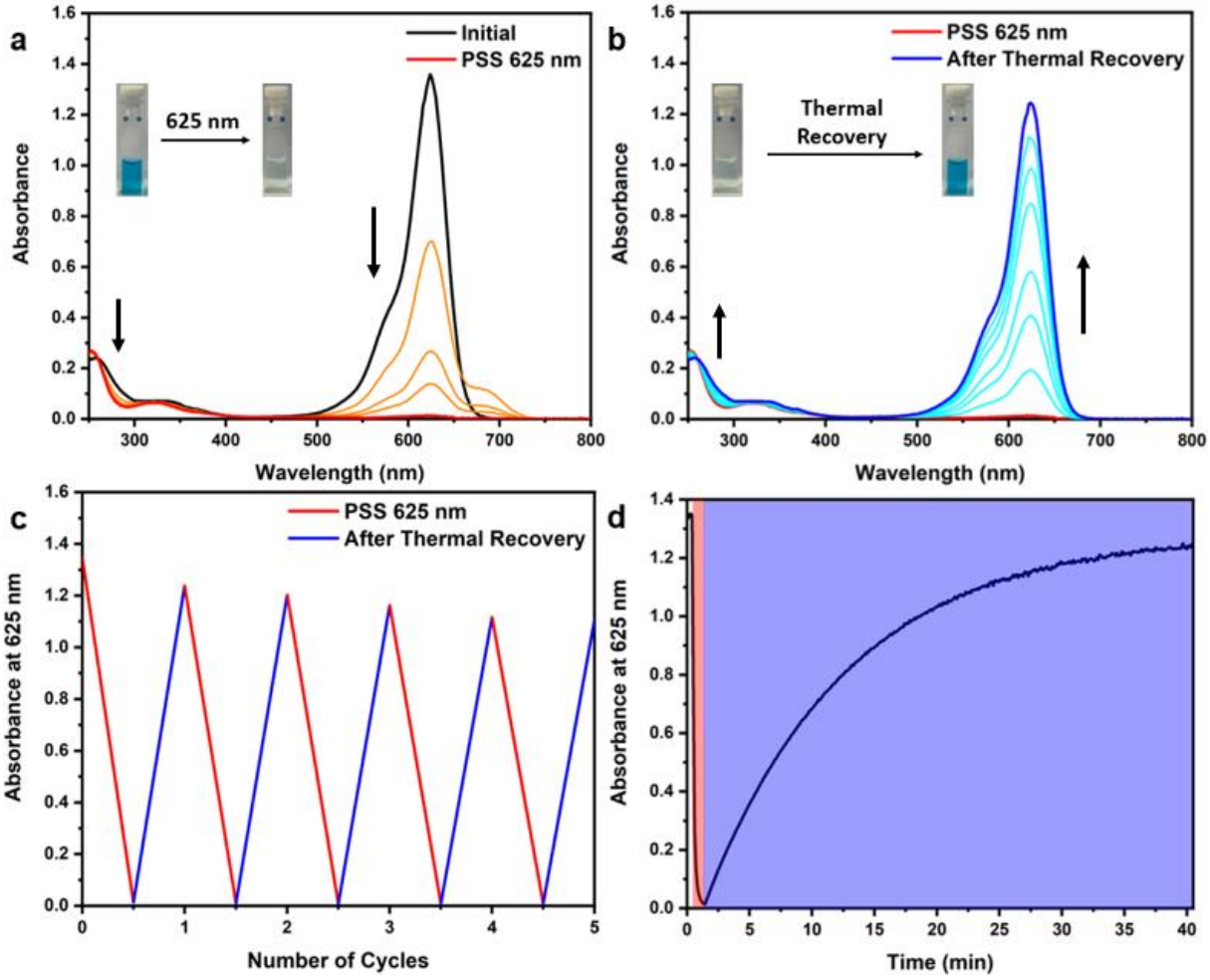

Supplementary Fig. 4 | Photoisomerisation and thermal recovery of DA$_{DPhe}$ in THF solution. UV-vis absorption spectra of **DA$_{DPhe}$** in THF (20 μM). **a** Absorption spectra of **DA$_{DPhe}$** at initial (black-line), photoirradiation of 625 nm over 1 min (orange-line) and after reached PSS 625 nm for 1 min (red-line). **b** Absorption spectra of **DA$_{DPhe}$** at PSS 625 nm (red-line), thermal recovery over 40 min (cyan-line) and after thermal recovery for 40 min (blue-line). **c** Multiple photoswitching cycles of **DA$_{DPhe}$** in THF (20 μM), alternative photoirradiation at 625 nm (red-line) for 1.0 min and thermal recovery for 40 min (blue-line). **d** Time-course of the photoisomerisation process of **DA$_{DPhe}$** in THF, monitored at λ_{max} 625 nm of **DA$_{DPhe}$** (red area: photoirradiation period and blue area: thermal recovery period).

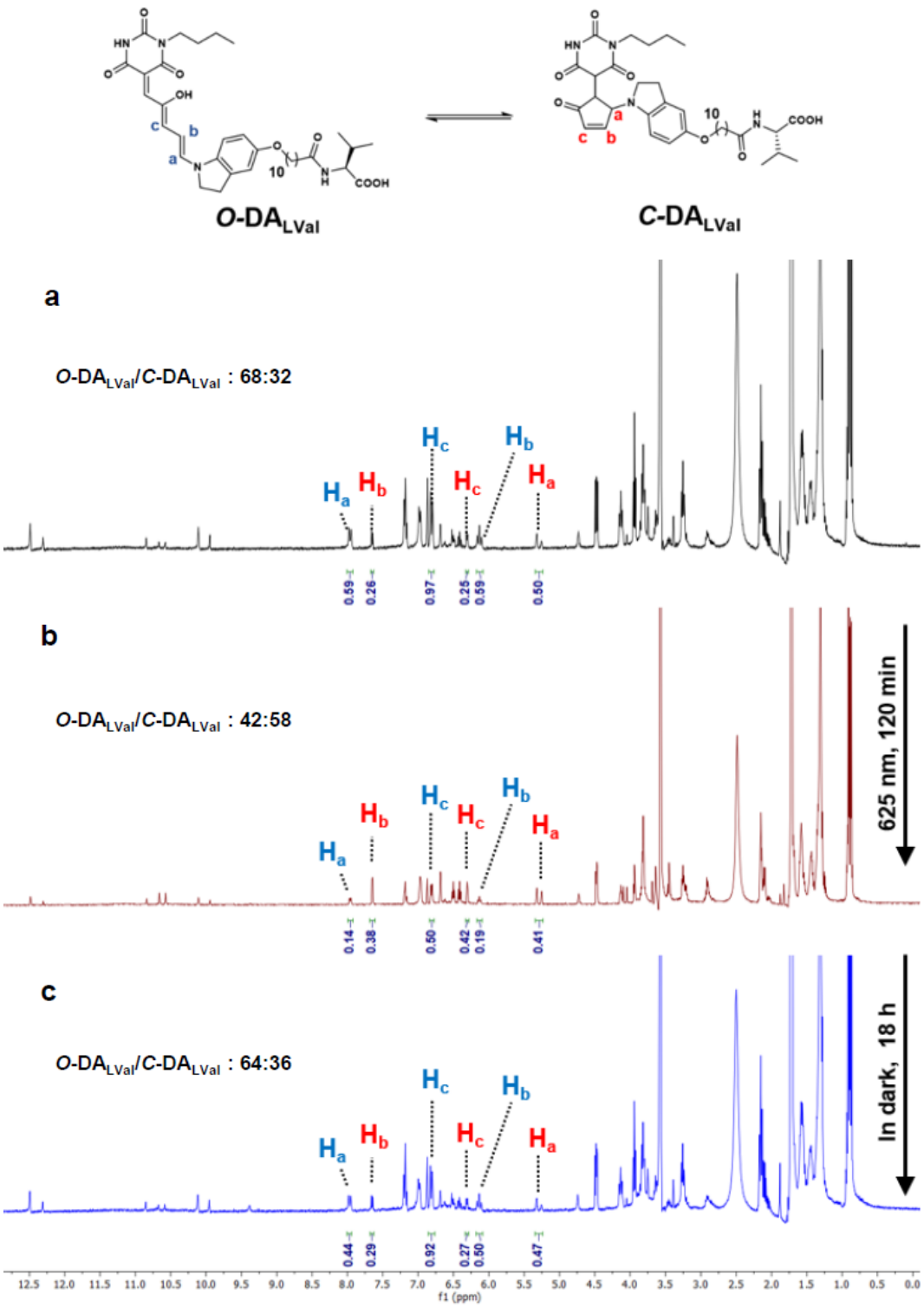

Supplementary Fig. 5 | Stacked ^{1}H NMR spectra of photoisomerisation and thermal recovery of DA$_{LVal}$. A THF-*d*$_8$ solution of synthetically prepared **DA$_{LVal}$** (5.7 mM 400 MHz, 25 °C). **a** before irradiation (black), **b** after irradiation with 625 nm light for 120 min (red), and **c** thermal recovery at 20 °C in dark for 18 h (blue) were recorded.

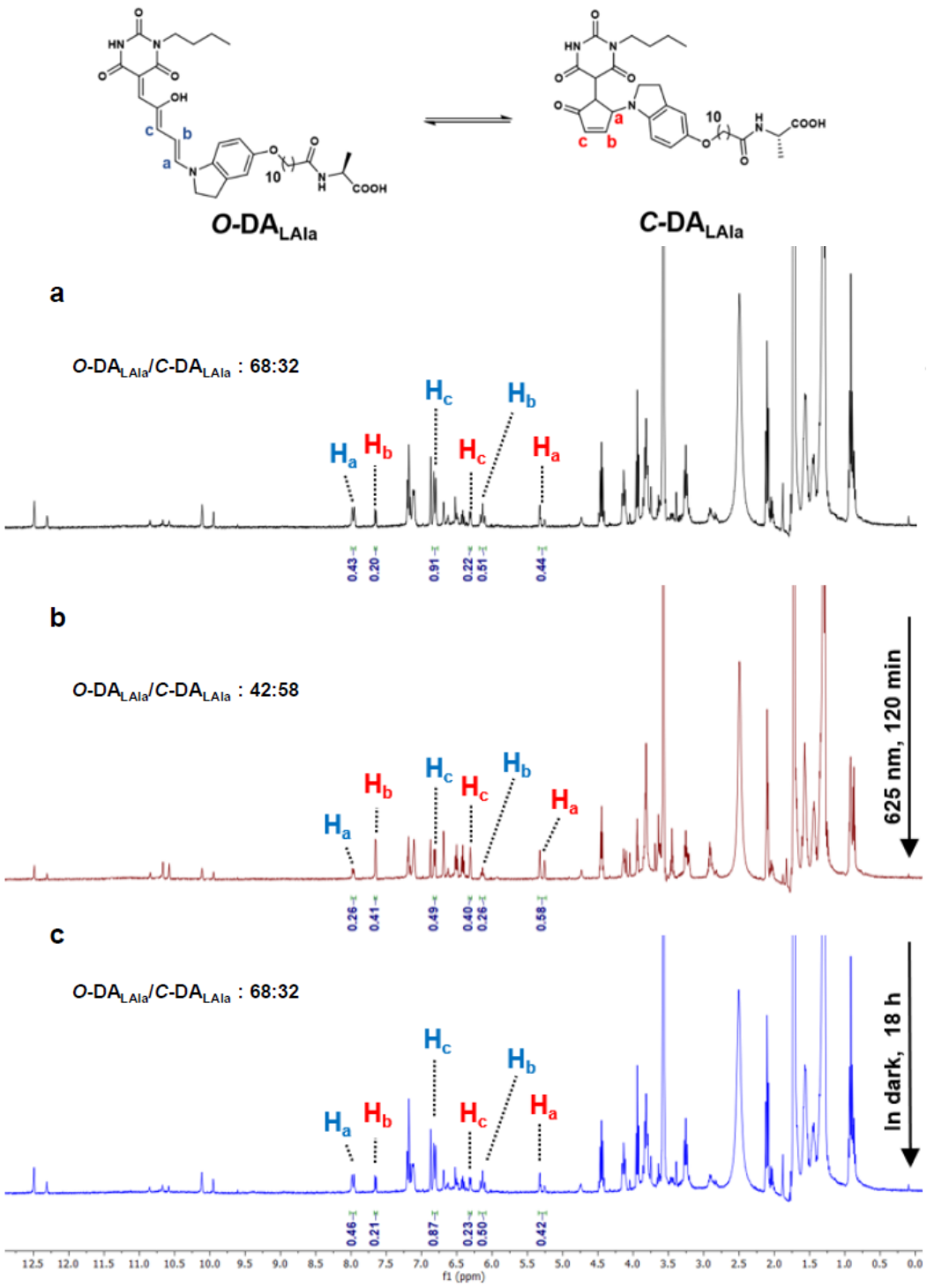

Supplementary Fig. 6 | Stacked ^{1}H NMR spectra of photoisomerisation and thermal recovery of DA$_{LAla}$. A THF-*d*$_8$ solution of synthetically prepared **DA$_{LAla}$** (5.9 mM, 400 MHz, 25 °C) **a** before irradiation (black), **b** after irradiation with 625 nm light for 120 min (red), and **c** thermal recovery at 20 °C in dark for 18 h (blue) were recorded.

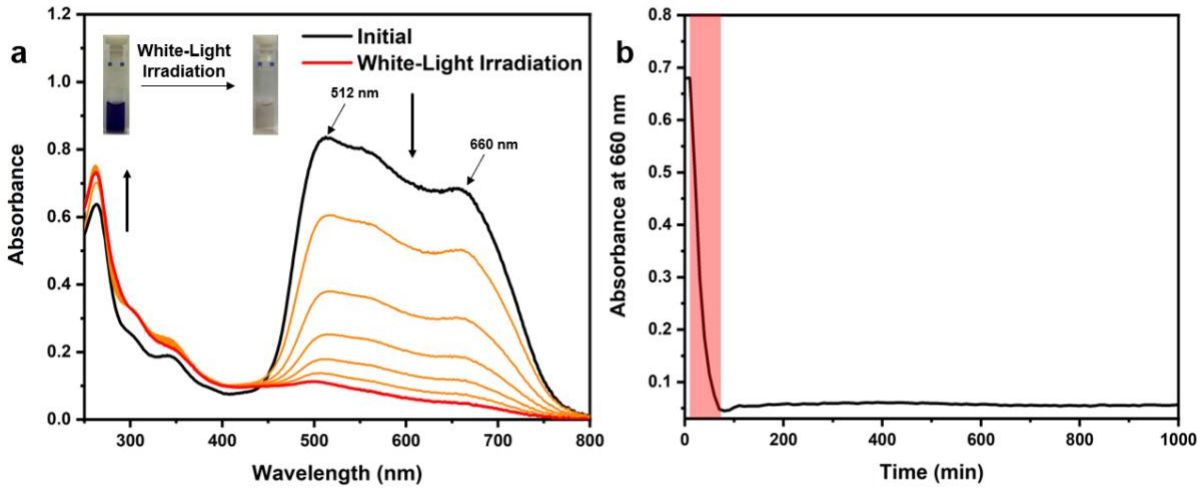

Supplementary Fig. 7 | Photoisomerisation of DA_{DPhe} in aqueous solution. UV-vis absorption spectra of DA_{DPhe} in aqueous solution (50 μM). **a** before irradiation, upon white-light irradiation over 60 min (orange-line) and after white-light irradiation for 60 min (red-line). **b** Time-course of the white-light irradiation of an aqueous solution of DA_{DPhe}, monitored at 660 nm (black-line). Photoirradiation of UV-vis sample was carried out at 20 °C using a light guide equipped BBZM-I xenon light source (380–800 nm, 300 W) positioned at a distance of 1 cm from the sample.

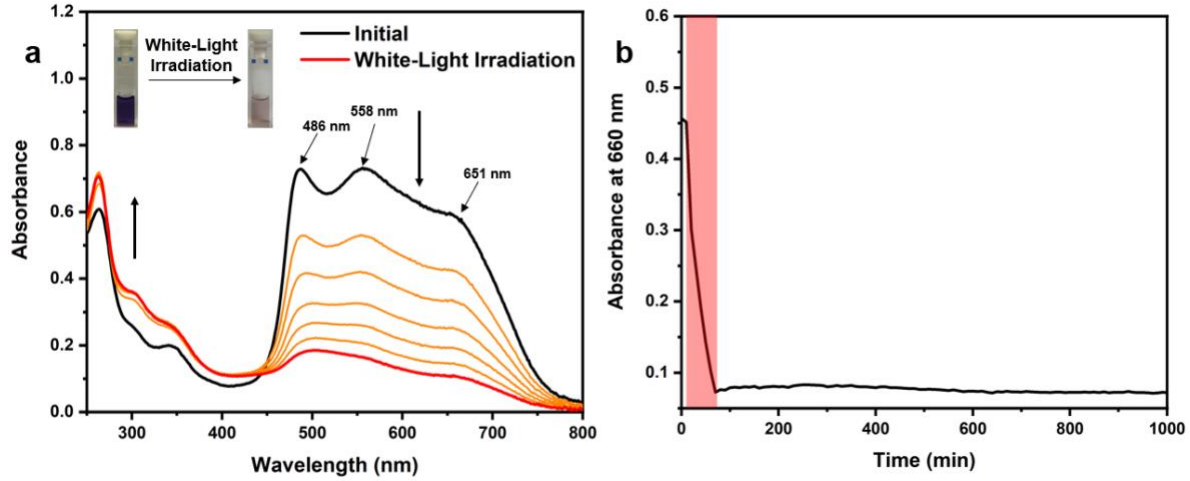

Supplementary Fig. 8 | Photoisomerisation of DA_{LVal} in aqueous solution. UV-vis absorption spectra of DA_{LVal} in aqueous solution (50 μM). **a** before irradiation, upon white-light irradiation over 60 min (orange-line) and after white-light irradiation for 60 min (red-line). **b** Time-course of the white-light irradiation of an aqueous solution of DA_{LVal}, monitored at 660 nm (black-line). Photoirradiation of UV-vis sample was carried out at 20 °C using a light guide equipped BBZM-I xenon light source (380–800 nm, 300 W) positioned at a distance of 1 cm from the sample.

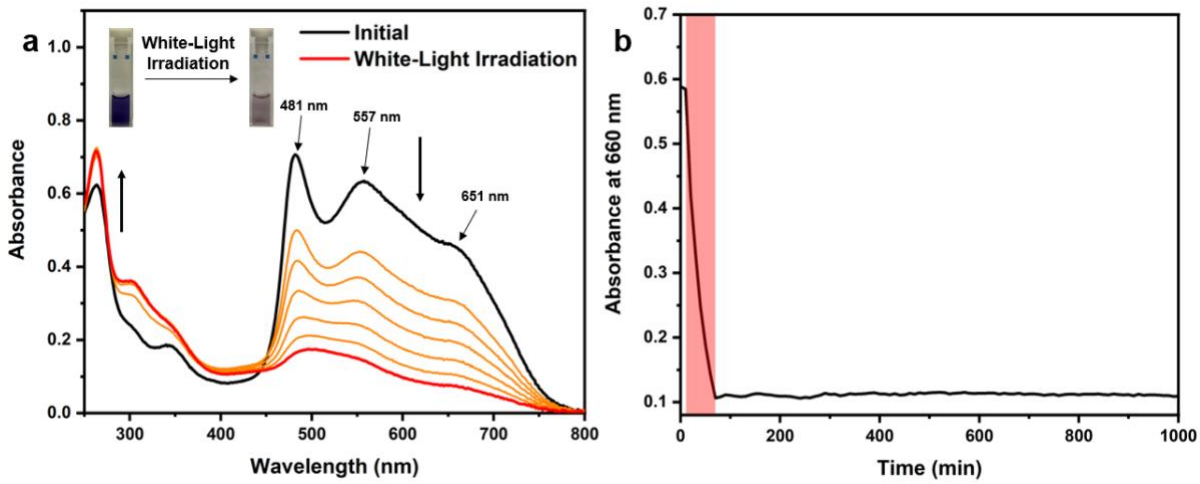

Supplementary Fig. 9 | Photoisomerisation of DA_{LAla} in aqueous solution. UV-vis absorption spectra of $\mathbf{DA_{LAla}}$ in aqueous solution (50 μM). **a** before irradiation, upon white-light irradiation over 60 min (orange-line) and after white-light irradiation for 60 min (red-line). **b** Time-course of the white-light irradiation of an aqueous solution of $\mathbf{DA_{LAla}}$, monitored at 660 nm (black-line). Photoirradiation of UV-vis sample was carried out at 20 °C using a light guide equipped BBZM-I xenon light source (380–800 nm, 300 W) positioned at a distance of 1 cm from the sample.

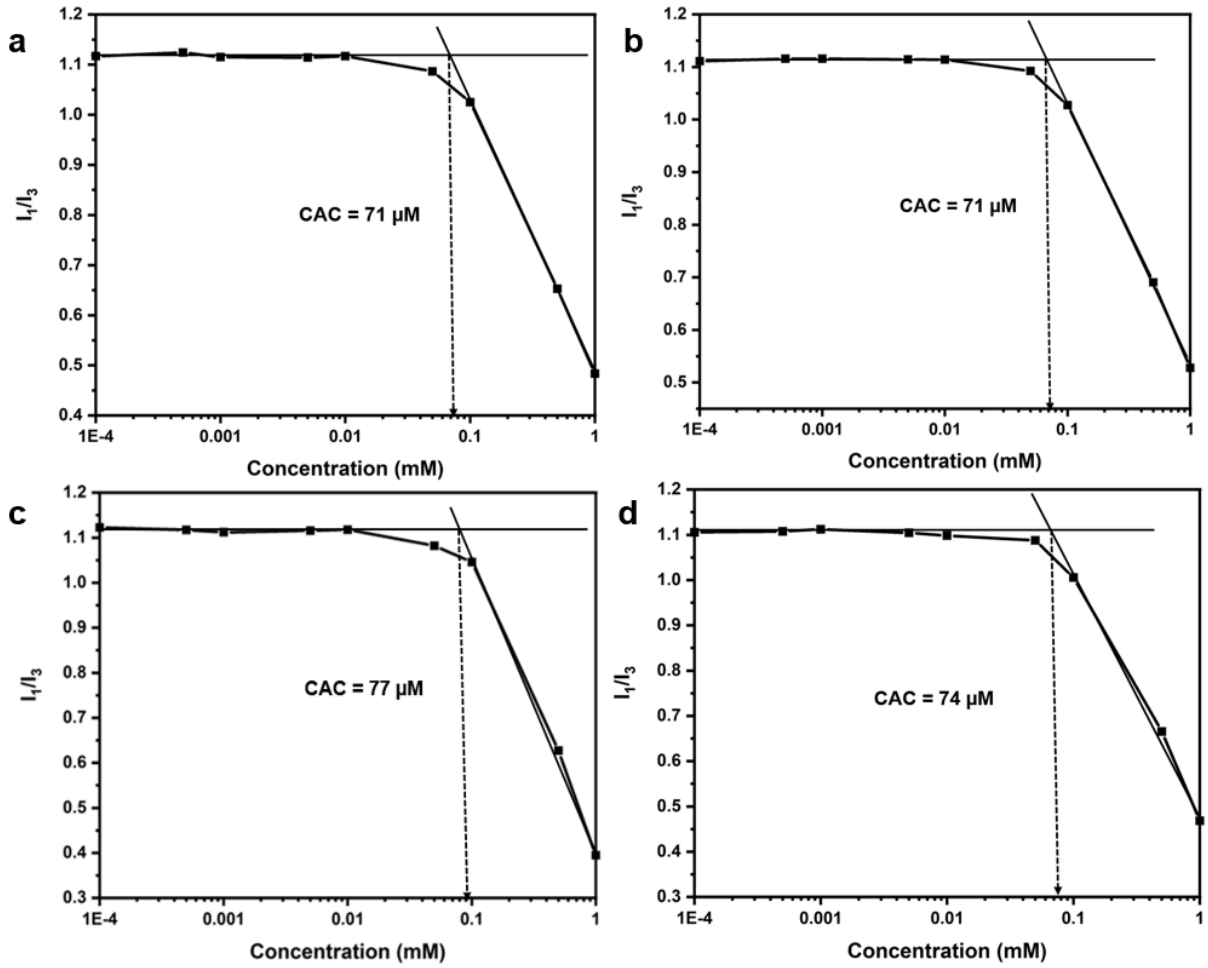

Supplementary Fig. 10 | Pyrene Fluorescent Assay of DA_A. Plot of pyrene fluorescence assay of I_{373}/I_{393} ratio for determination of the critical aggregation concentration of **a** DA_{LPhe}, **b** DA_{DPhe}, **c** DA_{LVal} and **d** DA_{LAla} with a ranged of concentration of 1.0×10^{-4} to 1.0 mM.

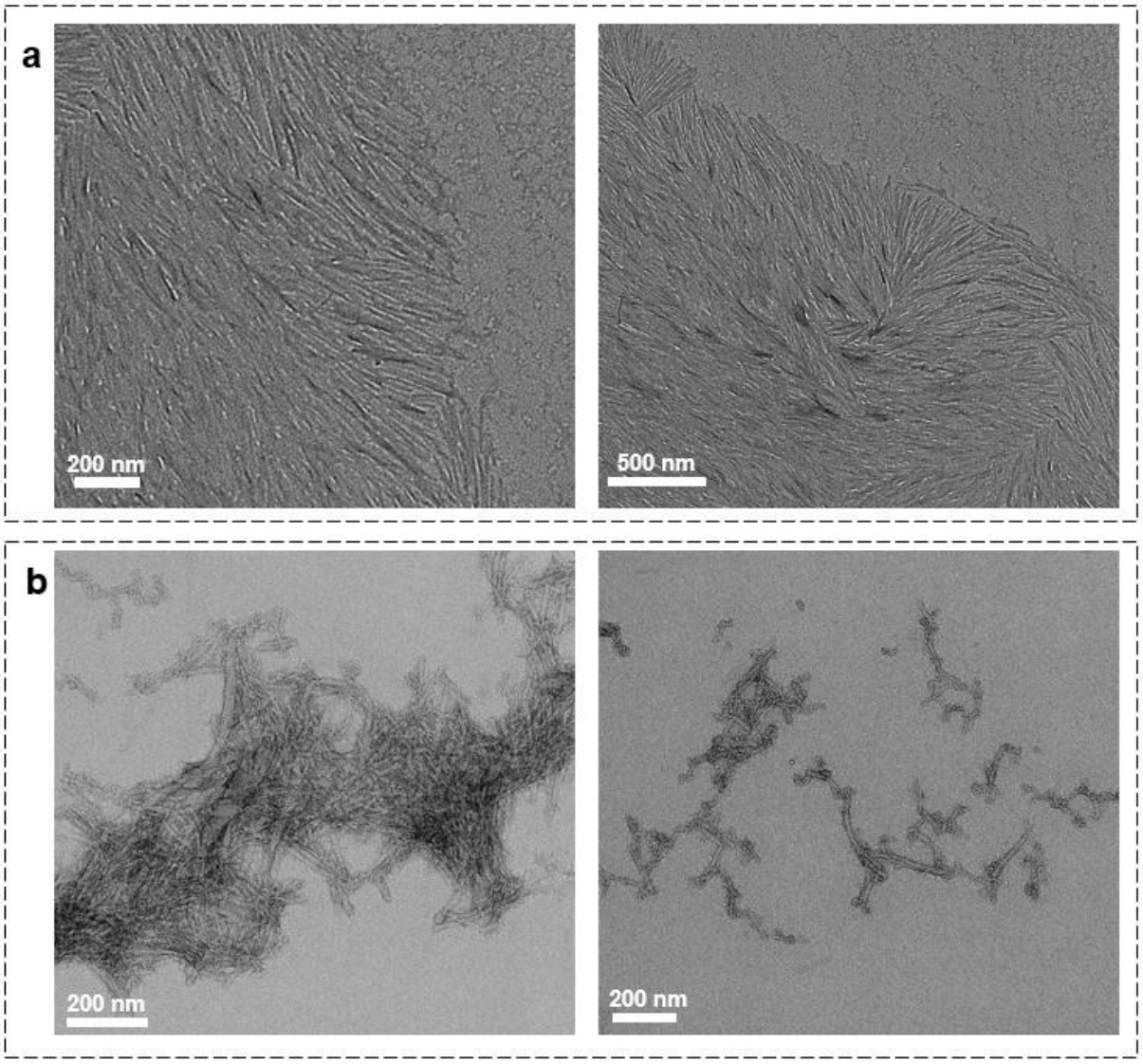

Supplementary Fig. 11 | TEM images of DA_{LPhe} in aqueous solution. Representative TEM images of aqueous solution of **a** DA_{LPhe} (0.25 wt.%, 3.43 mM) before and **b** after 60 min white light irradiation

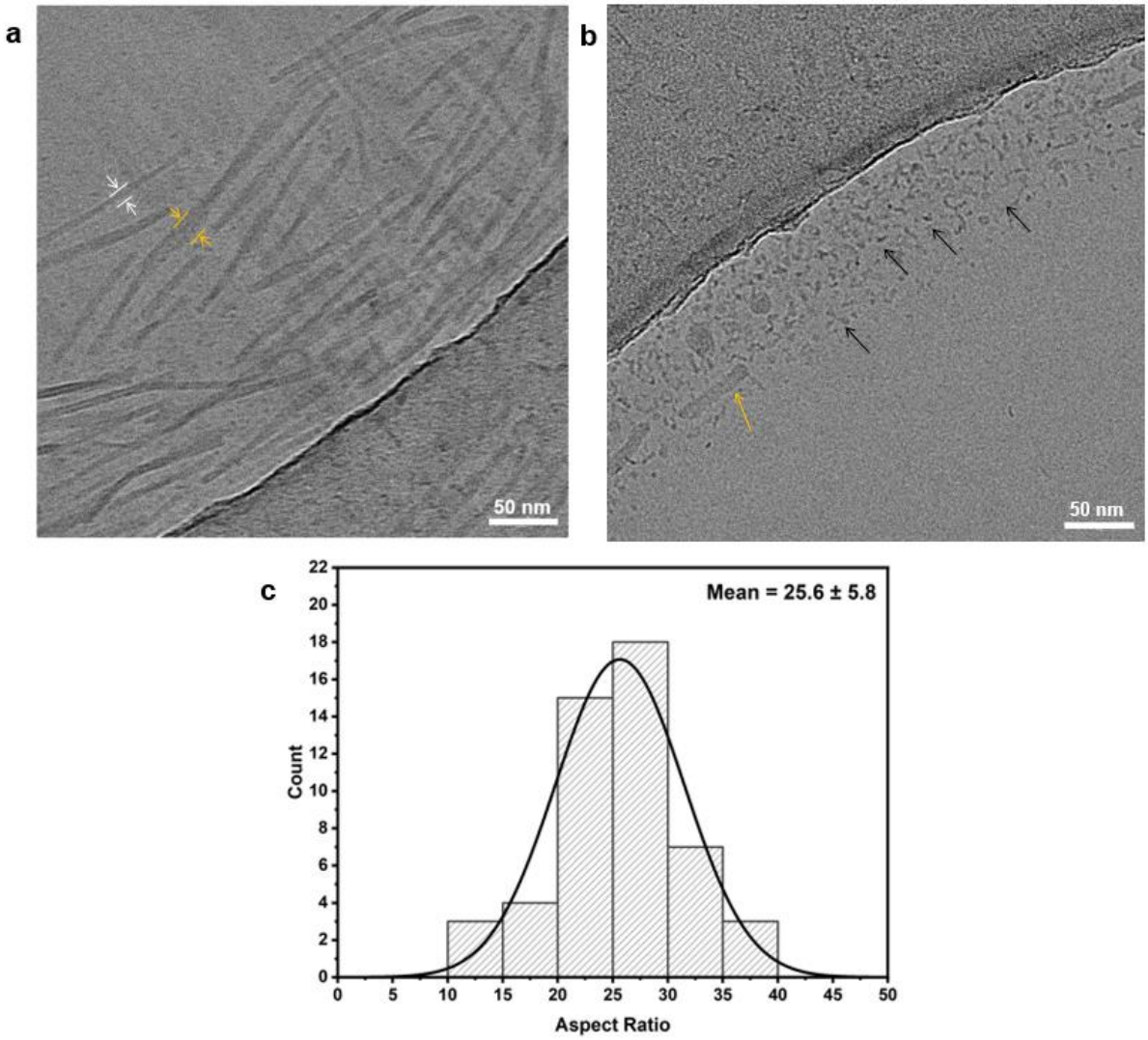

Supplementary Fig. 12 | Cryo-TEM images of DA_{DPhe} in aqueous solution. Representative of cryo-TEM images of **DA_{DPhe}** (1.0 wt. %, 13.7 mM) **a** before irradiation (yellow arrow: wide diameter and white arrow: narrow diameter) **b** after white light irradiation for 60 min (yellow arrows: shortened nanoribbon and black arrows: micelles). **c** Histogram profile of **DA_{DPhe}** aspect-ratio before irradiation.

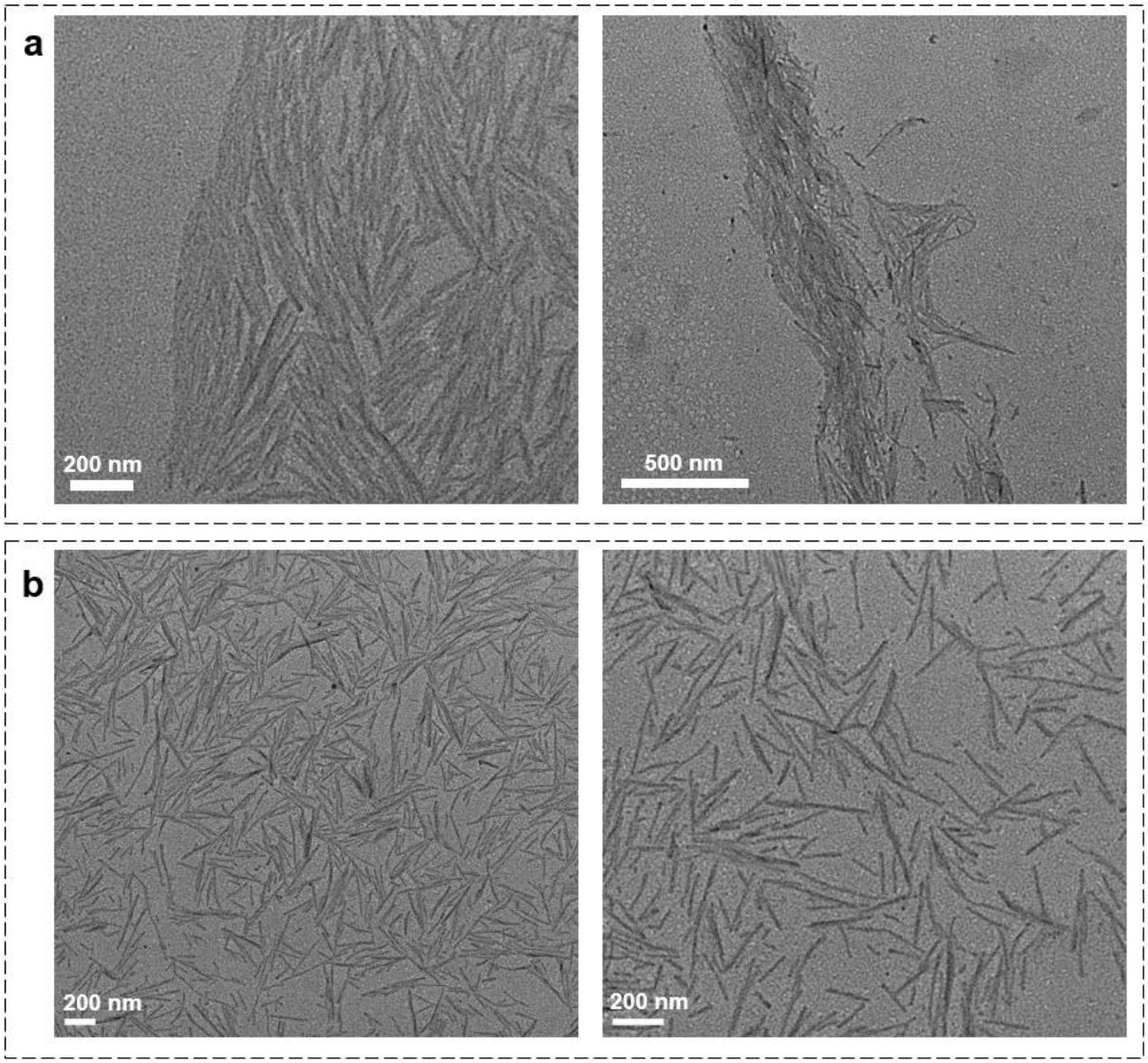

Supplementary Fig. 13 | TEM images of DA_{DPhe} in aqueous solution. Representative of TEM images of **DA_{DPhe}** (0.25 wt. %, 3.43 mM) **a** before and **b** after white light irradiation for 60 min.

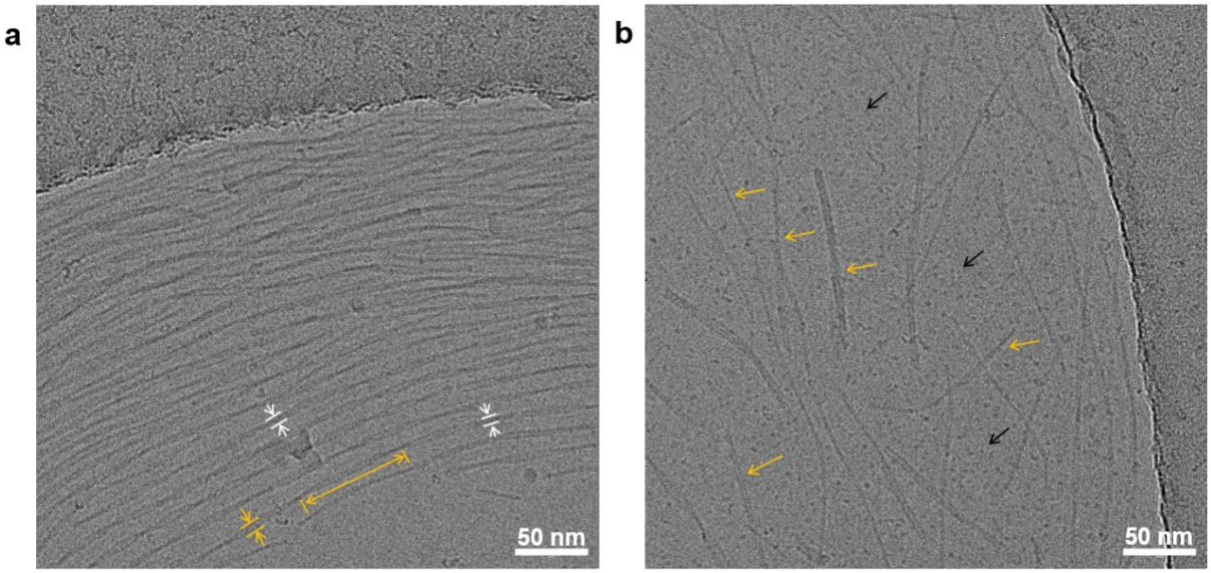

Supplementary Fig. 14 | Cryo-TEM images of DA_{LVal} in aqueous solution. Representative cryo-TEM images of aqueous solution of **DA_{LVal}** (1.0 wt.%, 14.7 mM) **a** before irradiation (white arrows: diameter of nanofibres and yellow arrows: helical pitch length). **b** After white light irradiation for 60 min (yellow arrows: shortened nanofibres and black arrows: micelles).

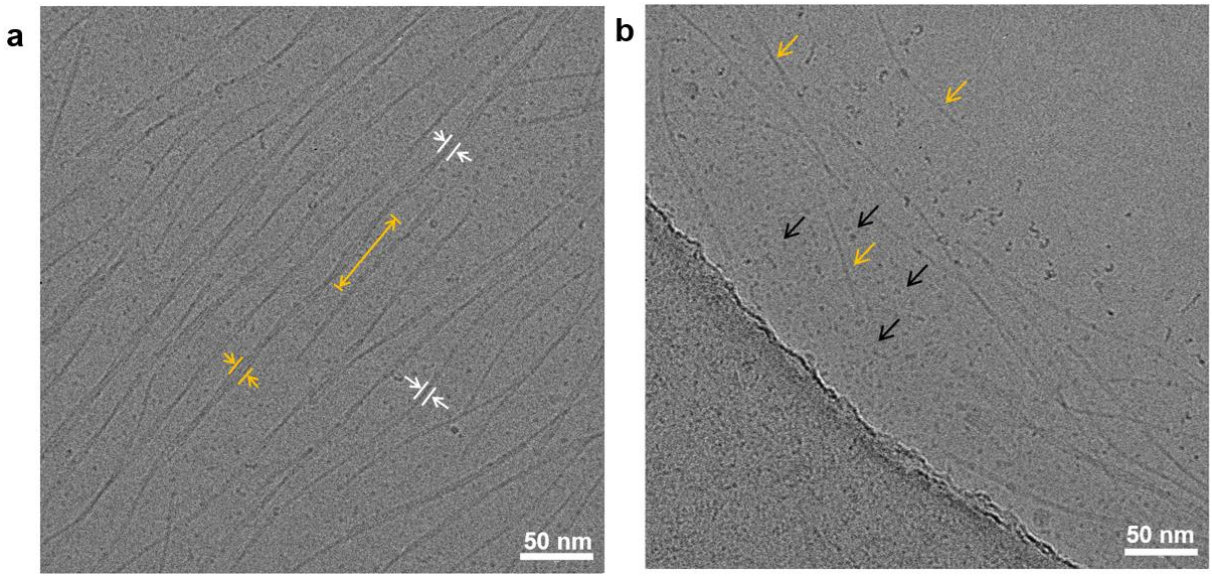

Supplementary Fig. 15 | Cryo-TEM images of DA_{LAla} in aqueous solution. Representative cryo-TEM images of aqueous solution of **DA_{LAla}** (1.0 wt.%, 15.3 mM) **a** before irradiation (white arrows: diameter of nanofibres and yellow arrows: helical pitch length). **b** After white light irradiation for 60 min (yellow arrows: shortened nanofibres and black arrows: micelles).

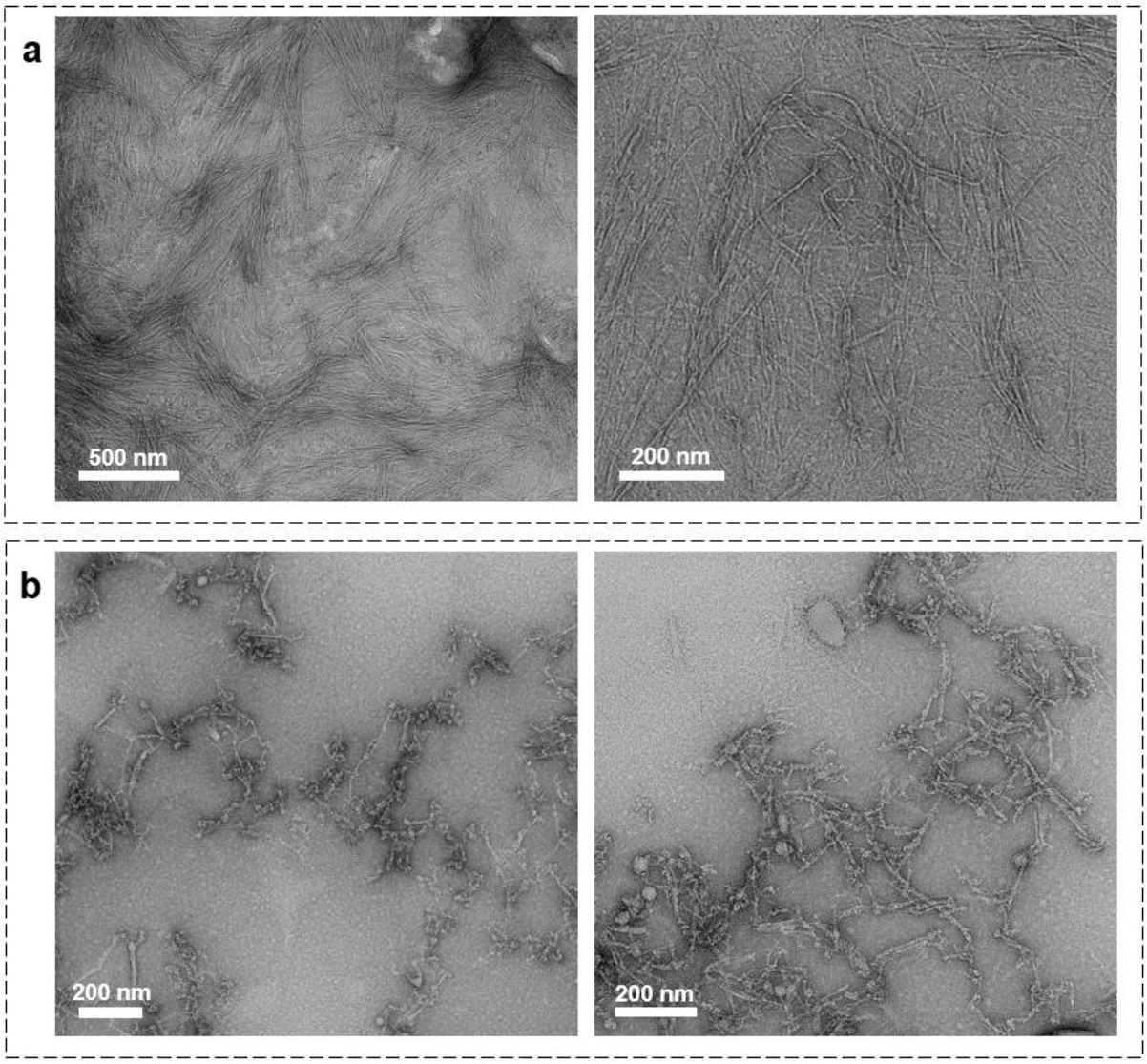

Supplementary Fig. 16 | TEM images of DA_{LVal} in aqueous solution. Representative of TEM images of **DA_{LVal}** (0.25 wt. %, 3.67 mM) **a** before and **b** after white light irradiation for 60 min.

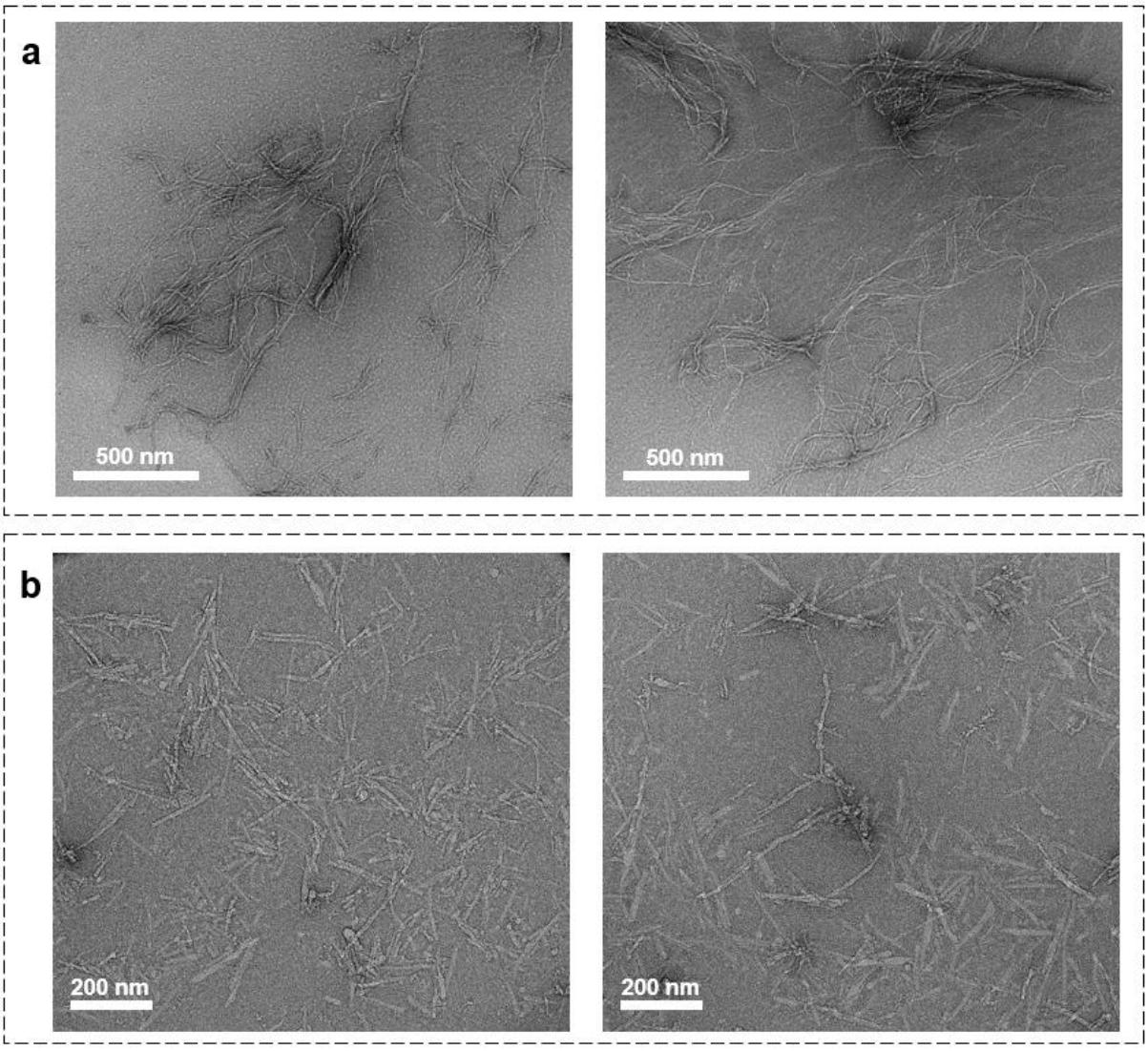

Supplementary Fig. 17 | TEM images of DA_{LAla} in aqueous solution. Representative of TEM images of **DA_{LAla}** (0.25 wt. %, 3.83 mM) **a** before irradiation and **b** after white light irradiation for 60 min.

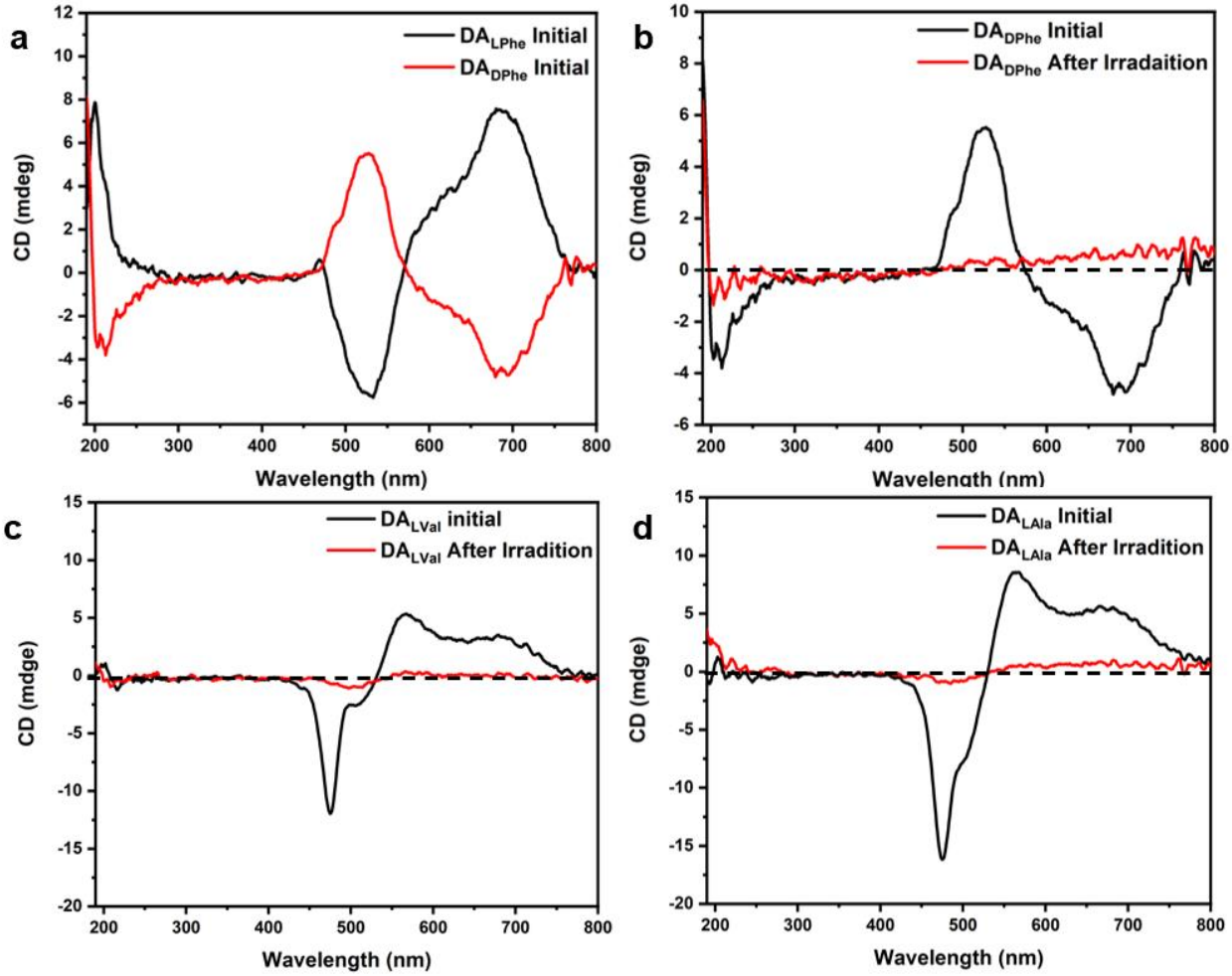

Supplementary Fig. 18 | Circular dichroism of DA$_A$ in aqueous solution. a Complementary circular dichroism spectrum of **DA$_{DPhe}$ and DA$_{LPhe}$** in aqueous solution before photoirradiation. **b** Circular dichroism spectra of the aqueous solution of **DA$_{DPhe}$** (50 μM, black-line) and after white-light irradiation for 60 min (red-line). **c** Circular dichroism spectra of the aqueous solution of **DA$_{LVal}$** (50 μM, black-line) and after white-light irradiation for 60 min (red-line). **d** Circular dichroism spectra of the aqueous solution of **DA$_{LAla}$** (50 μM, black-line) and after white-light irradiation for 60 min (red-line).

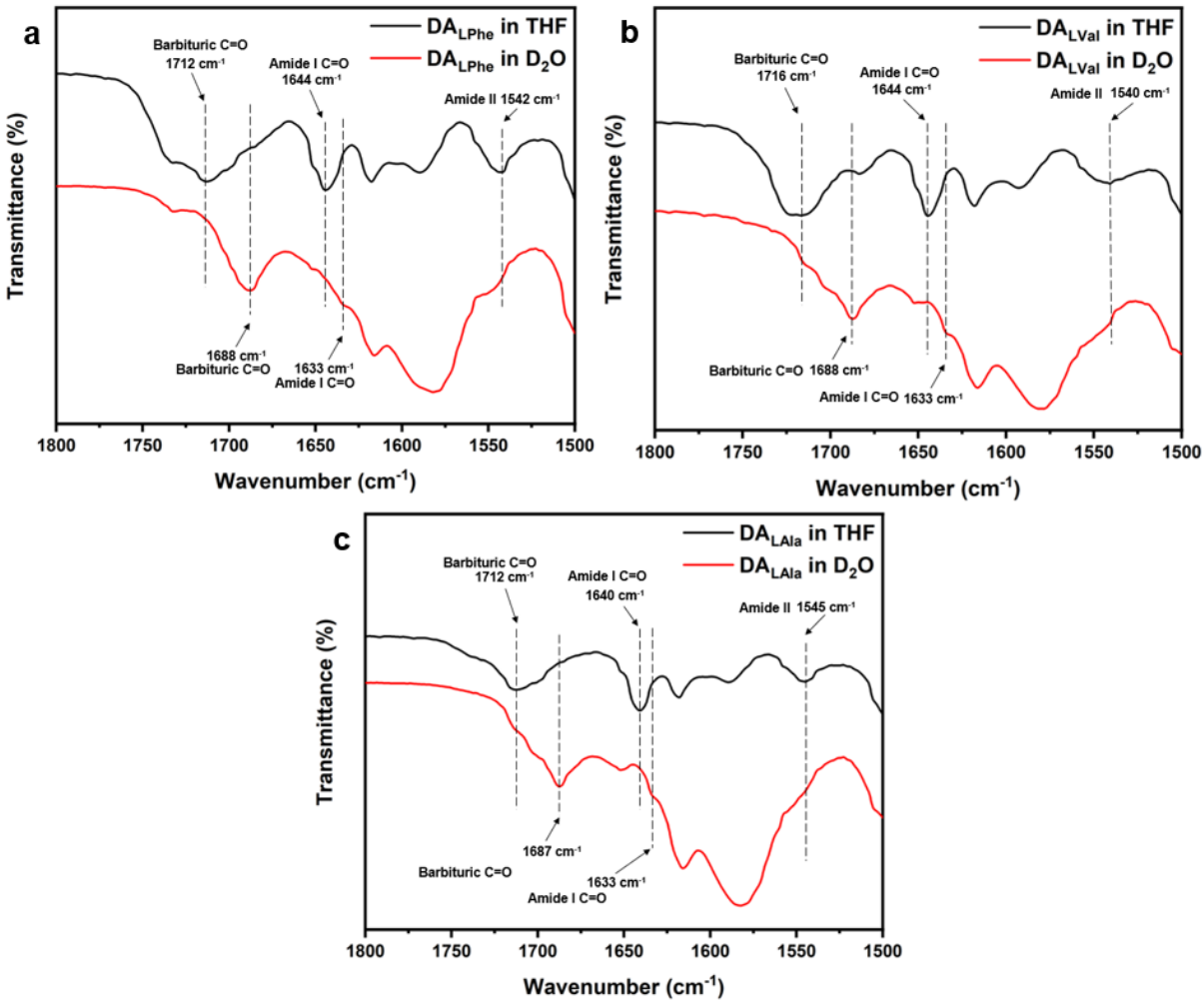

Supplementary Fig. 19 | FTIR of DA_A in organic and aqueous solution. Partial FTIR spectra of **a** $\mathbf{DA_{LPhe}}$ in THF and D_2O (8 wt.%), **b** $\mathbf{DA_{LVal}}$ in THF and D_2O (8 wt.%) and **c** $\mathbf{DA_{LAla}}$ in THF and D_2O (8 wt.%), recorded at 20 °C.

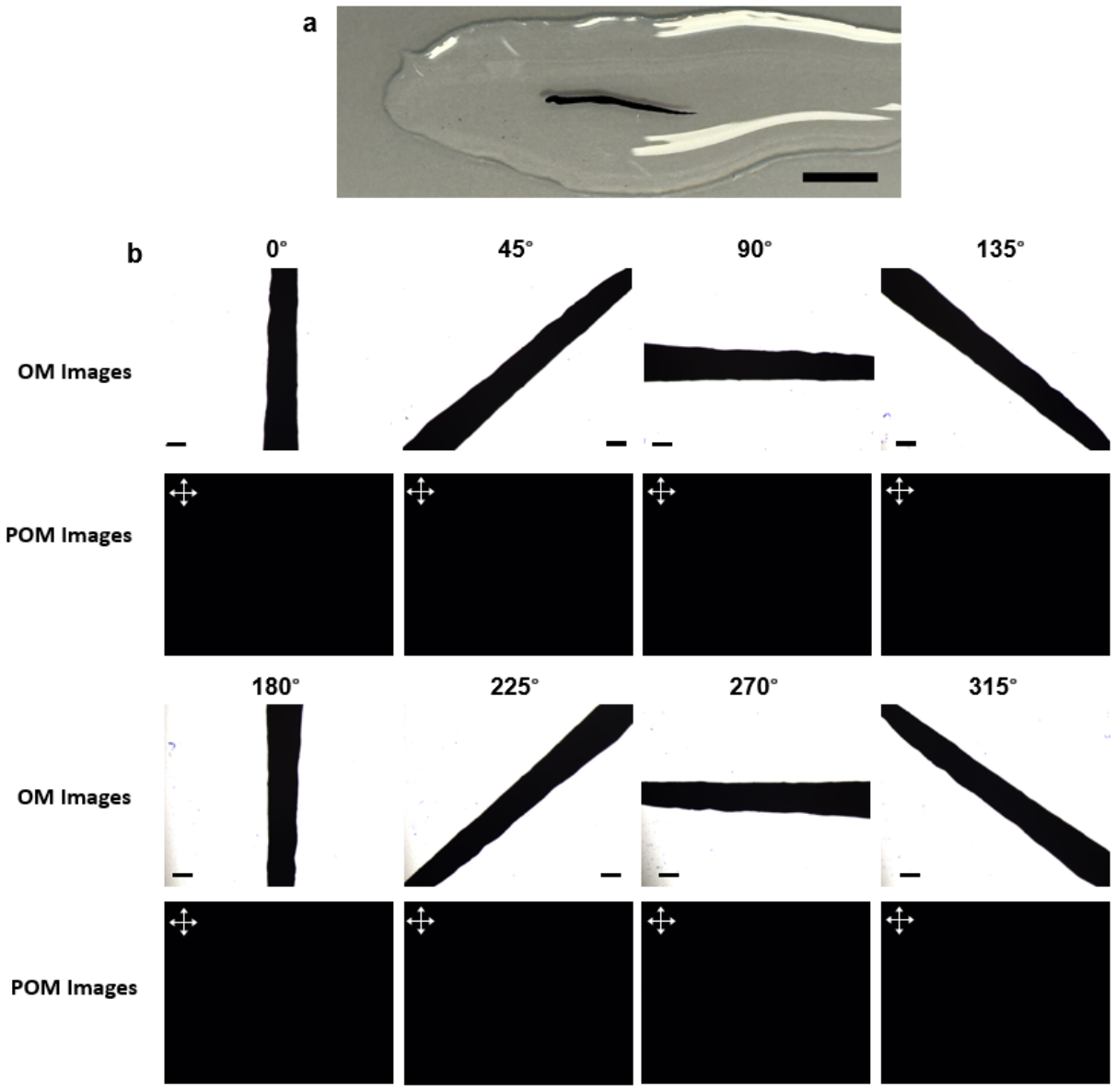

Supplementary Fig. 20 | Fabrication of macroscopic soft scaffold of DA_{LPhe} and optical microscopic images of a macroscopic soft scaffold of DA_{LPhe} under crossed polarisers. a Snapshot of a macroscopic soft scaffold of **DA_{LPhe}** (5.0 wt.%) prepared from an aqueous solution of $CaCl_2$ (150 mM), Scale bar 0.5 cm. **b** Optical microscopic images of a macroscopic soft scaffold of **DA_{LPhe}** (5.0 wt.%) prepared from a solution of $CaCl_2$ (150 mM) under crossed polarisers. The POM and OM images of the soft scaffold were tilted at 0°, 45°, 90°, 135°, 180°, 225°, 270° and 315° relative to the transmission axis of the analyser. Scale bar 200 μm for all panels.

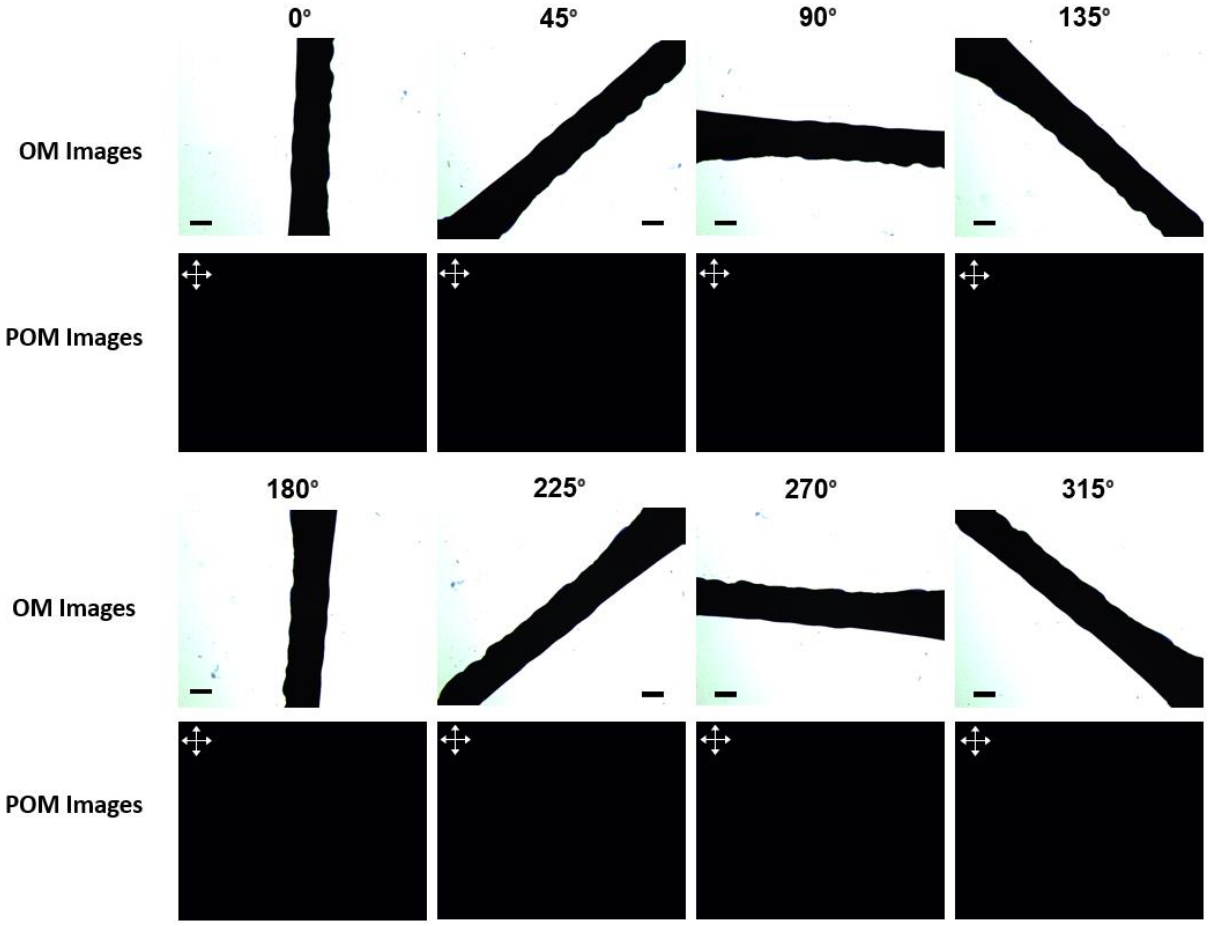

Supplementary Fig. 21 | Optical microscopic images of a macroscopic soft scaffold of DA_{LVal} under crossed polarisers. Optical microscopic images of a macroscopic soft scaffold of **DA_{LVal}** (5.0 wt.%) prepared from a solution of $CaCl_2$ (150 mM) under crossed polarisers. The POM and OM images of the soft scaffold were tilted at 0°, 45°, 90°, 135°, 180°, 225°, 270° and 315° relative to the transmission axis of the analyser. Scale bar 200 μm for all panels.

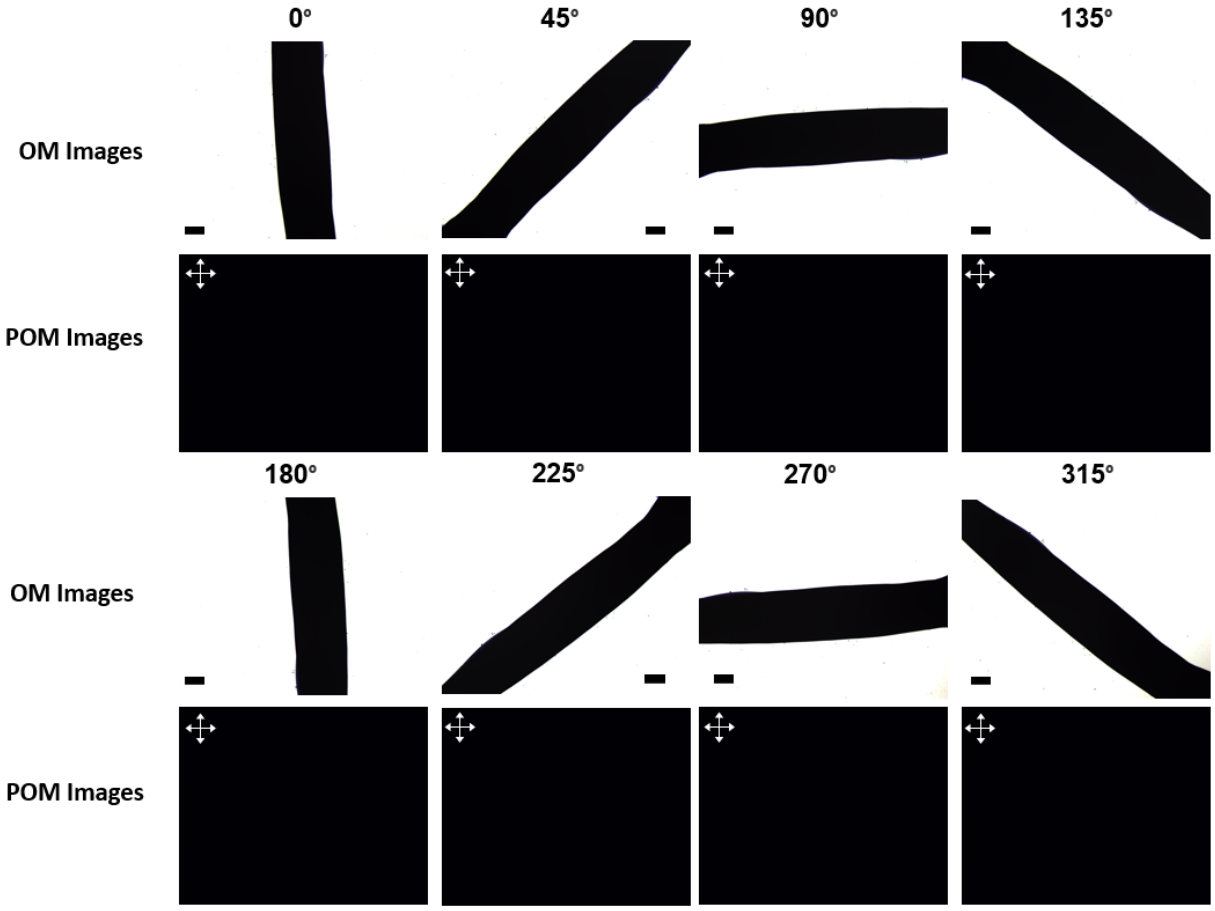

Supplementary Fig. 22 | Optical microscopic images of a macroscopic soft scaffold of DA_{LAla} under crossed polarisers. Optical microscopic images of a macroscopic soft scaffold of **DA_{LAla}** (5.0 wt.%) prepared from a solution of $CaCl_2$ (150 mM) under crossed polarisers. The POM and OM images of the soft scaffold were tilted at 0°, 45°, 90°, 135°, 180°, 225°, 270° and 315° relative to the transmission axis of the analyser. Scale bar 200 μm for all panels.

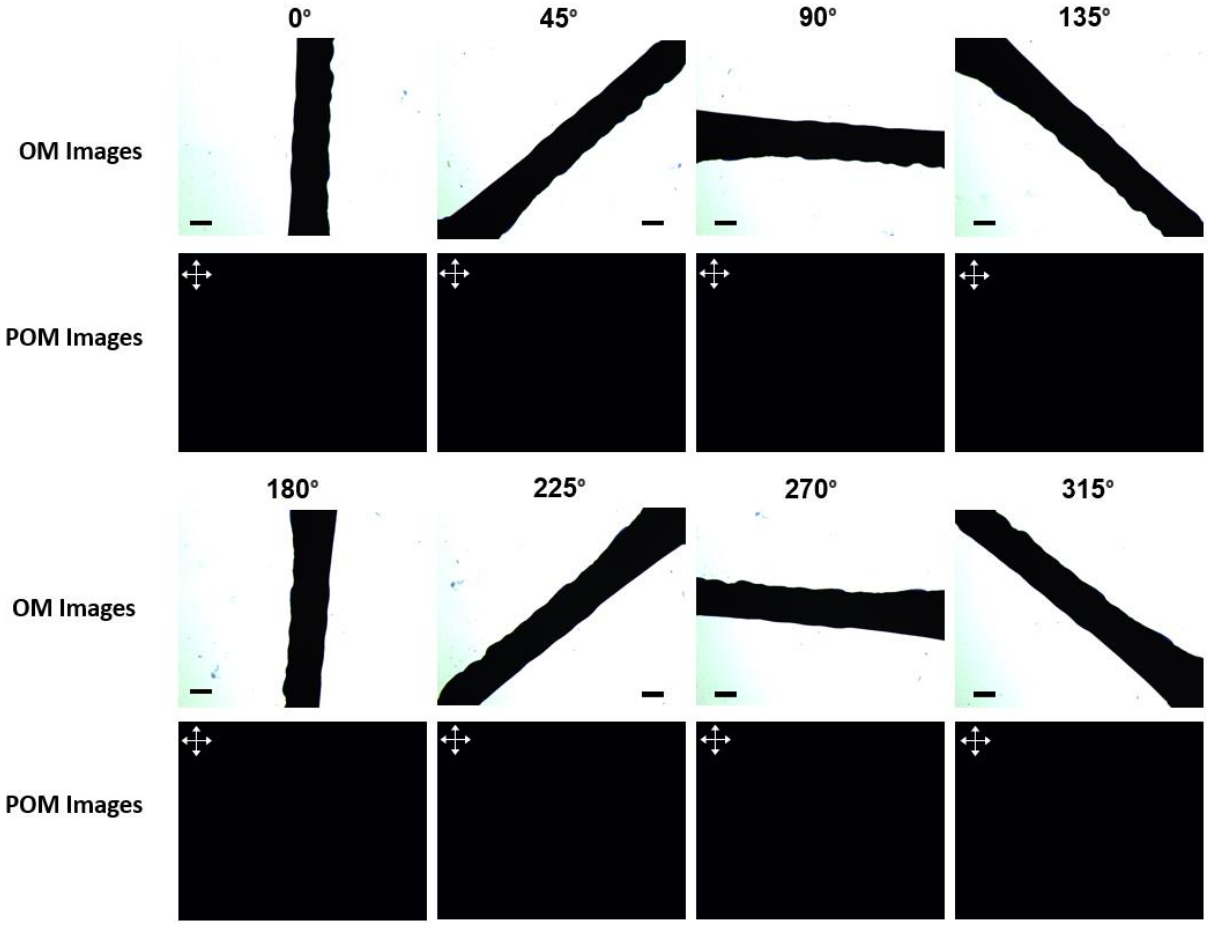

Supplementary Fig. 23 | Optical microscopic images of a macroscopic soft scaffold of DA_{DPhe} under crossed polarisers. Optical microscopic images of a macroscopic soft scaffold of **DA_{DPhe}** (5.0 wt.%) prepared from a solution of $CaCl_2$ (150 mM) under crossed polarisers. The POM and OM images of the soft scaffold were tilted at 0°, 45°, 90°, 135°, 180°, 225°, 270° and 315° relative to the transmission axis of the analyser. Scale bar 200 μm for all panels.

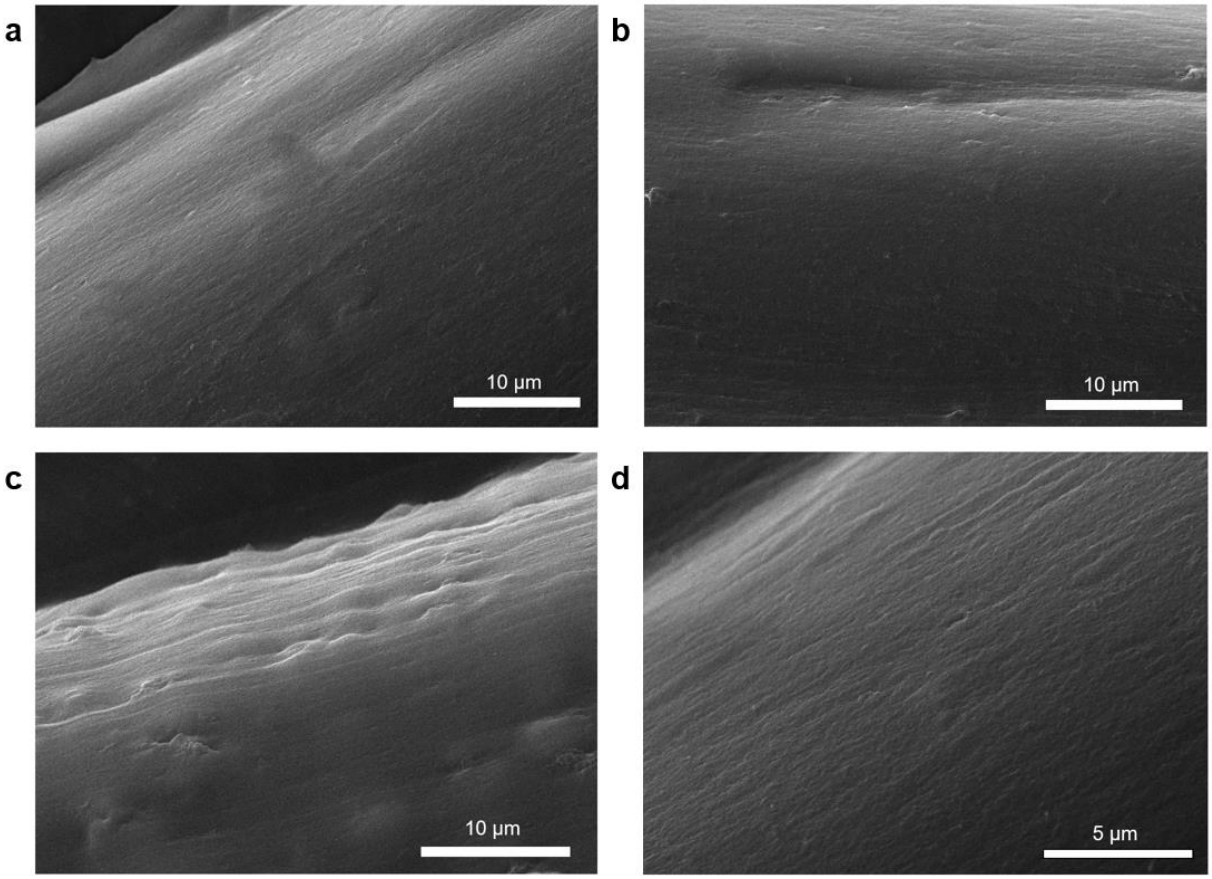

Supplementary Fig. 24 | SEM images of macroscopic soft scaffold of DA_A. Scanning electron microscopy images of an air-dried macroscopic soft scaffold of **a** DA_{LPhe}, **b** DA_{LVal}, **c** DA_{LAla} and **d** DA_{DPhe} (5.0 wt.%).

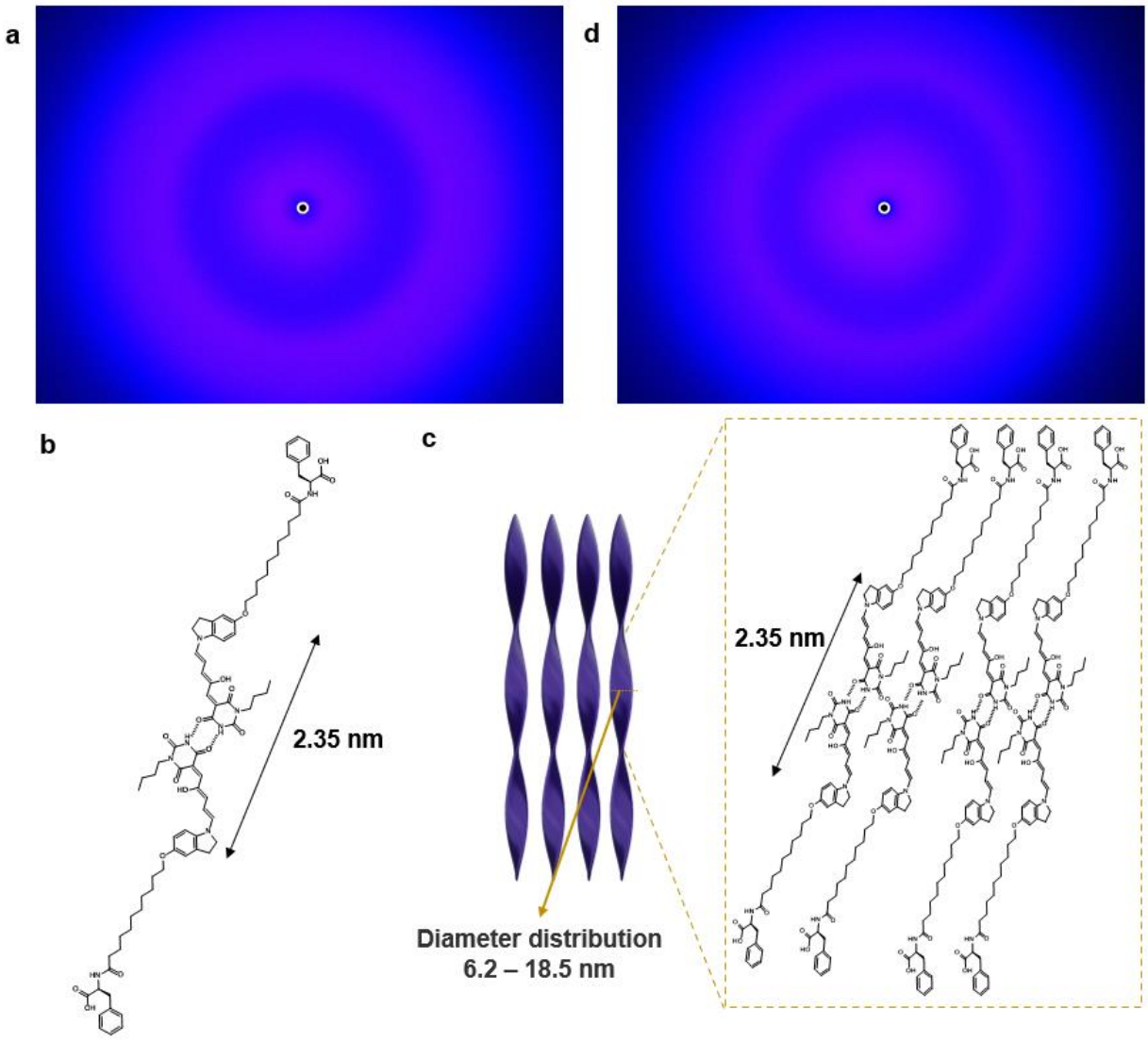

Supplementary Fig. 25 | WAXD image of a macroscopic soft scaffold of DA_{LPhe} and schematic illustration of supramolecular packing. a 2D-WAXD image of a macroscopic soft scaffold of **DA_{LPhe}** (5.0 wt.%, 68.6 mM) before irradiation **b** Schematic illustration of supramolecular assembled **DA_{LPhe}** in a dimeric form leads to diffraction in WAXD of the macroscopic soft scaffold. **c** Schematic illustration of **DA_{LPhe}** due to slightly twisted π-π packing of the phenyl-groups of phenylalanines within the pre-defined out-of-plane intermolecular distance **d** 2D-WAXD image of a macroscopic soft scaffold of **DA_{LPhe}** (5.0 wt.%, 68.6 mM) after red-laser irradiation for 120 min (0.2W, 650 nm).

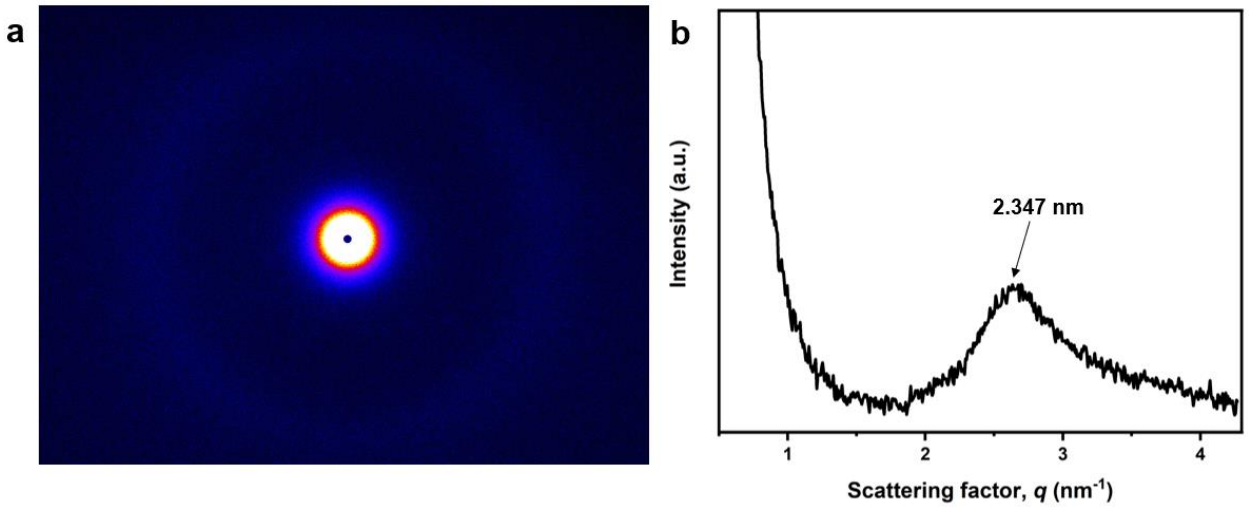

Supplementary Fig. 26 | SAXS image of a macroscopic soft scaffold of DA_{LPhe}. a 2D-SAXS image of a macroscopic soft scaffold of $\mathbf{DA_{LPhe}}$ (5.0 wt.%, 68.6 mM) before irradiation. **b** Converted 1D-SAXS profile from 2D-SAXS image of macroscopic soft scaffold of $\mathbf{DA_{LPhe}}$ in **a**.

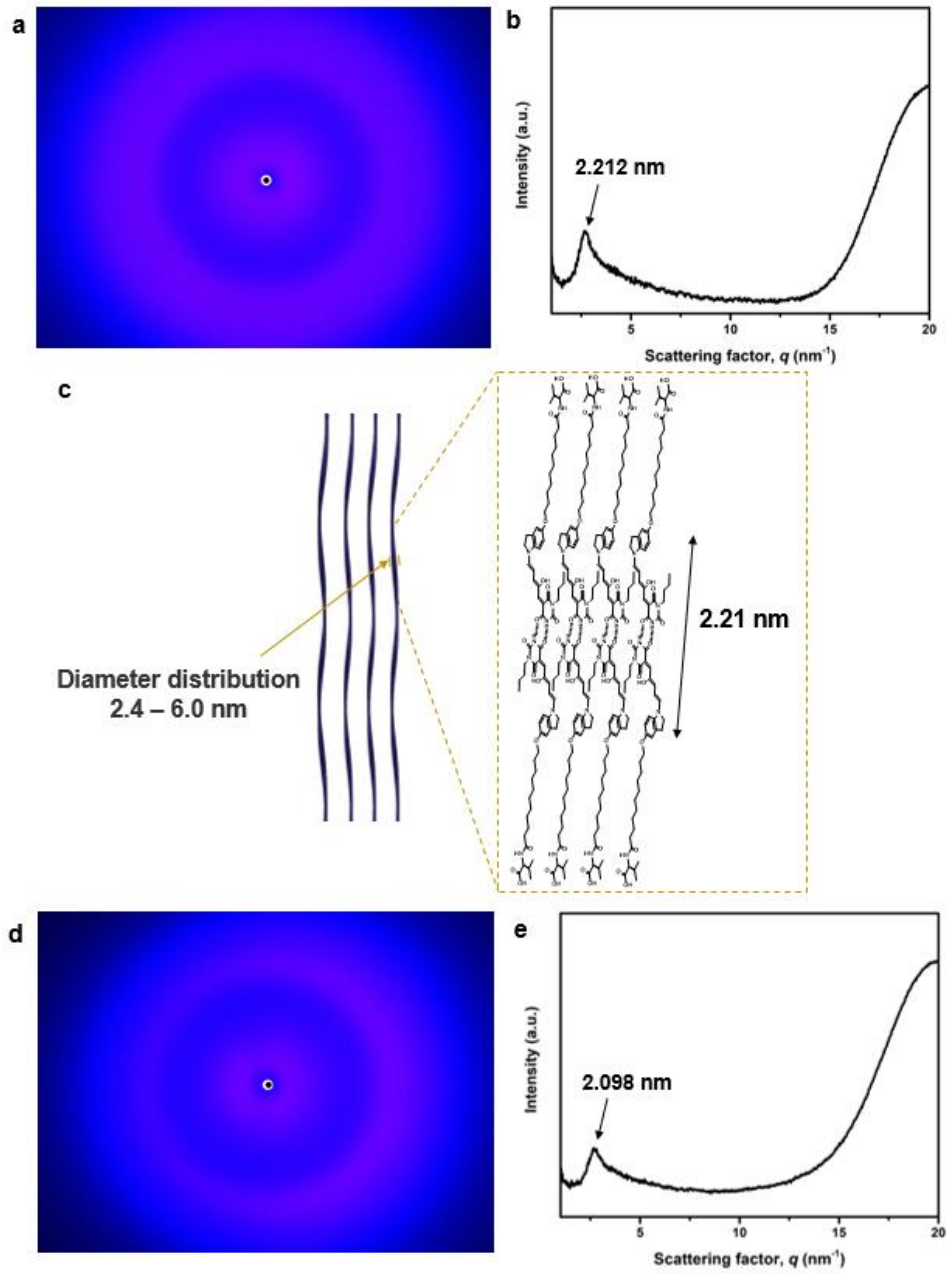

Supplementary Fig. 27 | WAXD image of a macroscopic soft scaffold of DA_{LVal} and schematic illustration of supramolecular packing. a 2D-WAXD image of a macroscopic soft scaffold of **DA_{LVal}** (5.0 wt.%, 73.4 mM) before irradiation. **b** Converted 1D-WAXD profile from 2D-WAXD image of macroscopic soft scaffold of **DA_{LVal}** in **a**. **c** Schematic illustration of supramolecular assembled **DA_{LVal}** in a dimeric form leads to diffraction in WAXD of the macroscopic soft scaffold and helical nanofibres diameters. **d** 2D-WAXD image of a macroscopic soft scaffold of **DA_{LVal}** (5.0 wt.%, 73.4 mM) after red-laser irradiation for 120 min (0.2W, 650 nm). **e** Converted 1D-WAXD profile from 2D-WAXD image of macroscopic soft scaffold of **DA_{LVal}** in **d**.

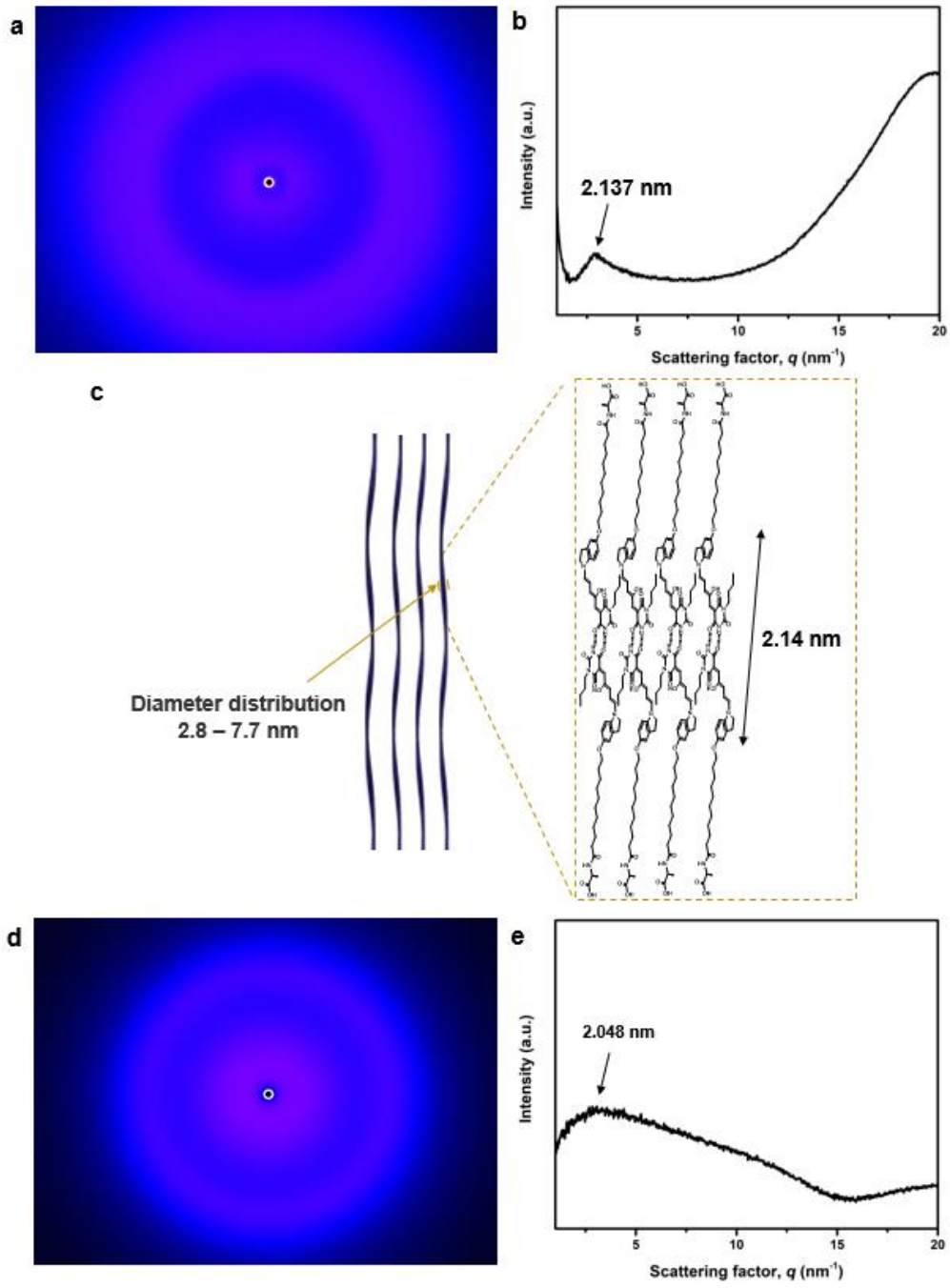

Supplementary Fig. 28 | WAXD image of a macroscopic soft scaffold of DA_{LAla} and schematic illustration of supramolecular packing. a 2D-WAXD image of a macroscopic soft scaffold of **DA_{LAla}** (5.0 wt.%, 76.6 mM) before irradiation. **b** Converted 1D-WAXD profile from 2D-WAXD image of macroscopic soft scaffold of **DA_{LAla}** in **a**. **c** Schematic illustration of supramolecular assembled **DA_{LAla}** in a dimeric form leads to diffraction in WAXD of the macroscopic soft scaffold and helical nanofibres diameters. **d** 2D-WAXD image of a macroscopic soft scaffold of **DA_{LAla}** (5.0 wt.%, 76.6 mM) after red-laser irradiation. **e** Converted 1D-WAXD profile from 2D-WAXD image of macroscopic soft scaffold of **DA_{LAla}** in **d**.

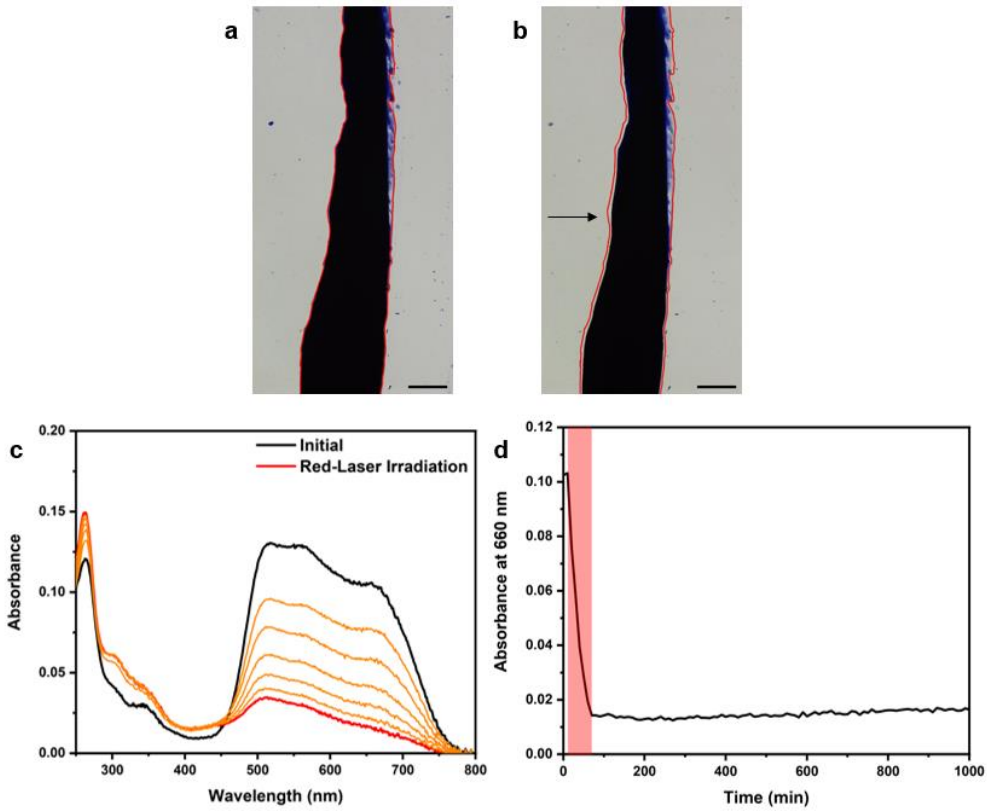

Supplementary Fig. 29 | Photoirradiation of a macroscopic soft scaffold of DA_{LPhe} and photoisomerisation of DA_{LPhe} in aqueous solution with red-laser. a Snapshot of a macroscopic soft scaffold of **DA_{LPhe}** (5.0 wt.%, 68.6 mM) before and **b** after 60 min white-light irradiation. (Black arrow indicates the irradiation position) Scale bar 200 μm for all panels. **c** UV-vis absorption spectra of **DA_{LPhe}** in aqueous solution (50 μM) before irradiation (black-line), upon red-laser irradiation over 60 min (orange-line) and after red-laser irradiation for 60 min (red-line). **d** Time-course of the red-laser irradiation of an aqueous solution of **DA_{LPhe}**, monitored at 660 nm (black-line). Photoirradiation of UV-vis sample was carried out at 20 °C using a red-laser (650 nm, 0.2 W) positioned at a distance of 1.0 cm from the sample.

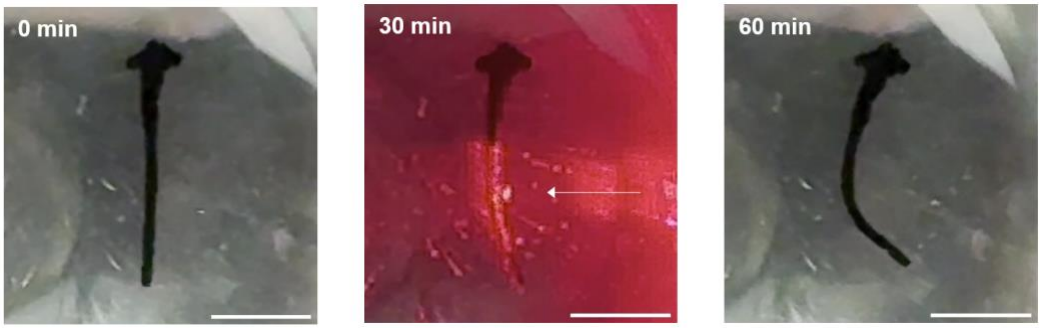

Supplementary Fig. 30 | Photoactuation of a macroscopic soft scaffold of DA_{DPhe} in aqueous solution. Snapshots of macroscopic soft scaffold of **DA_{DPhe}** (3.0 wt.%, 41.2 mM) in $CaCl_2$ solution (150 mM) before and after irradiated over 60 min with 650 nm light source from right side. White arrows indicate the irradiation direction and scale bars for all panels: 0.5 cm.

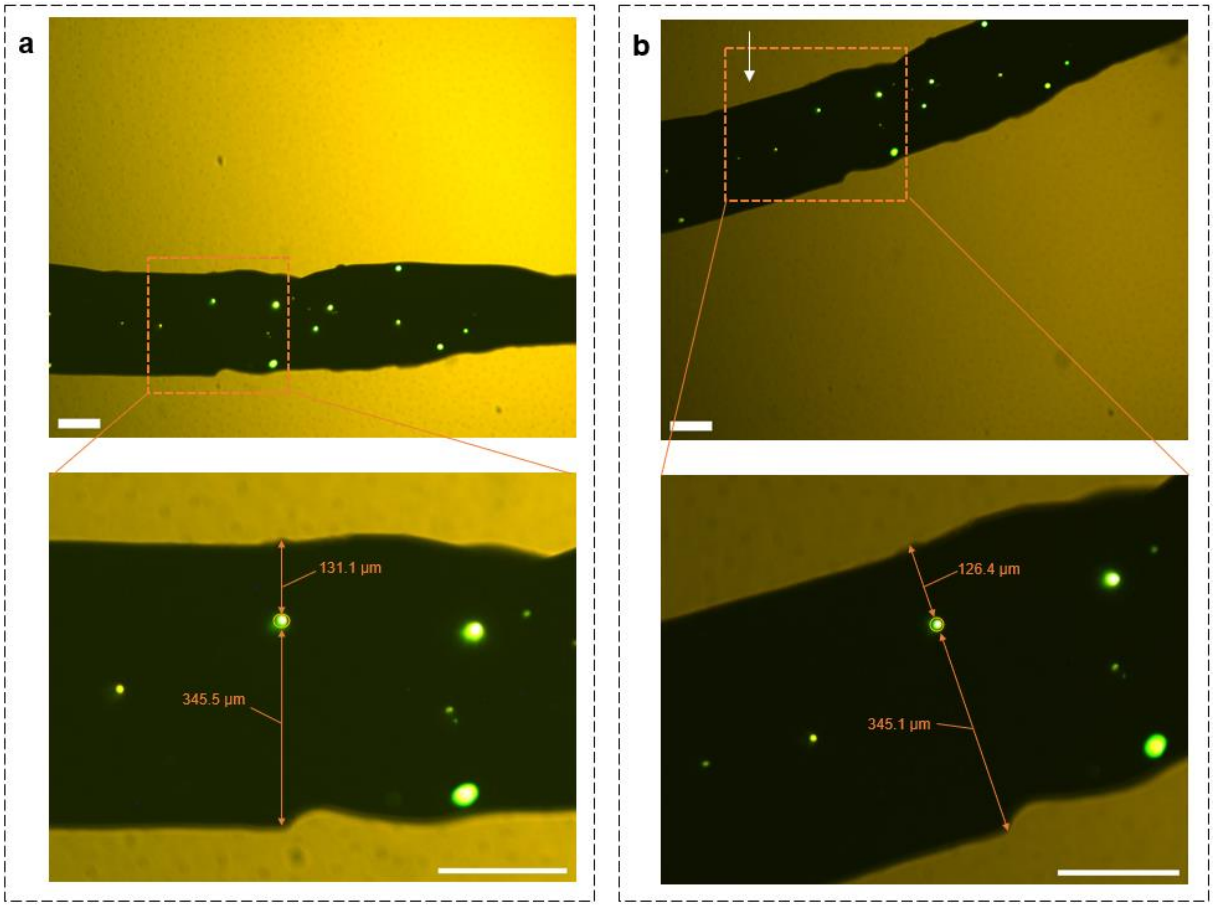

Supplementary Fig. 31 | Photoactuation of microbeads encapsulated macroscopic soft scaffold of DA_{LPhe} in aqueous solution. a Snapshots of a microbeads encapsulated (FluoSpheres™ Polystyrene Microspheres, Invitrogen™) macroscopic soft scaffold of **DA_{LPhe}** (3.0 wt.%, 41.2 mM) in $CaCl_2$ (150 mM) before irradiation and enlarged selected area. **b** After red laser irradiation to the macroscopic soft scaffold for 70 s and enlarged selected area. Direction of photoirradiation is indicated by the white arrow. Scale bar is 200 μm for all panels.

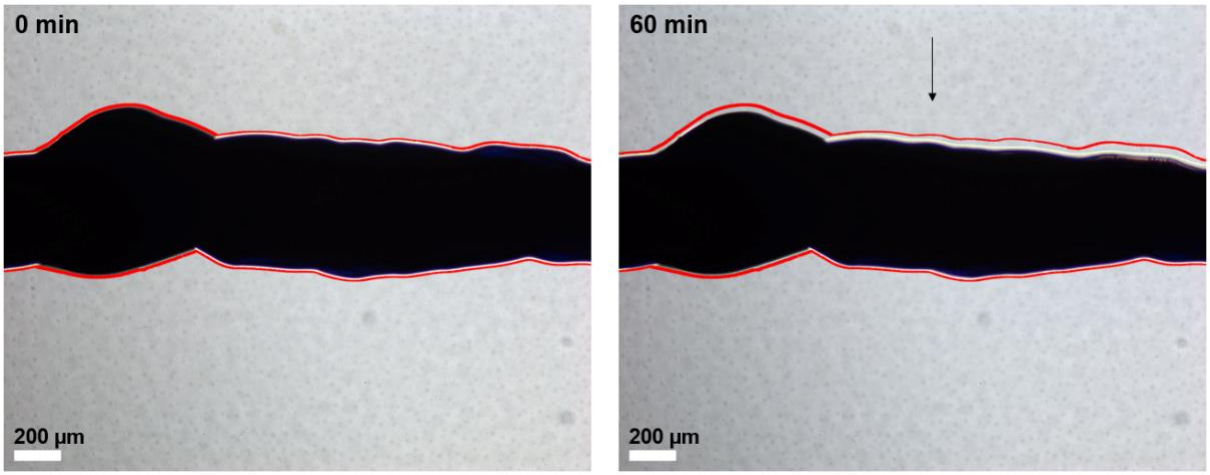

Supplementary Fig. 32 | Photoirradiation of a macroscopic soft scaffold of DA_{LPhe} in *n*-dodecane solution. Snapshots of macroscopic soft scaffold of **DA_{LPhe}** (3.0 wt.%) immersed in *n*-dodecane solution. The macroscopic soft scaffold of **DA_{LPhe}** was applied red laser irradiation over 60 min. Direction of the irradiation is indicated by the black arrow. Scale bar is 200 μm for all panels.

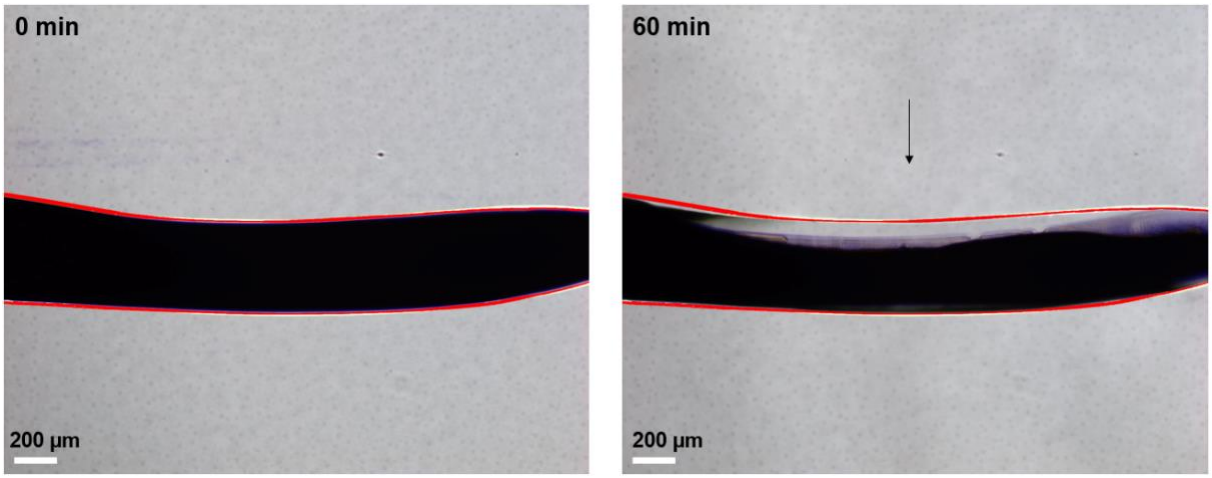

Supplementary Fig. 33 | Photoirradiation of a macroscopic soft scaffold of DA_{LVal} in *n*-dodecane solution. Snapshots of macroscopic soft scaffold of **DA_{LVal}** (3.0 wt.%) immersed in *n*-dodecane solution. The macroscopic soft scaffold of **DA_{LVal}** was applied red laser irradiation over 60 min. Direction of the irradiation is indicated by the black arrow. Scale bar is 200 μm for all panels.

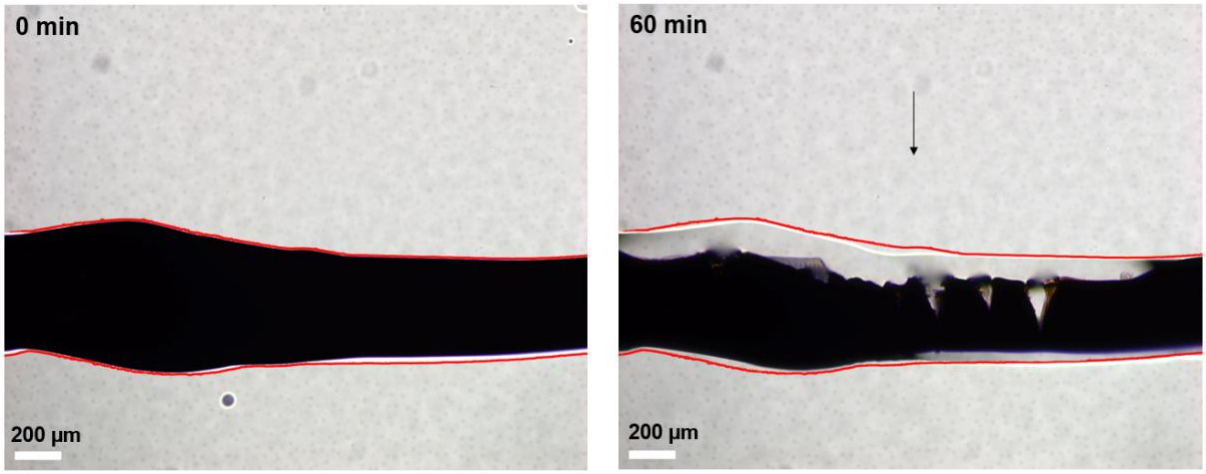

Supplementary Fig. 34 | Photoirradiation of a macroscopic soft scaffold of DA_{LAla} in *n*-dodecane solution. Snapshots of macroscopic soft scaffold of **DA_{LAla}** (3.0 wt.%) immersed in *n*-dodecane solution. The macroscopic soft scaffold of **DA_{LAla}** was applied red laser irradiation over 60 min. Direction of the irradiation is indicated by the black arrow. Scale bar is 200 μm for all panels.

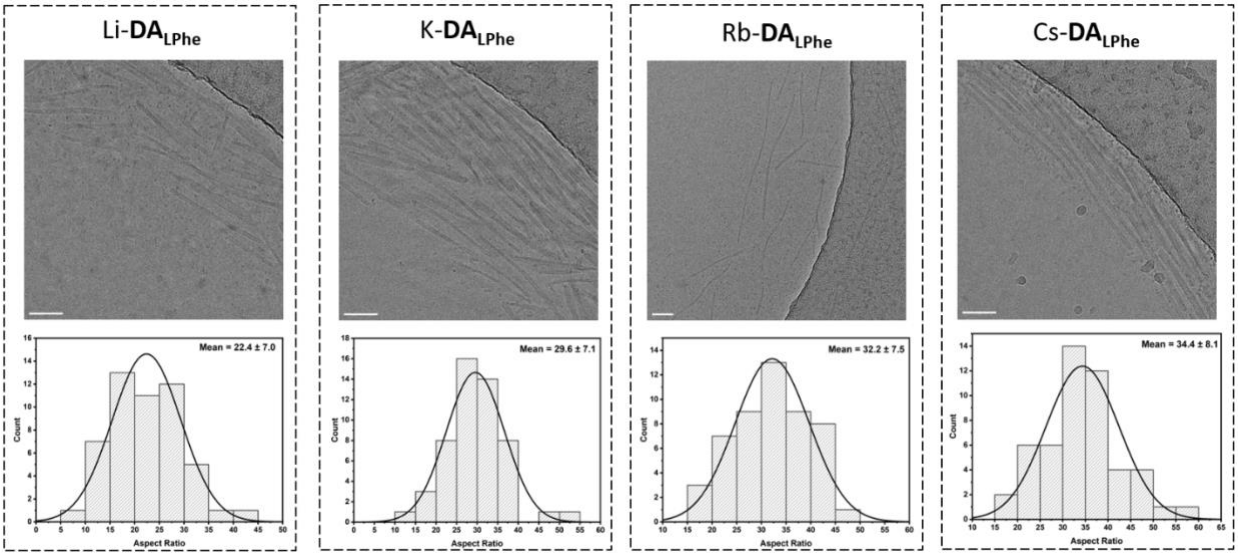

Supplementary Fig. 35 | Cryo-TEM images of M-DA_{LPhe} in aqueous solution and corresponding aspect-ratio histogram profile. Representative of cryo-TEM images and histogram of aspect-ratio distribution of **M-DA_{LPhe}** (1.0 wt.%, 13.7 mM). Scale bar is 50 nm for all panels.

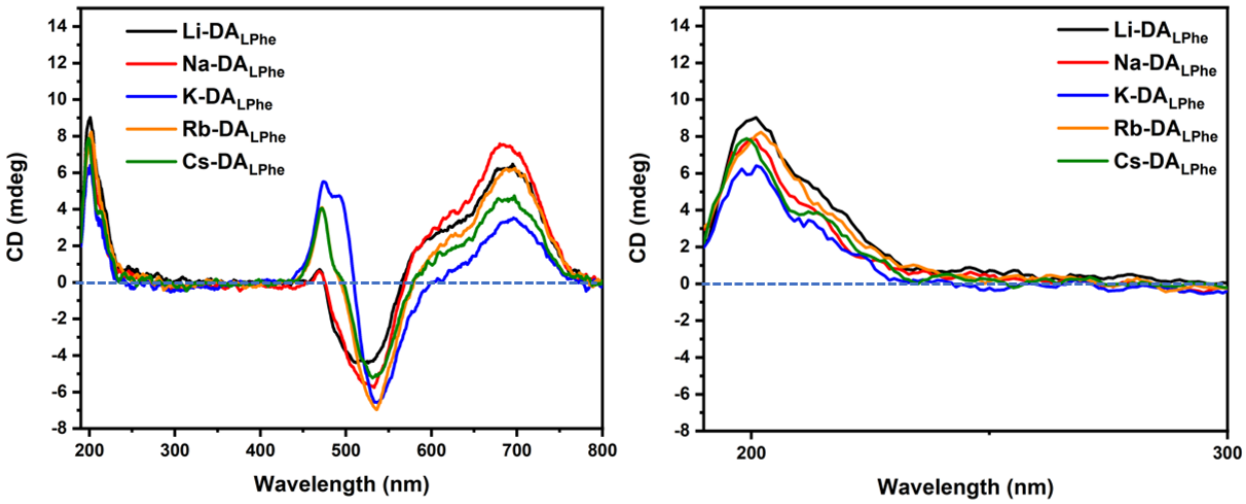

Supplementary Fig. 36 | Circular dichroism of M-DA$_{LPhe}$ in aqueous solution. Circular dichroism spectra of the aqueous solution of M-**DA$_{LPhe}$** (50 μM) and enlarged circular dichroism spectra at 190 – 250 nm wavelength.

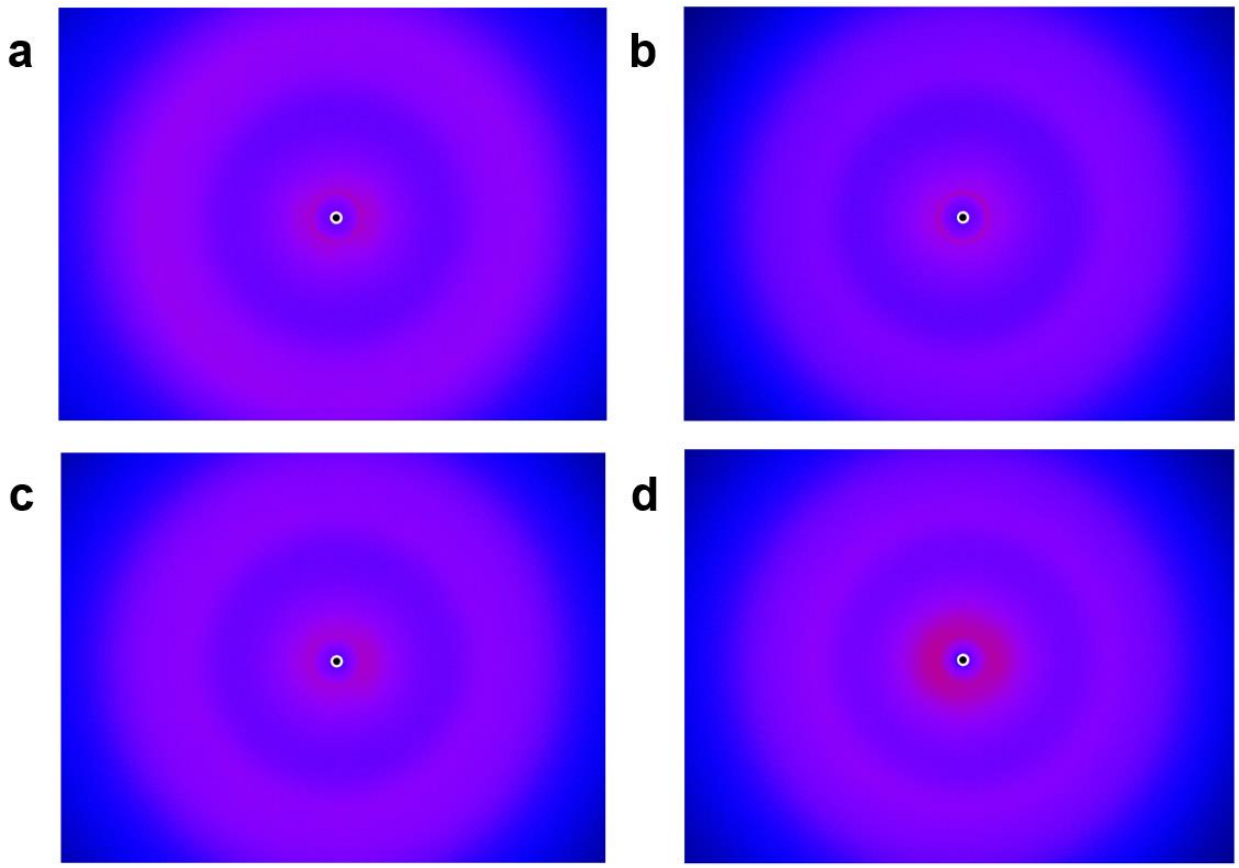

Supplementary Fig. 37 | 2D-WAXD image of a macroscopic soft scaffold of M-DA$_{LPhe}$. 2D-WAXD images of a macroscopic soft scaffold of **a** Li-**DA$_{Phe}$**, **b** K-**DA$_{Phe}$**, **c** Rb-**DA$_{Phe}$**, and **d** Cs-**DA$_{Phe}$** (5.0 wt.%, 73.4 mM) before irradiation.

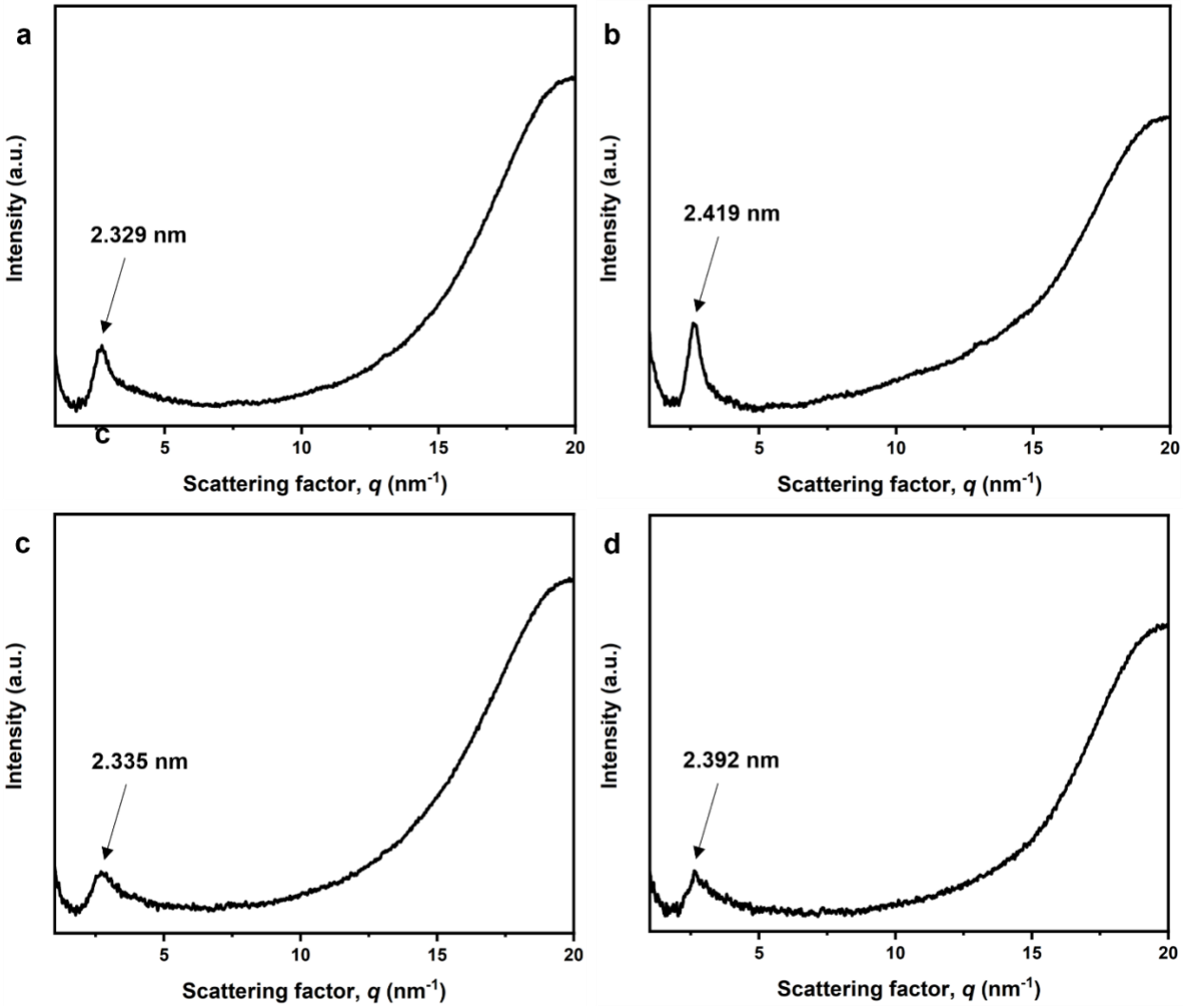

Supplementary Fig. 38 | 1D-WAXD profile of a macroscopic soft scaffold of M-DA$_{LPhe}$. Corresponding converted 1D-WAXD profiles of a macroscopic soft scaffold of **a** Li-**DA$_{Phe}$**, **b** K-**DA$_{Phe}$**, **c** Rb-**DA$_{Phe}$**, and **d** Cs-**DA$_{Phe}$** (5.0 wt.%, 73.4 mM) before irradiation.

M-DA_{LPhe}	Length (nm)	Width (nm)
Li-DA_{LPhe}	147.10 ± 41.61	6.80 ± 1.57
Na-DA_{LPhe}	147.47 ± 37.57	6.21 ±1.30
K-DA_{LPhe}	206.96 ± 51.22	7.16 ± 1.63
Rb-DA_{LPhe}	196.77 ± 60.65	6.04 ± 1.07
Cs-DA_{LPhe}	222.15 ± 55.39	6.55 ±0.95

Supplementary Table 1 | Length and width distribution of M-DA_{LPhe} measured from cryo-TEM images. The length and width distribution from corresponding cryo-TEM images with 50 numbers of nanoribbons of M-**DA_{LPhe}** (1.0 wt.% 13.7 mM).

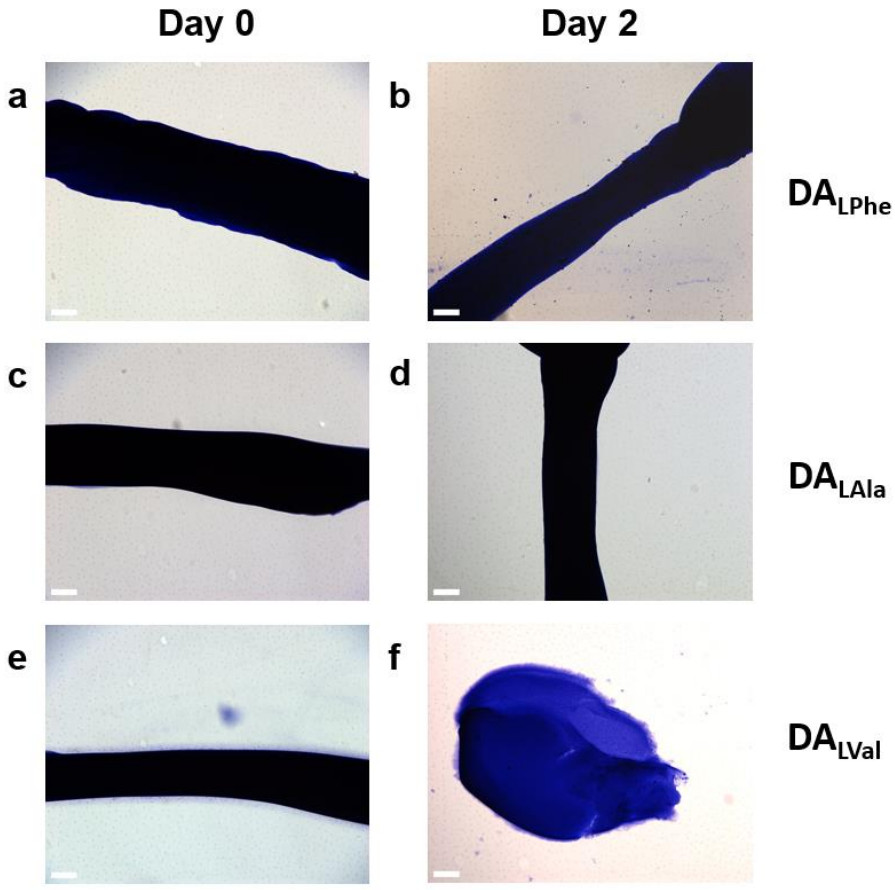

Supplementary Fig. 39 | Stability of macroscopic soft scaffolds of DA_A in 10% FBS medium over 2 days incubation. Snapshots of macroscopic soft scaffolds of **DA_{LPhe}** (3.0 wt.%), **DA_{LVal}** (3.0 wt.%) and **DA_{LAla}** (3.0 wt.%) were immersed in 10% FBS medium over 2 days of incubation at 37°C and 5% CO_2. Scale bar is 200 μm for all panels.

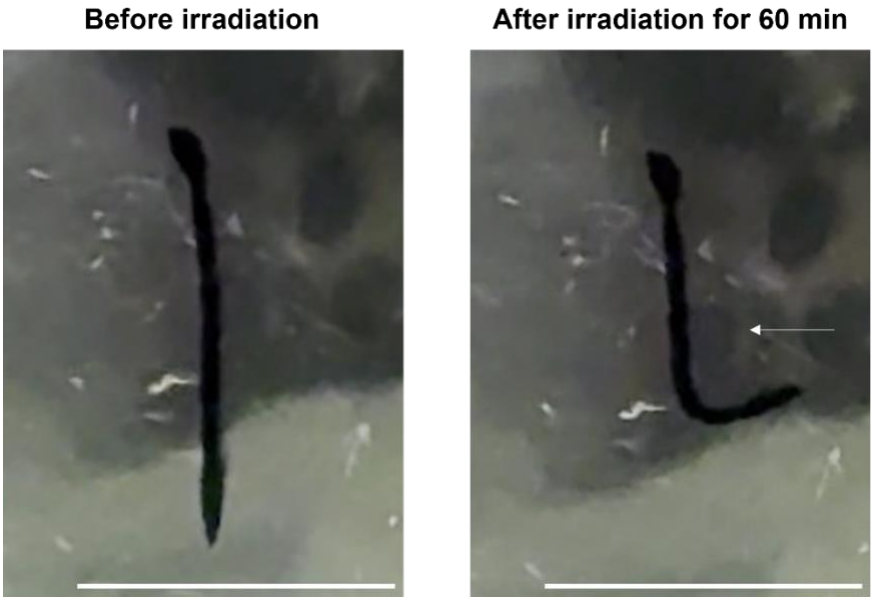

Supplementary Fig. 40 | Photoactuation of macroscopic soft scaffolds of DA_{LAla} after 10% FBS medium incubation over 2 days. Snapshots of before and after 60 min red-laser irradiation (0.2 W, 650 nm) of macroscopic soft scaffold of **DA_{LAla}** (3.0 wt.%) after 10% FBS medium incubation over 2 days. White arrow indicates photoirradiation position. Scale bar is 0.5 cm for all panels.

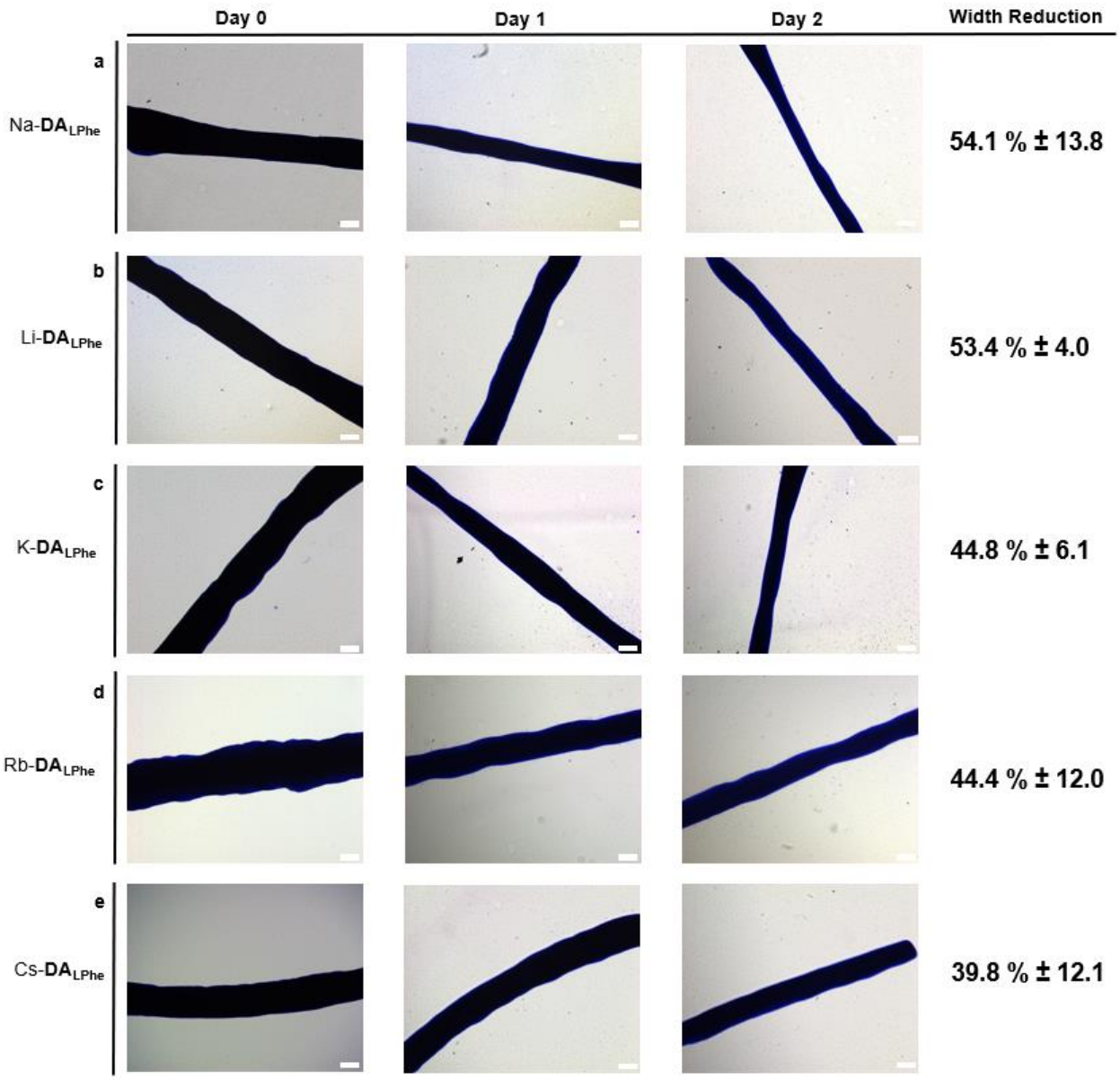

Supplementary Fig. 41 | Stability study of macroscopic soft scaffolds of M-DA$_{LPhe}$ 20% FBS medium over 2 days incubation. Snapshots of representative macroscopic soft scaffold of **a** Na-**DA$_{LPhe}$ b** Li-**DA$_{LPhe}$ c** K-**DA$_{LPhe}$ d** Rb-**DA$_{LPhe}$ and e** Cs-**DA$_{LPhe}$** (3.0 wt.%) immersed in 20% FBS medium over 2 days incubation. The corresponding width reduction percentage were obtained by averaging five macroscopic soft scaffold's widths. Scale bar is 200 μm for all panels.

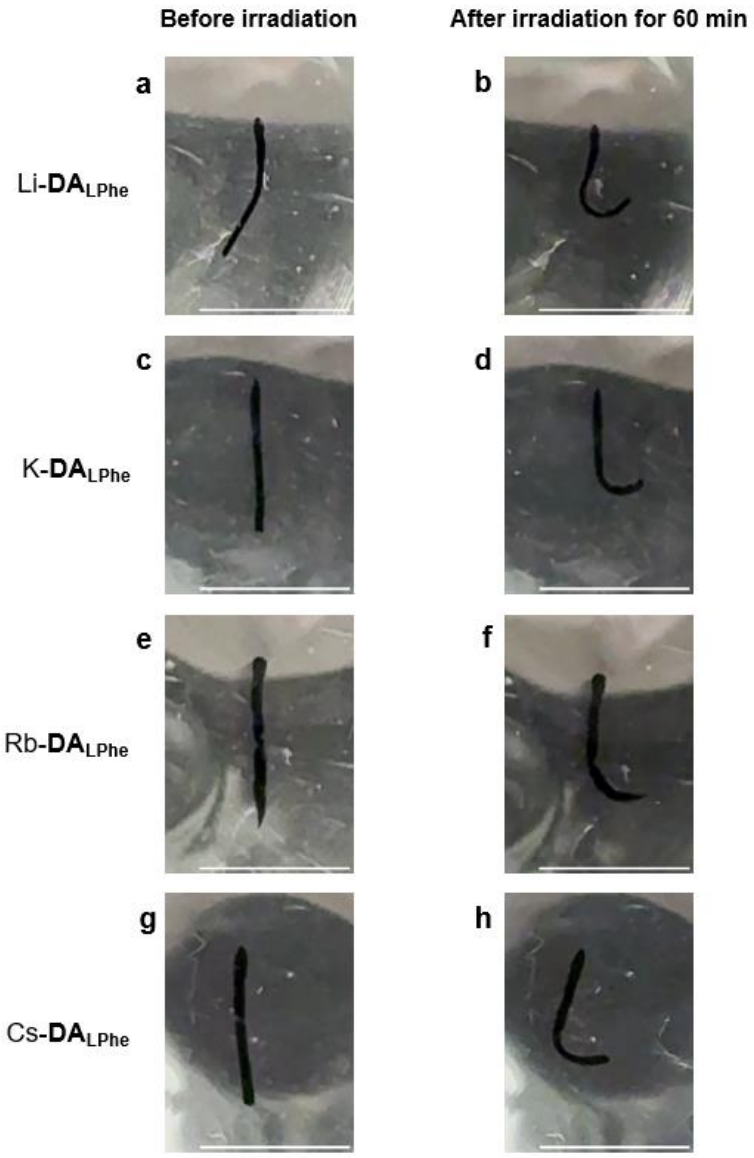

Supplementary Fig. 42 | Photoactuation of macroscopic soft scaffolds of M-DA$_{LPhe}$ after 10% FBS medium incubation over 2 days. The 10% FBS medium containing macroscopic soft scaffolds M-**DA$_{LPhe}$** were exchanged to $CaCl_2$ solution before performing actuation experiment. Snapshots of before irradiation of macroscopic soft scaffold of **a** Li-**DA$_{LPhe}$** **c** K-**DA$_{LPhe}$** **e** Rb-**DA$_{LPhe}$** **and g** Cs-**DA$_{LPhe}$** (3.0 wt.%) after 10% FBS medium incubation over 2 days. Snapshots of macroscopic soft scaffold of **b** Li-**DA$_{LPhe}$** **d** K-**DA$_{LPhe}$** **f** Rb-**DA$_{LPhe}$** **and h** Cs-**DA$_{LPhe}$** (3.0 wt.%) after 60 min red-laser irradiation (0.2 W, 650 nm). Scale bar is 0.5 cm for all panels.

M-$\mathbf{DA_{LPhe}}$	**Actuation Speed (°/min)**
Li-$\mathbf{DA_{LPhe}}$	1.62
Na-$\mathbf{DA_{LPhe}}$	1.73
K-$\mathbf{DA_{LPhe}}$	1.66
Rb-$\mathbf{DA_{LPhe}}$	1.53
Cs-$\mathbf{DA_{LPhe}}$	1.53

Supplementary Table 2 | Photo-induced actuation speed of macroscopic soft scaffolds of M-$\mathbf{DA_{LPhe}}$ after 2 days of 10% FBS medium incubation. The macroscopic soft scaffolds of M-$\mathbf{DA_{LPhe}}$ (3.0 wt.) were incubated in 10% FBS medium for 2 days. The 10% FBS medium containing macroscopic soft scaffolds M-$\mathbf{DA_{LPhe}}$ were exchanged to $CaCl_2$ solution before performing actuation experiment. All the macroscopic soft scaffolds were irradiated with red-laser for 60 min (0.2W, 650 nm).

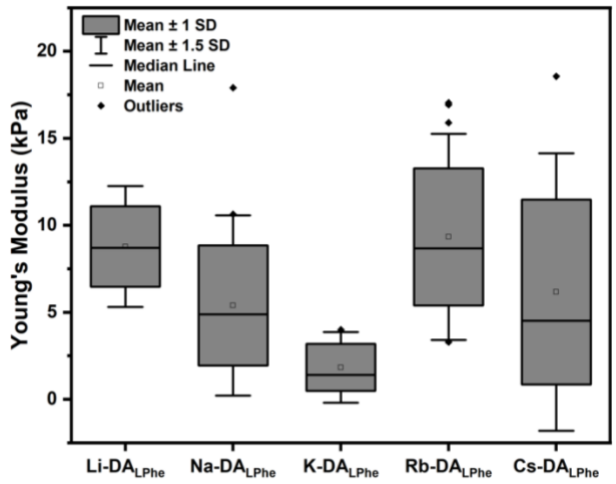

Supplementary Fig. 43 | Probing of Young's modulus of macroscopic soft scaffolds of M-$\mathbf{DA_{LPhe}}$ through AFM nanoindentation. Young's modulus values of macroscopic soft scaffolds of M-$\mathbf{DA_{LPhe}}$ (3.0 wt.%) without photoirradiation.

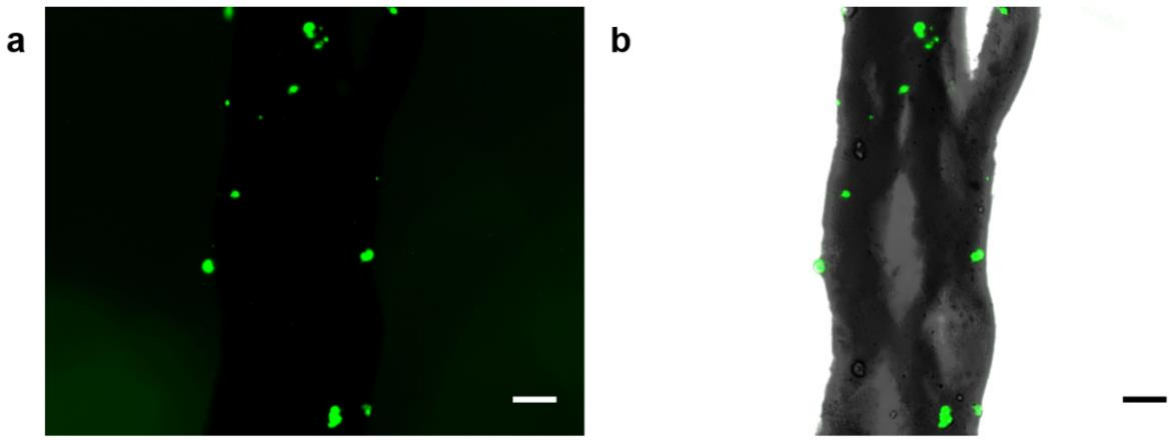

Supplementary Fig. 44 | Cell cultured macroscopic soft scaffold of Na-DA$_{LPhe}$ in 10% FBS medium for 1 day. Snapshot of **a** Calcein AM live cell staining and **b** merged with bright field of hMSCs cultured with macroscopic soft scaffold of **DA$_{LPhe}$** (3.0 wt.%) after 1 day of incubation in 10% FBS supplemented medium at 37 °C and 5% CO_2. Scale bar is 200 μm for all panels.

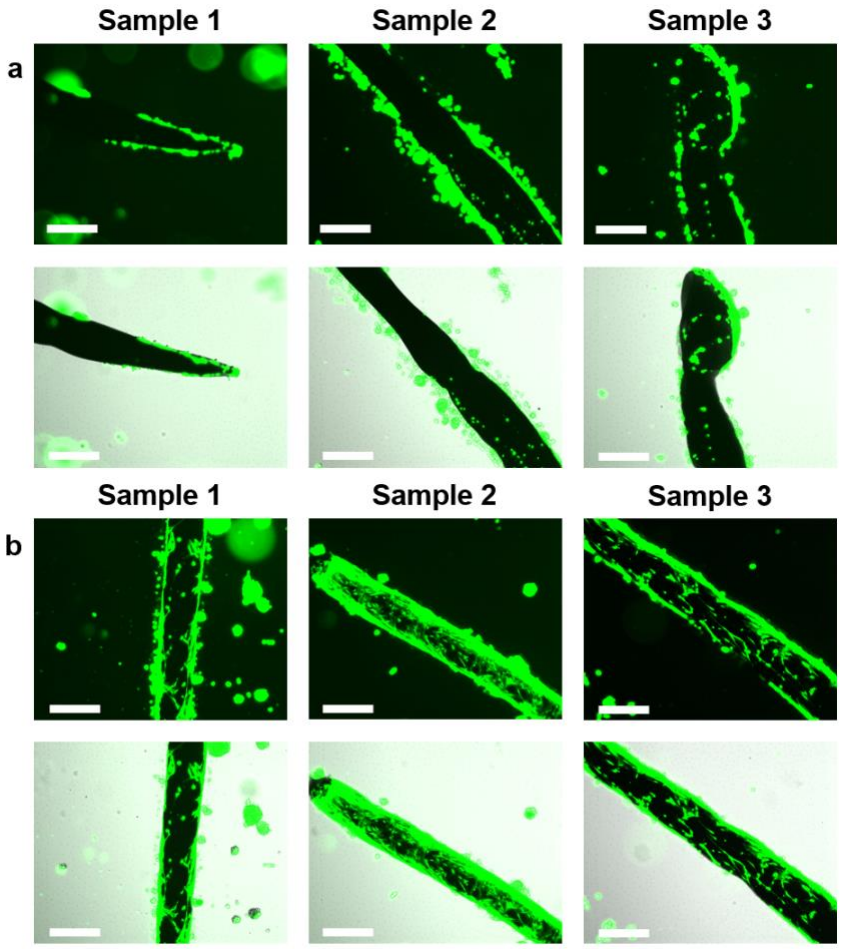

Supplementary Fig. 45 | Cell cultured macroscopic soft scaffolds of Na-DA_{Lala} and Na-DA_{DPhe} in 2% FBS medium for 1 day. Snapshots of Calcein AM live cell staining and merged with bright field of hMSCs cultured with macroscopic soft scaffold of **a** Na-**DA_{LAla}** (3.0 wt.%) and **b** Na-**DA_{DPhe}** (3.0 wt.%) after 1 day of incubation in 2% FBS supplemented medium at 37 °C and 5% CO_2. Scale bar is 500 μm for all panels.

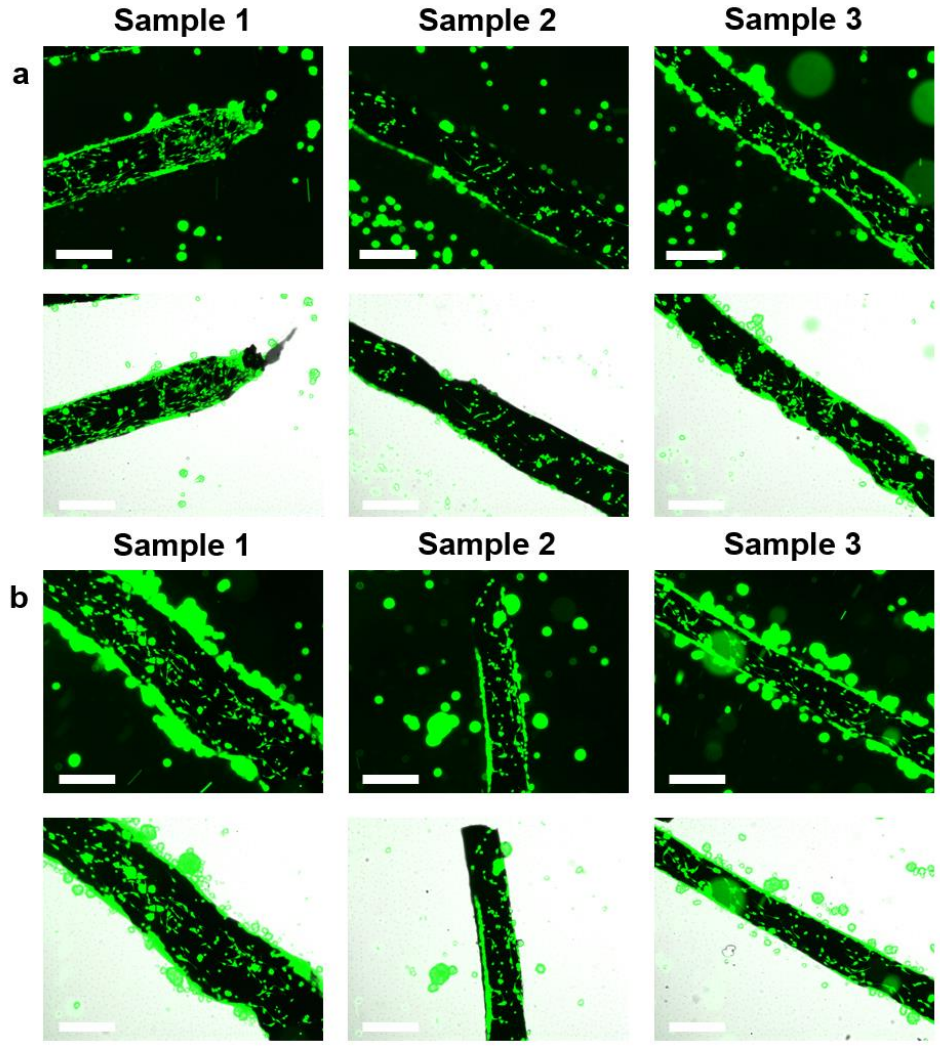

Supplementary Fig. 46 | Cell cultured macroscopic soft scaffolds of Li-DA$_{LPhe}$ and Cs-DA$_{LPhe}$ in 2% FBS medium for 1 day. Snapshots of Calcein AM live cell staining and merged with bright field of hMSCs cultured with macroscopic soft scaffold of **a** Li-**DA$_{LPhe}$** (3.0 wt.%) and **b** Cs-**DA$_{LPhe}$** (3.0 wt.%) after 1 day of incubation in 2% FBS supplemented medium at 37 °C and 5% CO_2. Scale bar is 500 μm for all panels.

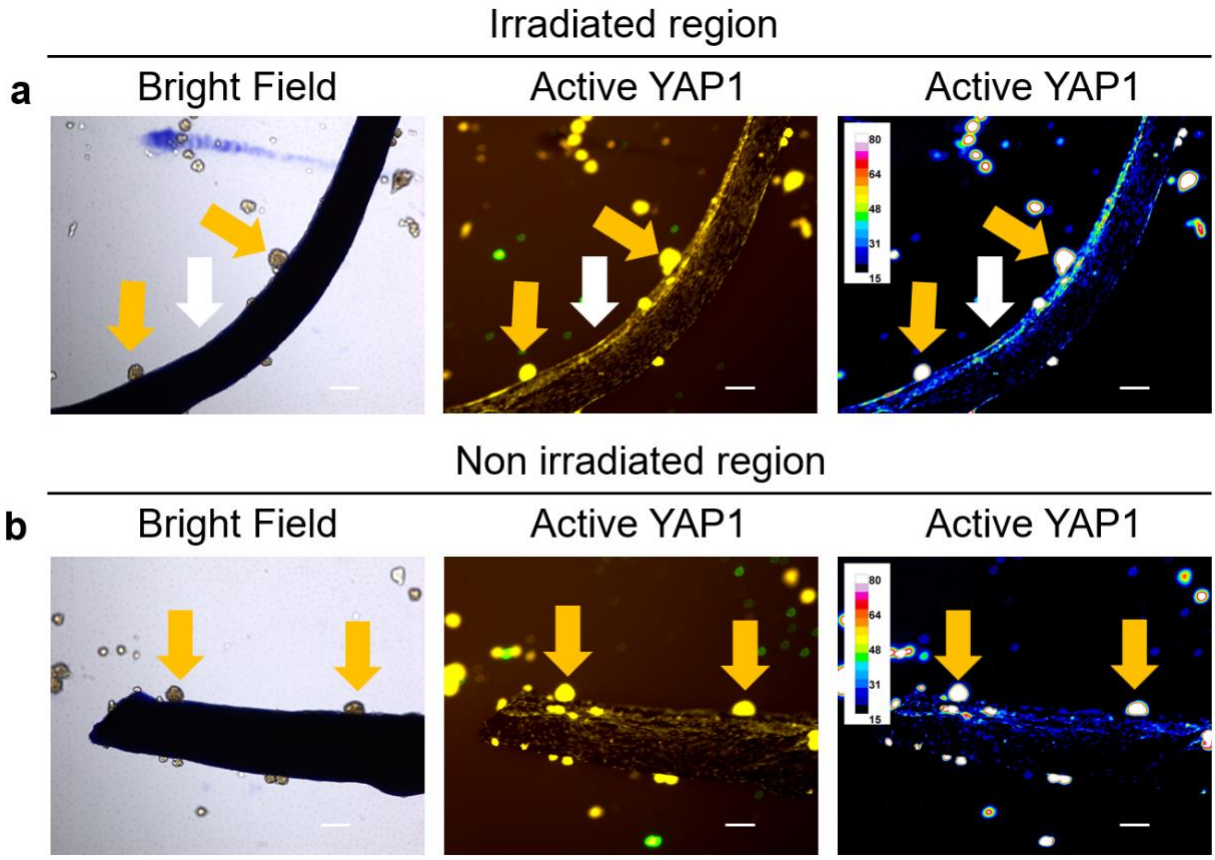

Supplementary Fig. 47 | Mechano-transduction study of hMSCs using marcoscopic soft scaffold of DA_{LPhe}. Lower magnification view (5x) of the mechano-transduction sample (as shown in Fig. 7). White arrow: irradiated region. Blue arrow: examples of cell aggregate attached on the scaffold. Scale bar: 200 μm

4. Analytical Data

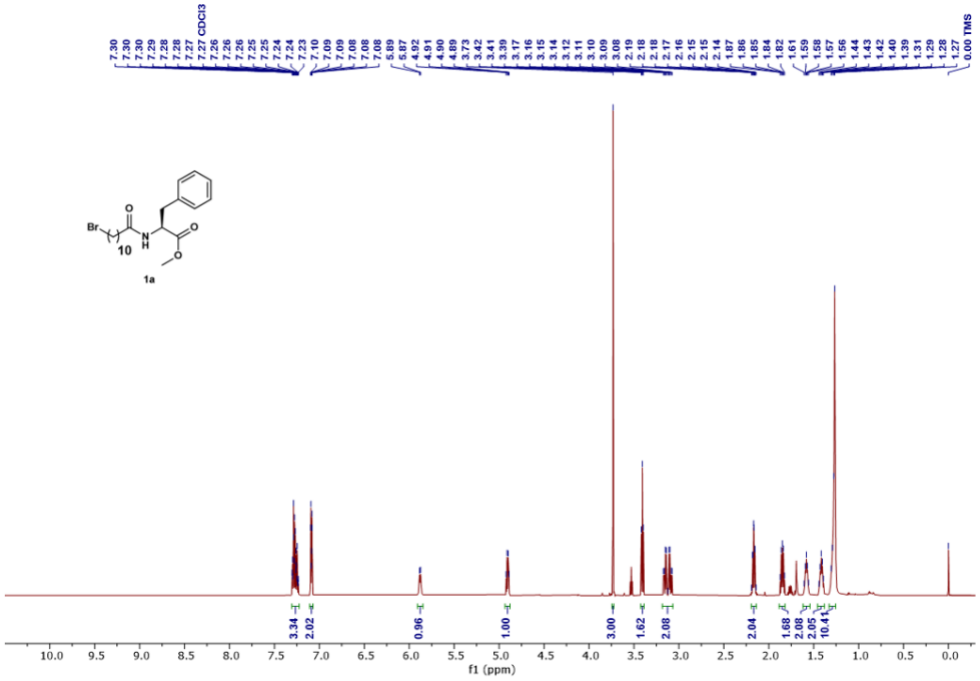

Supplementary Fig. 48 | ^{1}H NMR spectrum (600 MHz, 25 °C) of compound **1a** in $CDCl_3$ with 0.03% v/v TMS

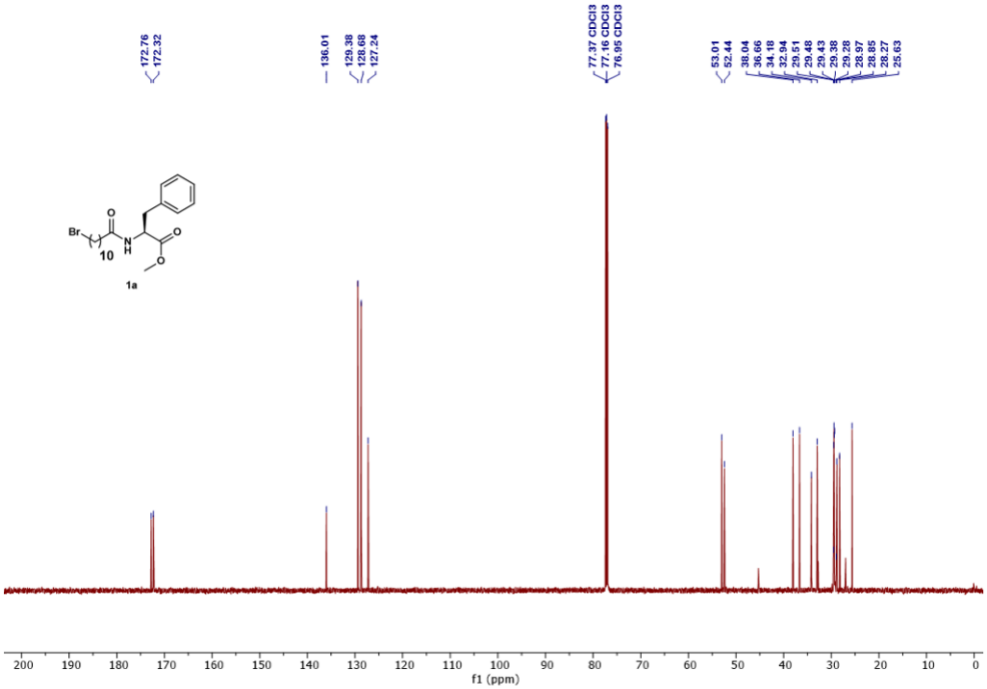

Supplementary Fig. 49 | ^{13}C NMR spectrum (151 MHz, 25 °C) of compound **1a** in $CDCl_3$ with 0.03% v/v TMS.

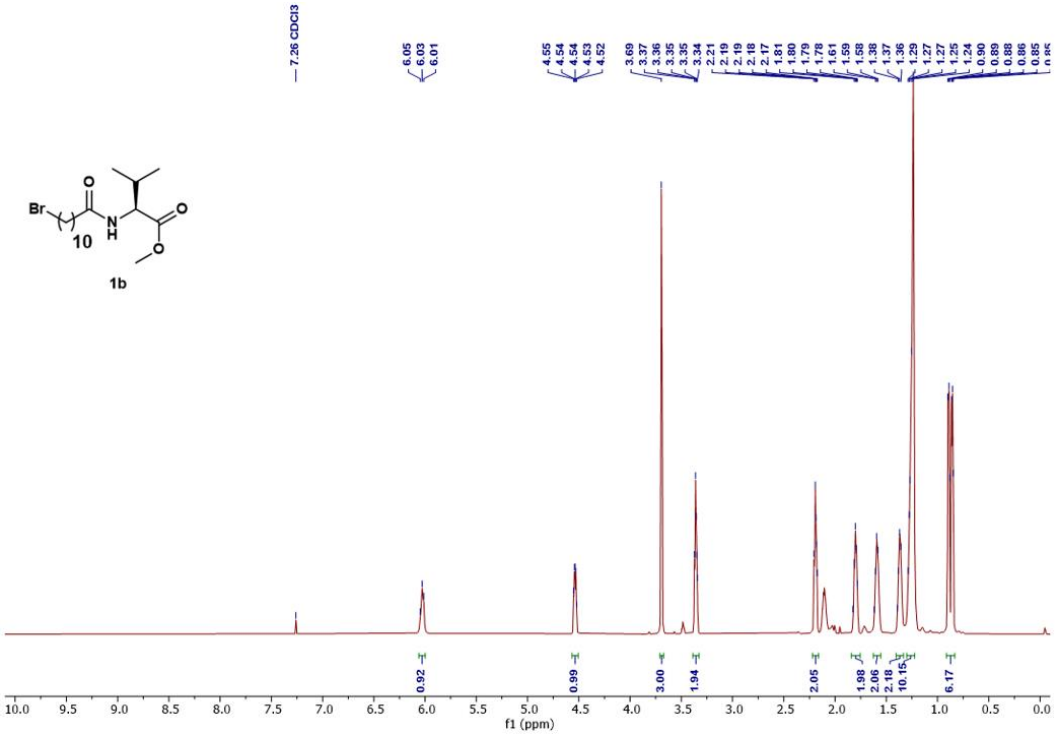

Supplementary Fig. 50 | ^{1}H NMR spectrum (600 MHz, 25 °C) of compound **1b** in $CDCl_3$ with 0.03% v/v TMS

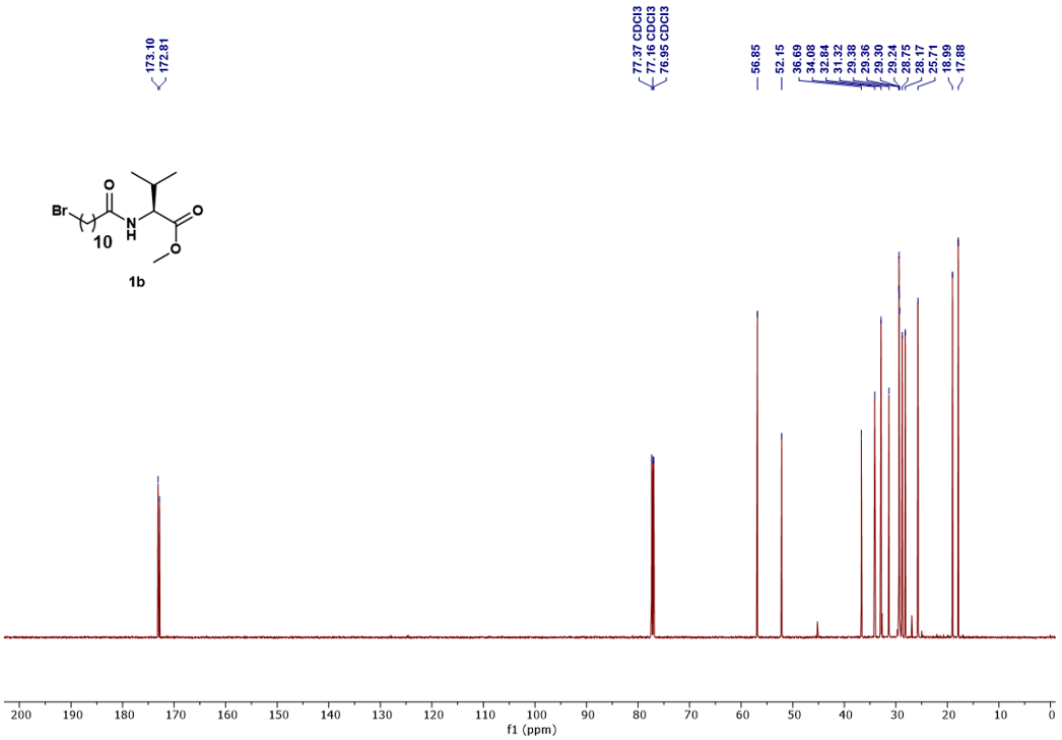

Supplementary Fig. 51 | ^{13}C NMR spectrum (151 MHz, 25 °C) of compound **1b** in $CDCl_3$ with 0.03% v/v TMS.

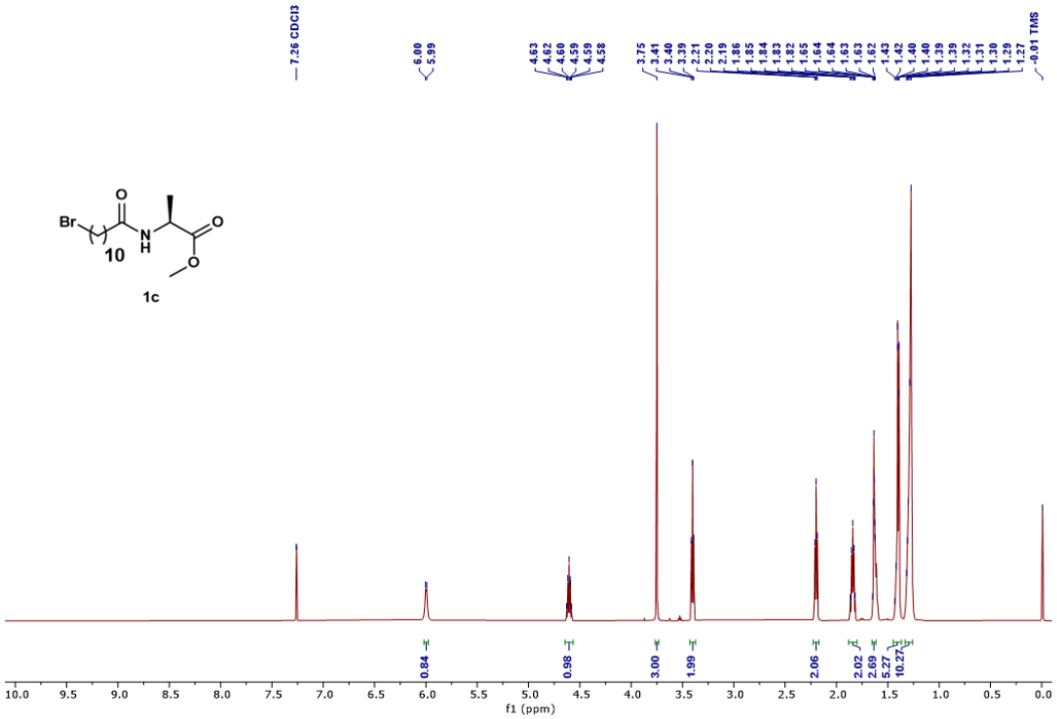

Supplementary Fig. 52 | ^{1}H NMR spectrum (600 MHz, 25 °C) of compound **1c** in $CDCl_3$ with 0.03% v/v TMS

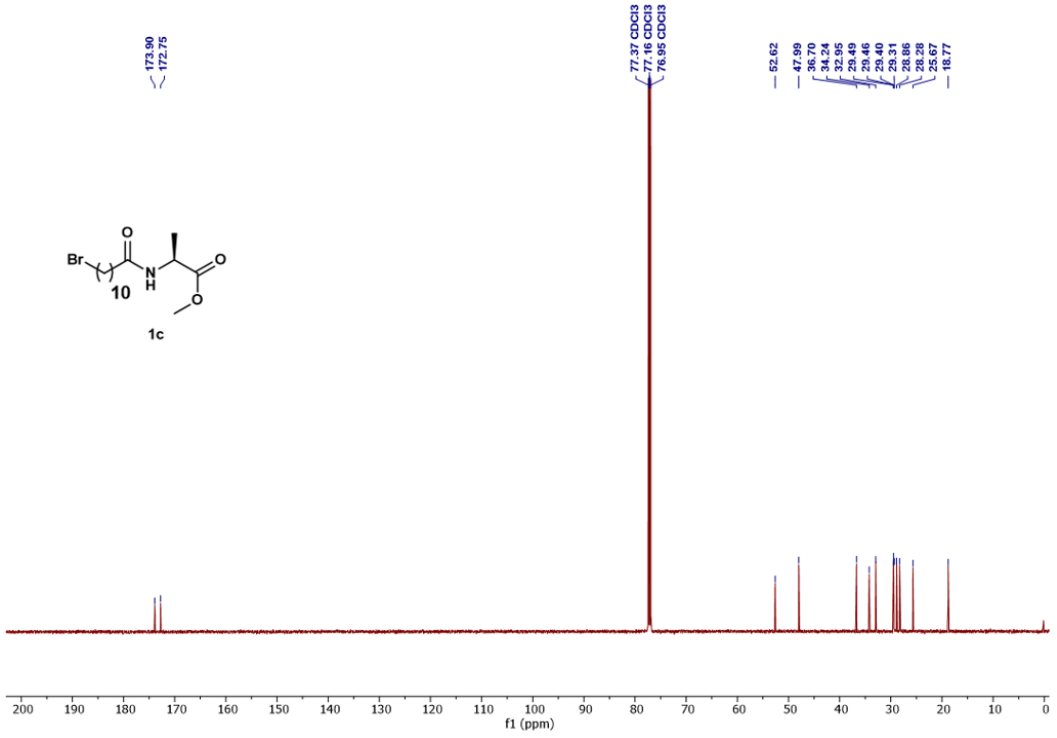

Supplementary Fig. 53 | ^{13}C NMR spectrum (151 MHz, 25 °C) of compound **1c** in $CDCl_3$ with 0.03% v/v TMS.

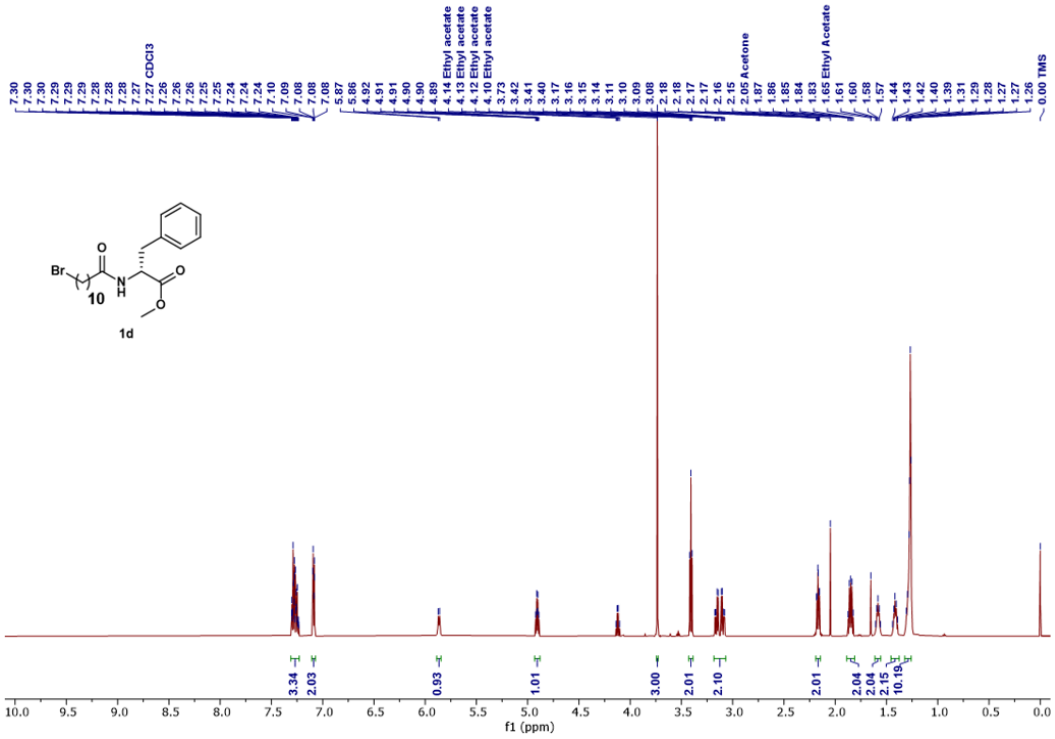

Supplementary Fig. 54 | ^{1}H NMR spectrum (600 MHz, 25 °C) of compound **1d** in $CDCl_3$ with 0.03% v/v TMS

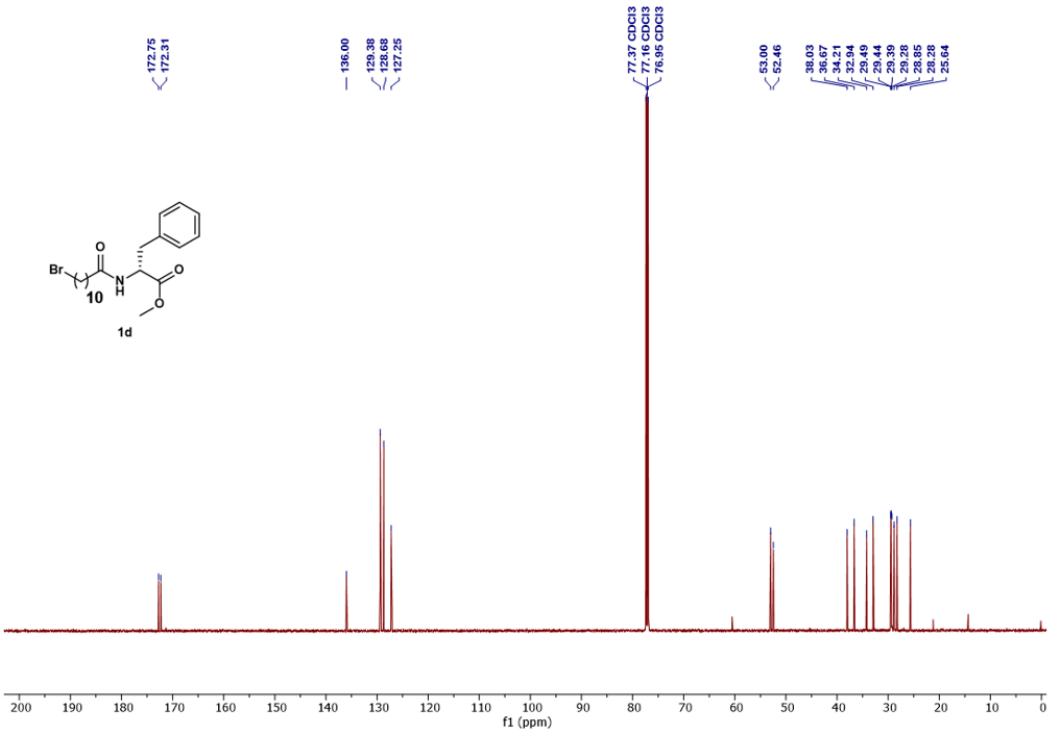

Supplementary Fig. 55 | ^{13}C NMR spectrum (151 MHz, 25 °C) of compound **1d** in $CDCl_3$ with 0.03% v/v TMS.

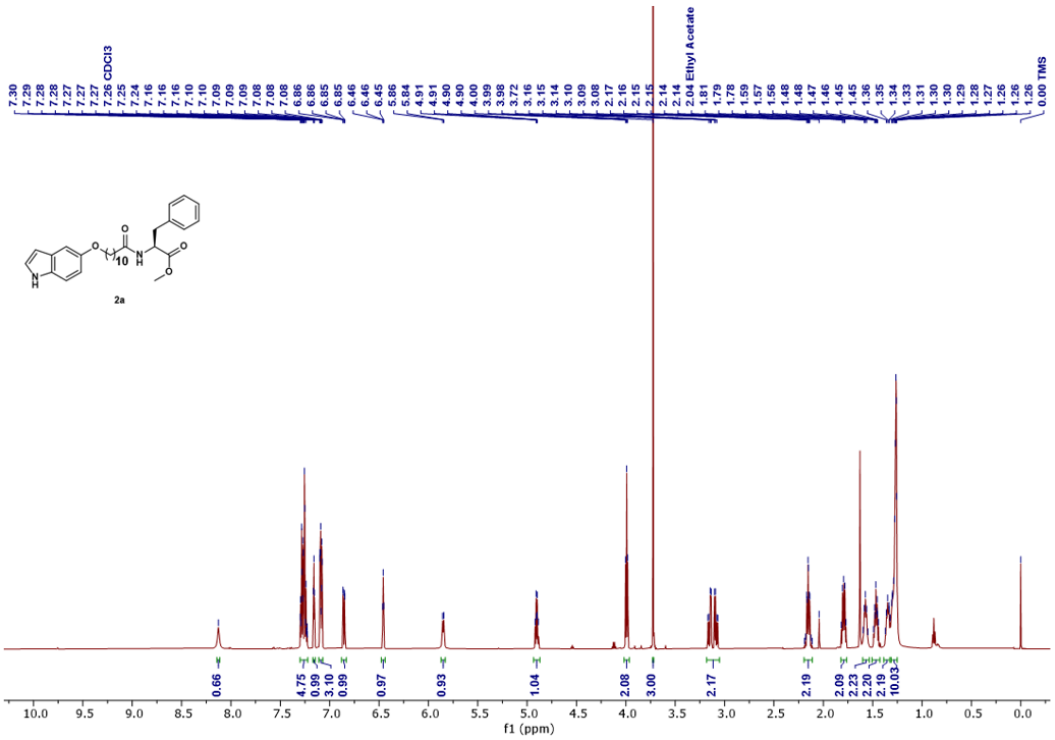

Supplementary Fig. 56 | ^{1}H NMR spectrum (600 MHz, 25 °C) of compound **2a** in $CDCl_3$ with 0.03% v/v TMS

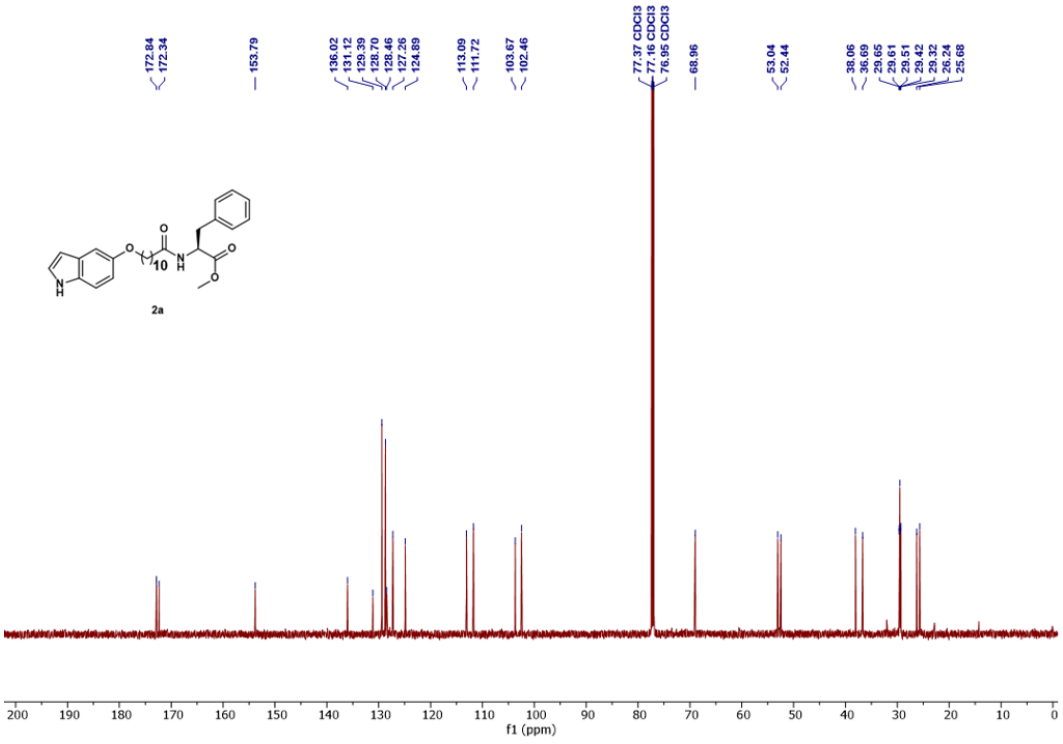

Supplementary Fig. 57 | ^{13}C NMR spectrum (151 MHz, 25 °C) of compound **2a** in $CDCl_3$ with 0.03% v/v TMS.

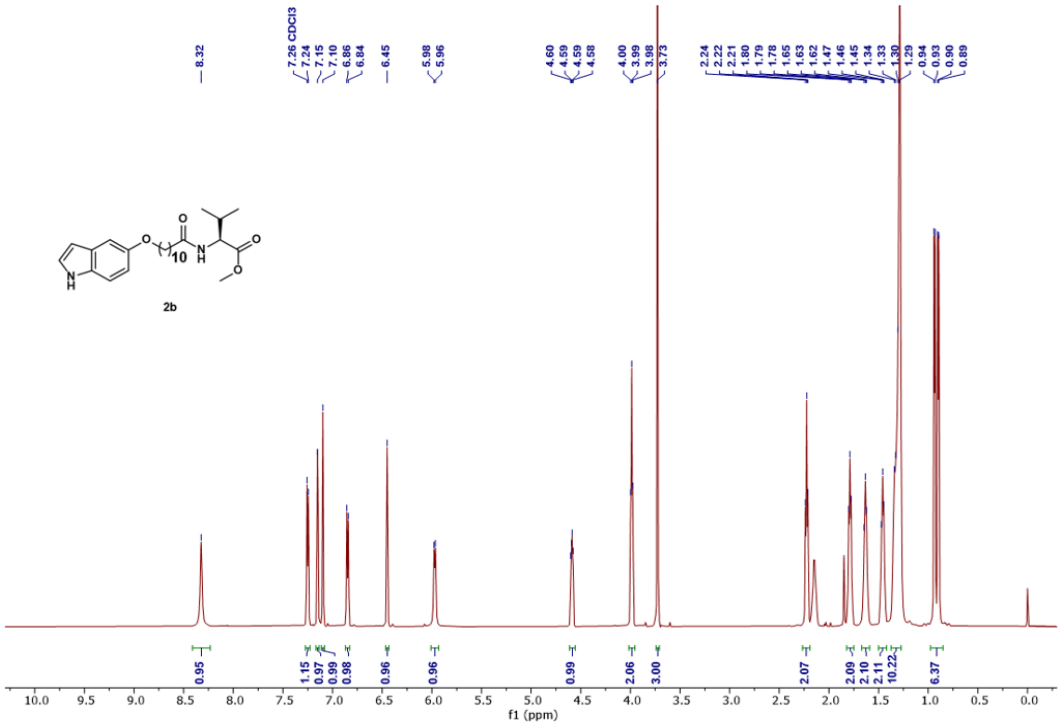

Supplementary Fig. 58 | ^{1}H NMR spectrum (600 MHz, 25 °C) of compound **2b** in $CDCl_3$ with 0.03% v/v TMS

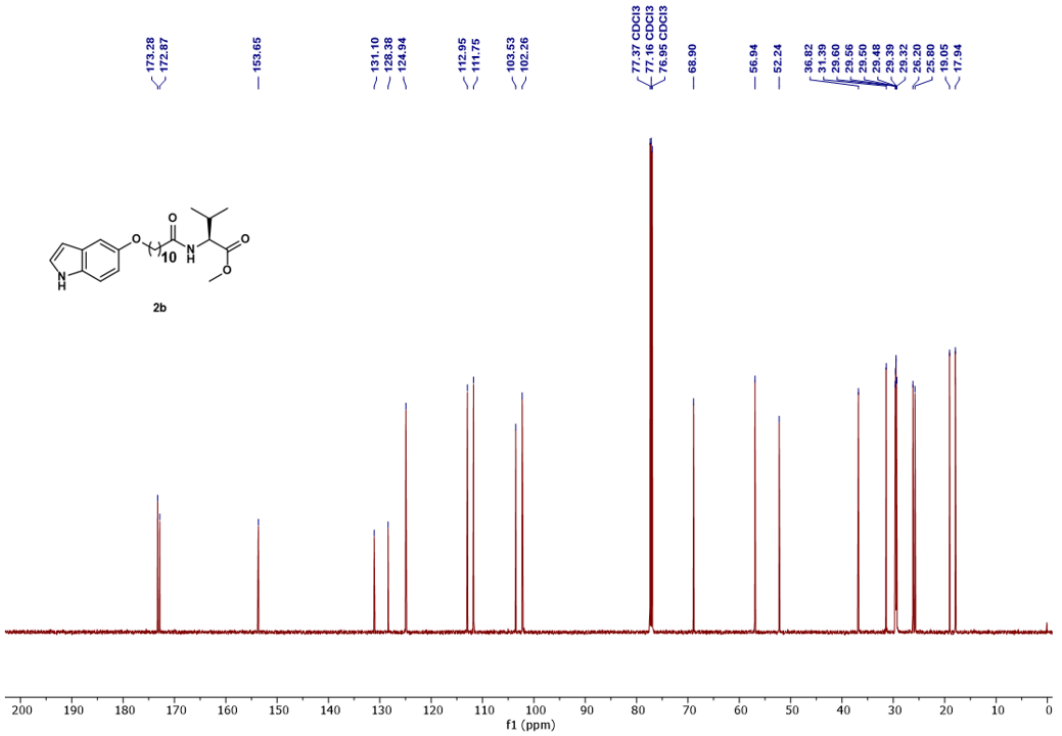

Supplementary Fig. 59 | ^{13}C NMR spectrum (151 MHz, 25 °C) of compound **2b** in $CDCl_3$ with 0.03% v/v TMS.

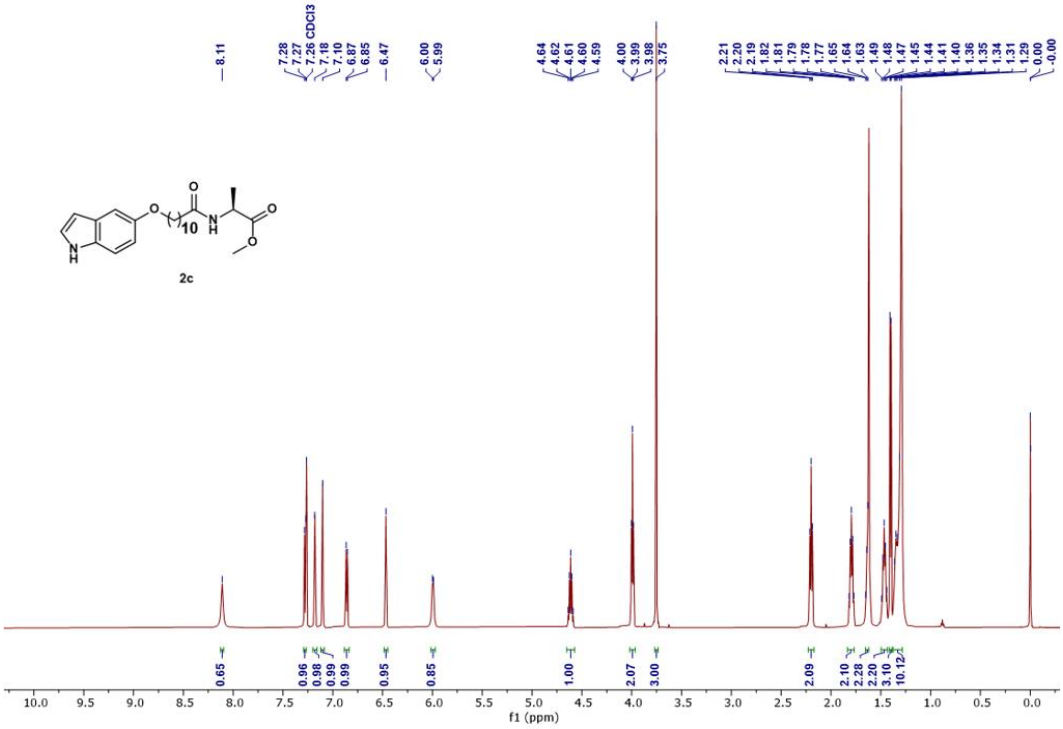

Supplementary Fig. 60 | ^{1}H NMR spectrum (600 MHz, 25 °C) of compound **2c** in $CDCl_3$ with 0.03% v/v TMS

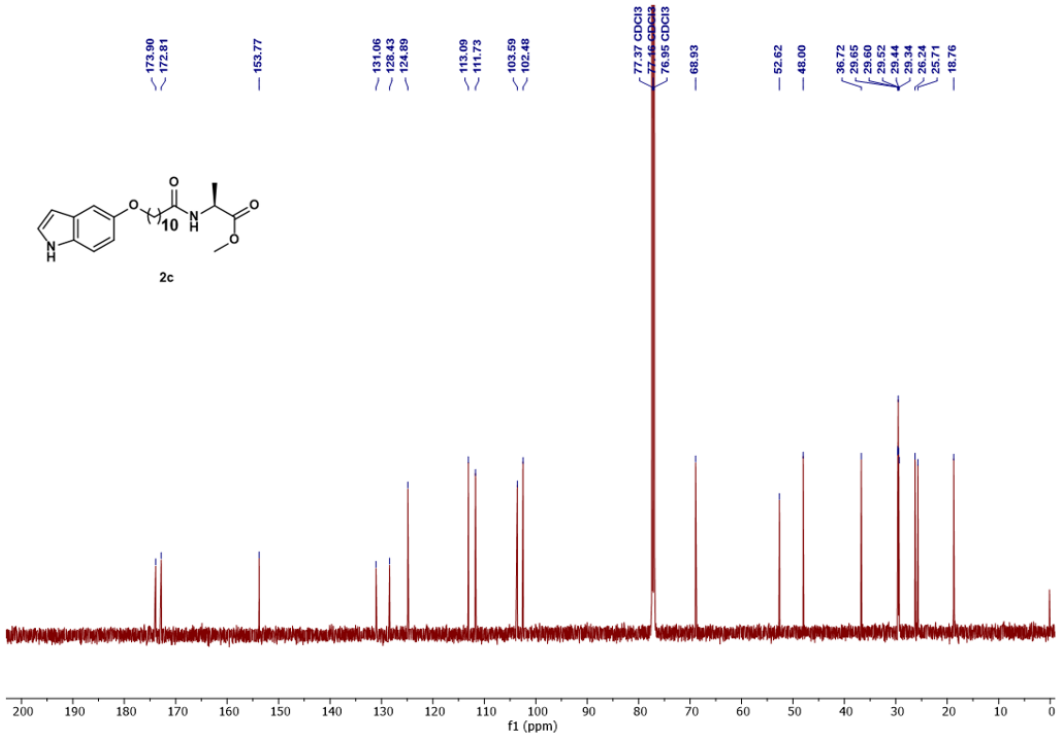

Supplementary Fig. 61 | ^{13}C NMR spectrum (151 MHz, 25 °C) of compound **2c** in $CDCl_3$ with 0.03% v/v TMS.

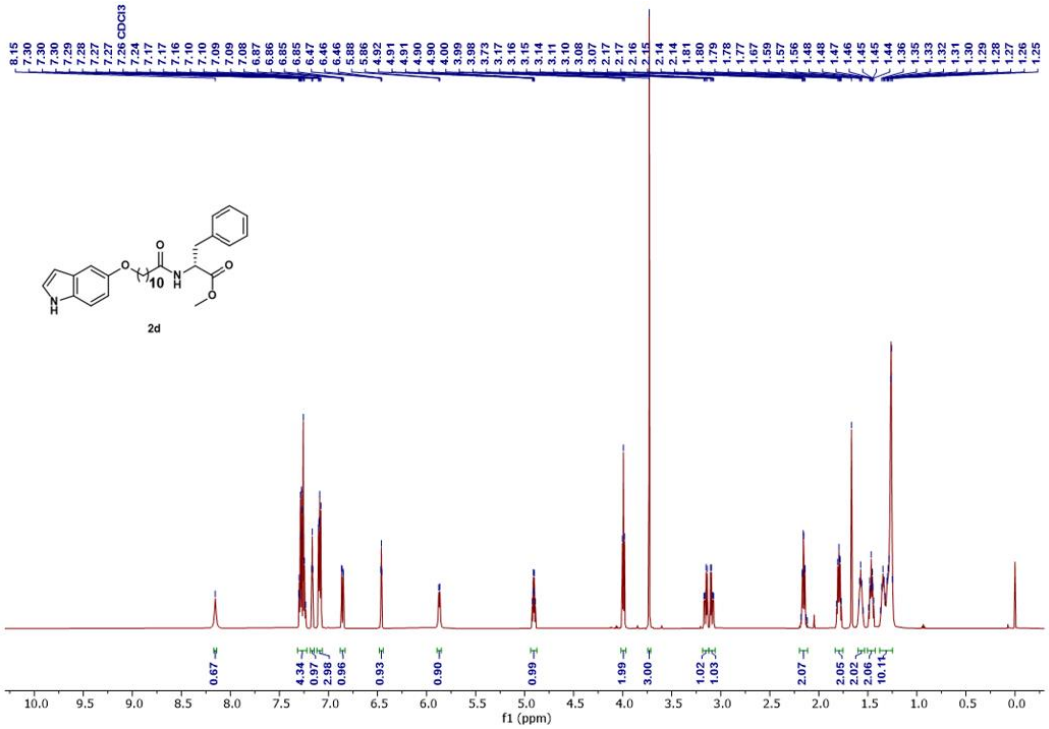

Supplementary Fig. 62 | ^{1}H NMR spectrum (600 MHz, 25 °C) of compound **2d** in $CDCl_3$ with 0.03% v/v TMS

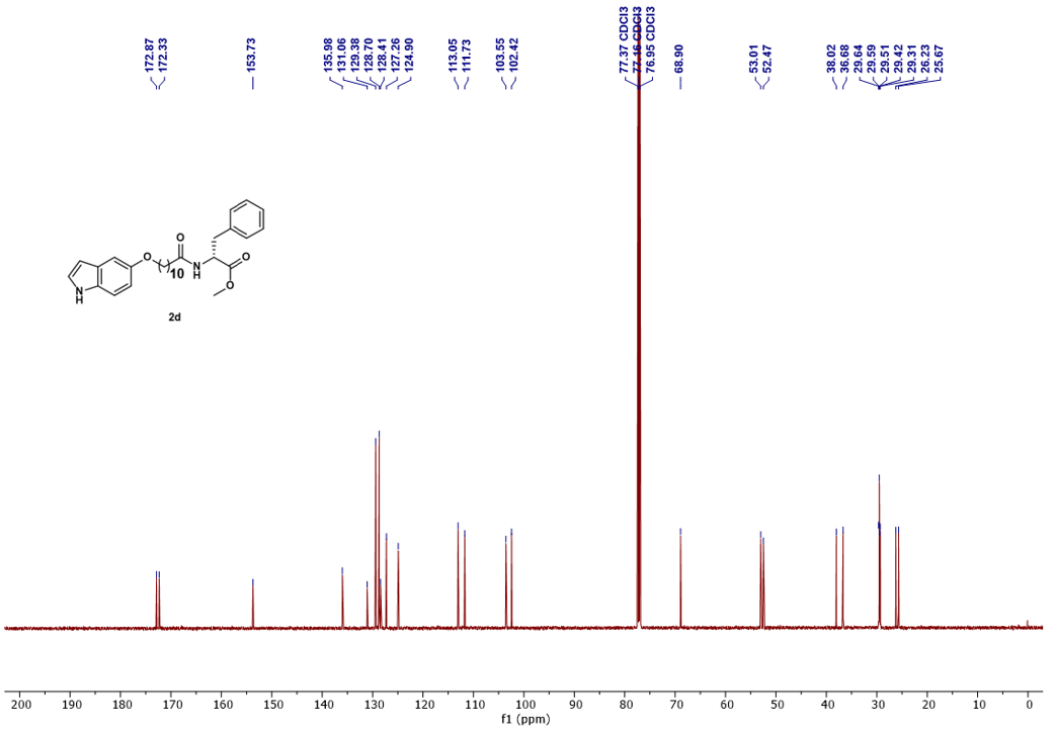

Supplementary Fig. 63 | ^{13}C NMR spectrum (151 MHz, 25 °C) of compound **2d** in $CDCl_3$ with 0.03% v/v TMS.

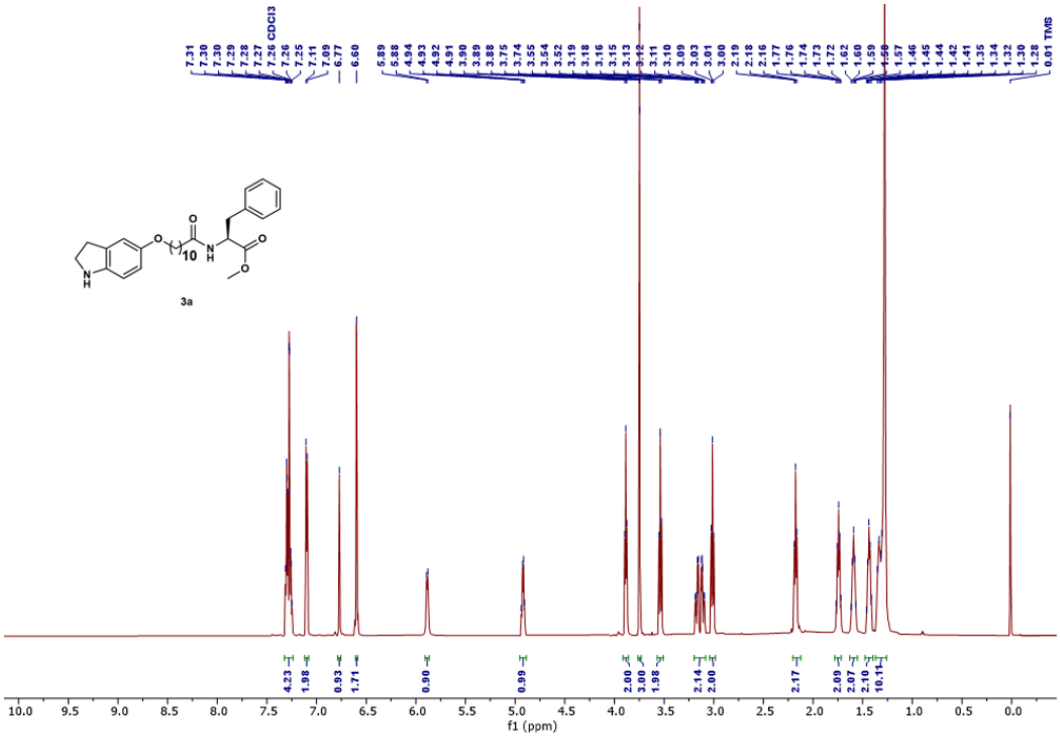

Supplementary Fig. 64 | ^{1}H NMR spectrum (600 MHz, 25 °C) of compound **3a** in $CDCl_3$ with 0.03% v/v TMS

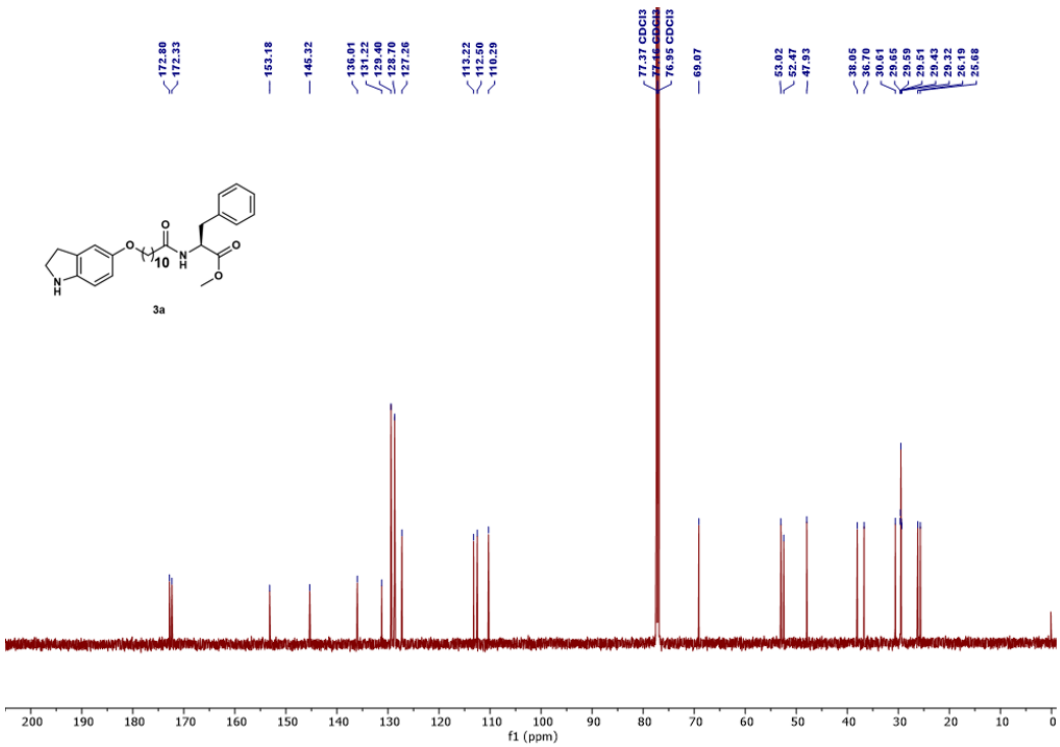

Supplementary Fig. 65 | ^{13}C NMR spectrum (151 MHz, 25 °C) of compound **3a** in $CDCl_3$ with 0.03% v/v TMS.

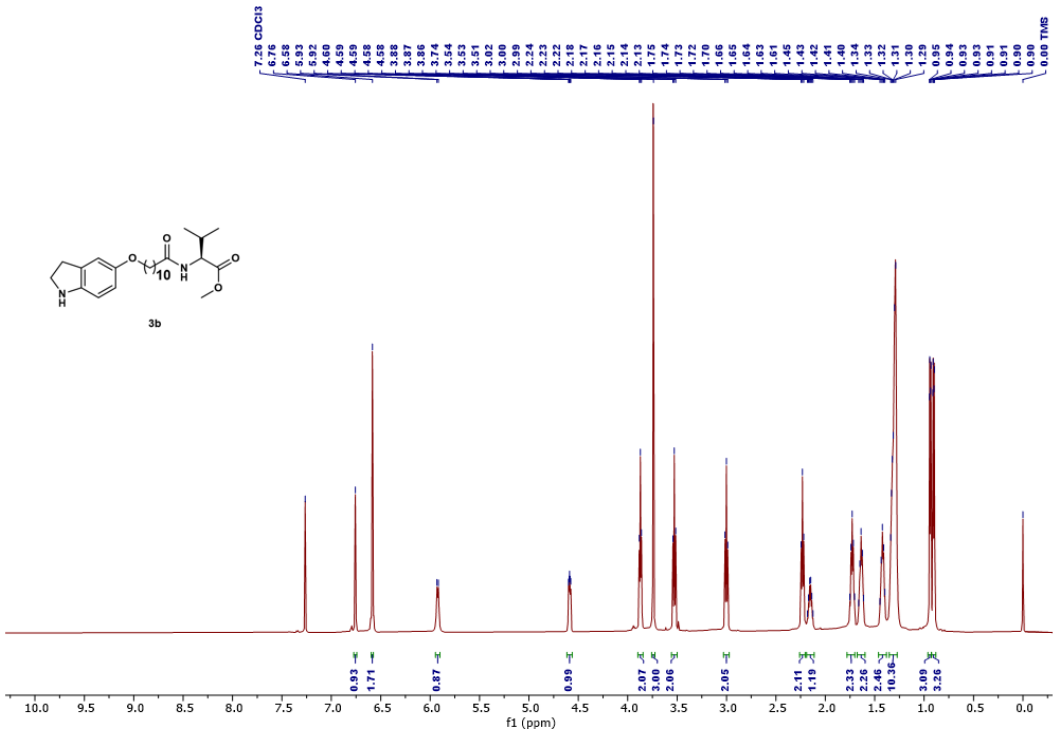

Supplementary Fig. 66 | ^{1}H NMR spectrum (600 MHz, 25 °C) of compound **3b** in $CDCl_3$ with 0.03% v/v TMS

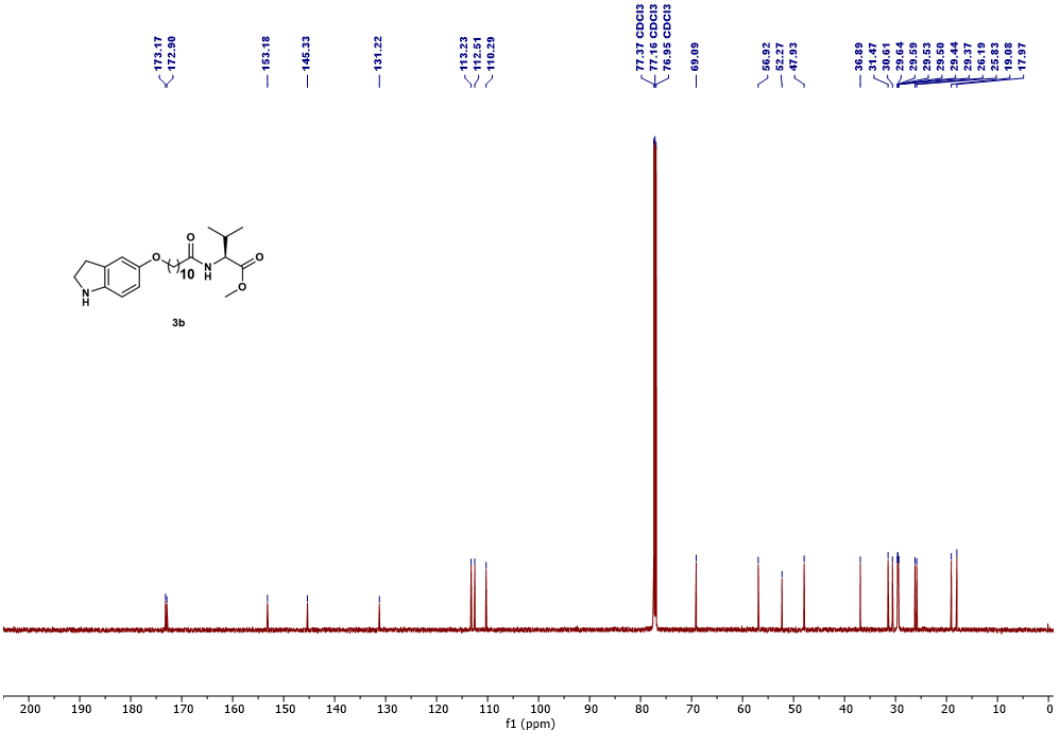

Supplementary Fig. 67 | ^{13}C NMR spectrum (151 MHz, 25 °C) of compound **3b** in $CDCl_3$ with 0.03% v/v TMS.

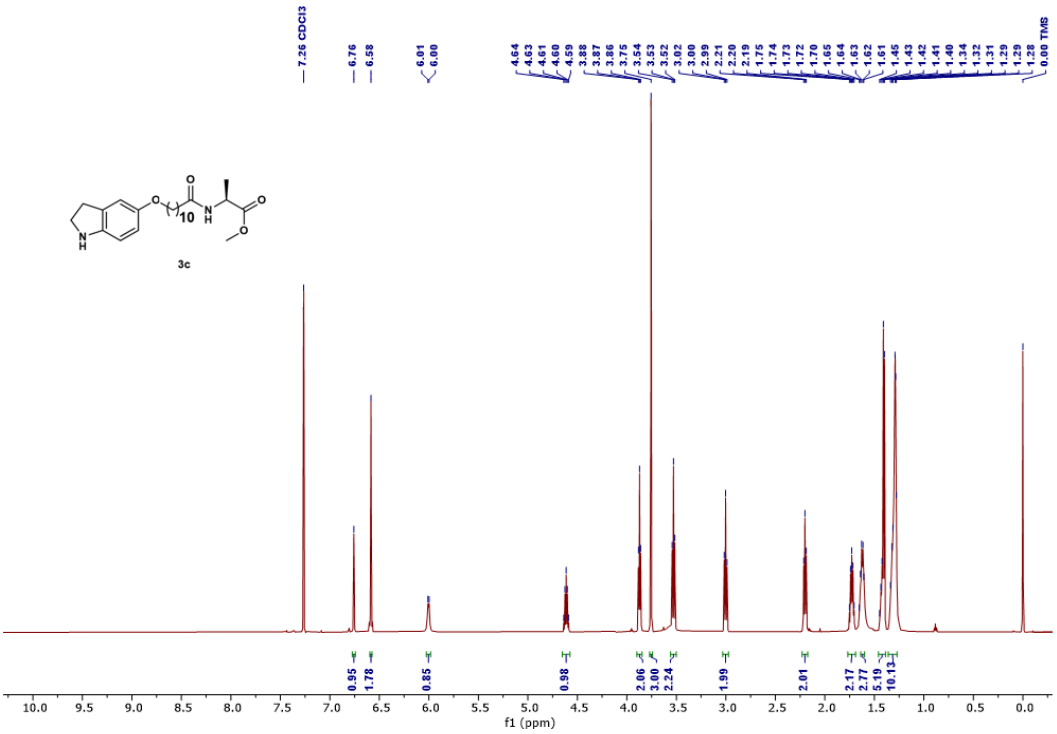

Supplementary Fig. 68 | ^{1}H NMR spectrum (600 MHz, 25 °C) of compound **3c** in $CDCl_3$ with 0.03% v/v TMS

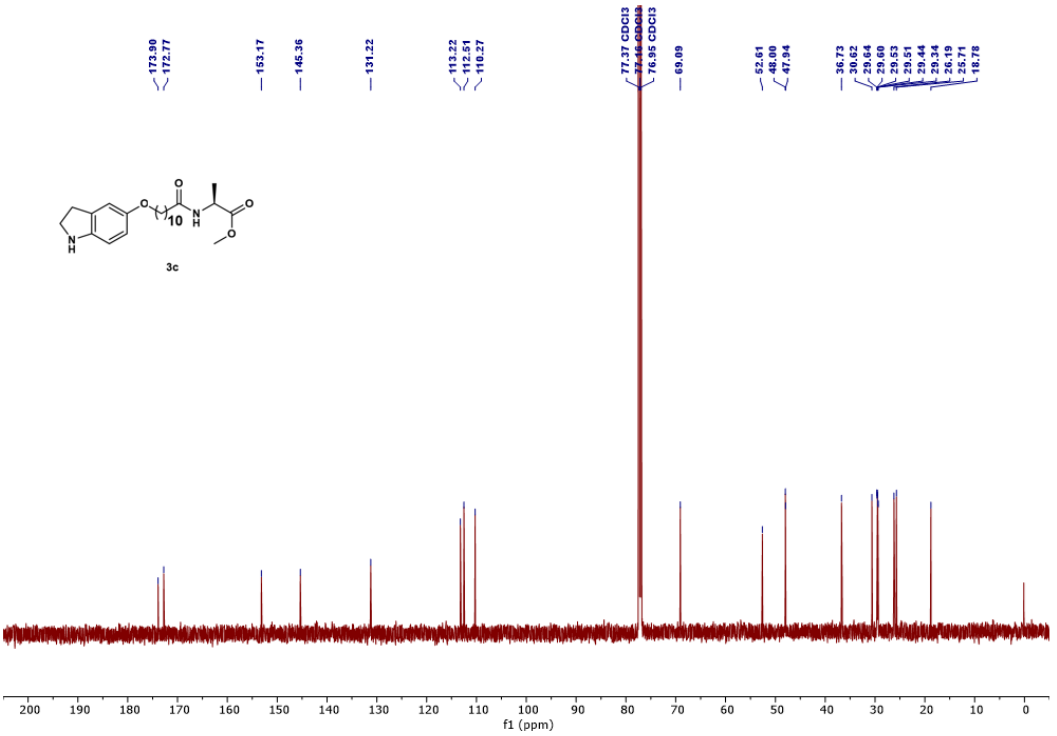

Supplementary Fig. 69 | ^{13}C NMR spectrum (151 MHz, 25 °C) of compound **3c** in $CDCl_3$ with 0.03% v/v TMS.

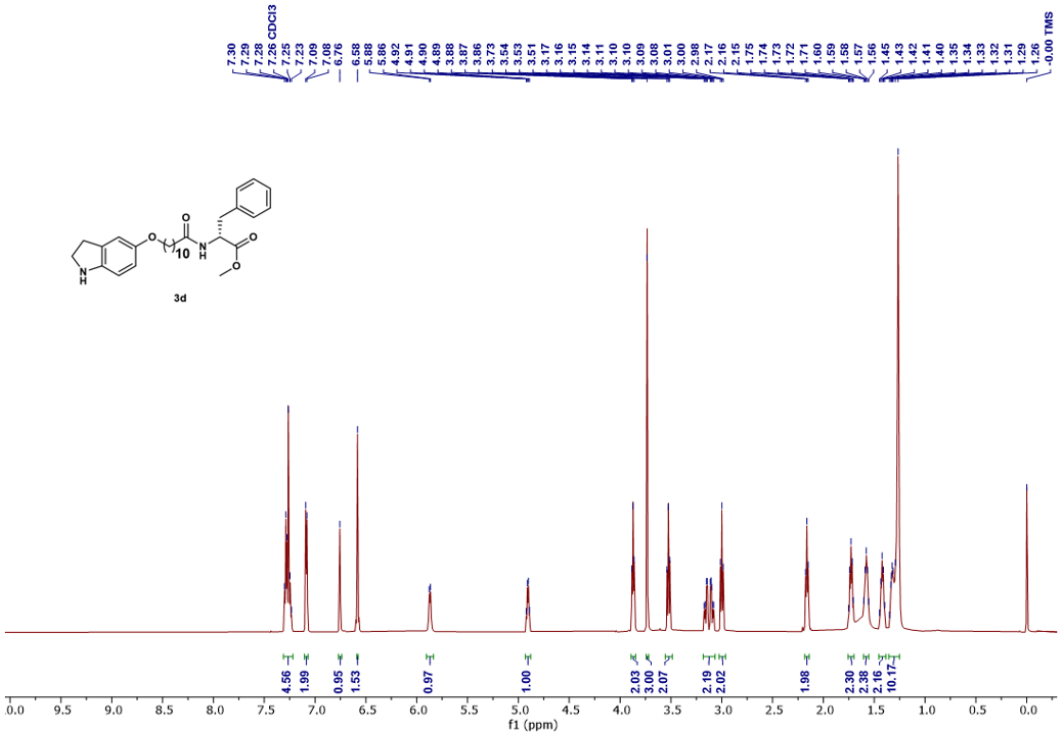

Supplementary Fig. 70 | ^{1}H NMR spectrum (600 MHz, 25 °C) of compound **3d** in $CDCl_3$ with 0.03% v/v TMS

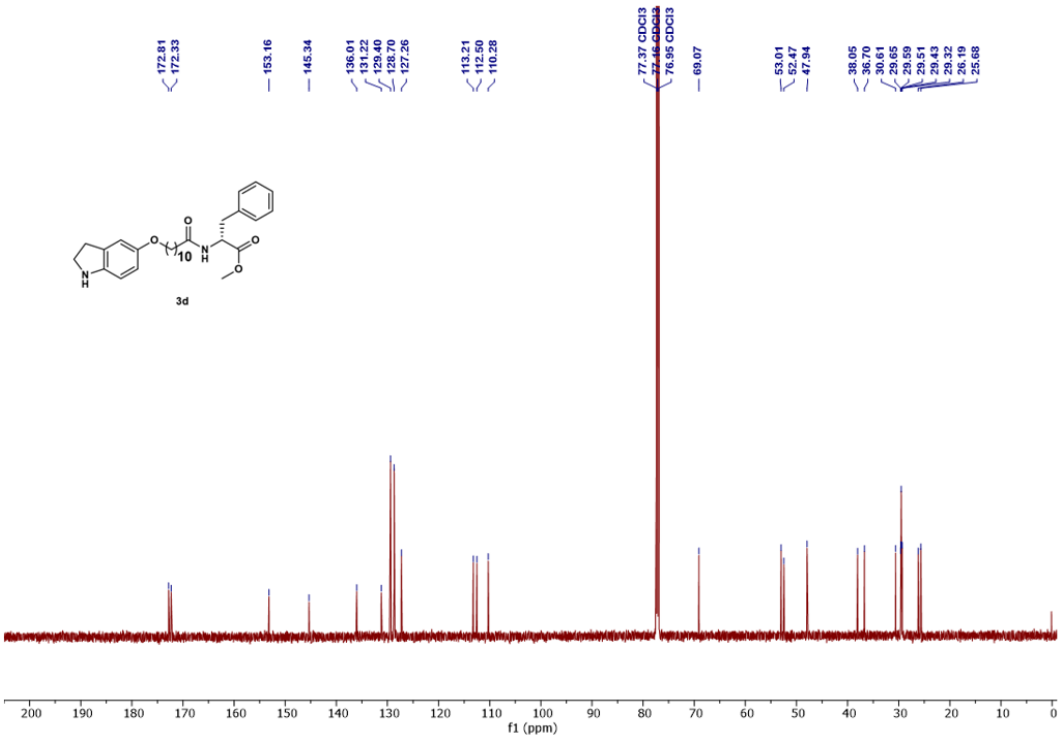

Supplementary Fig. 71 | ^{13}C NMR spectrum (151 MHz, 25 °C) of compound **3d** in $CDCl_3$ with 0.03% v/v TMS.

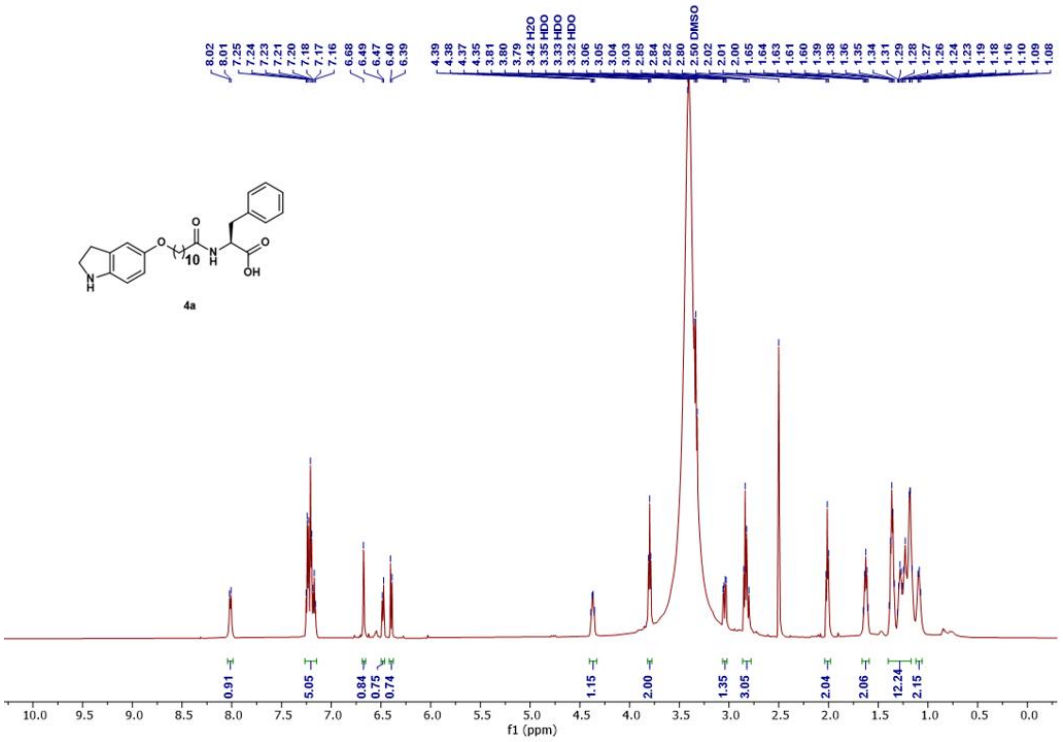

Supplementary Fig. 72 | ^{1}H NMR spectrum (600 MHz, 25 °C) of compound **4a** in DMSO-d_6

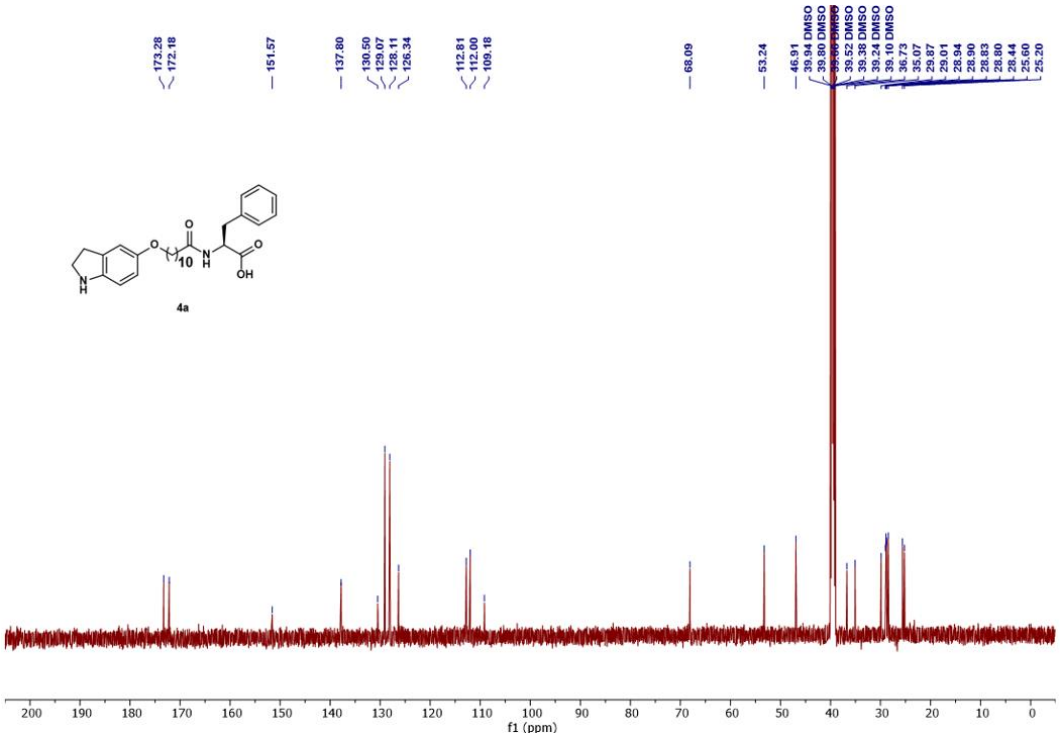

Supplementary Fig. 73 | ^{13}C NMR spectrum (151 MHz, 25 °C) of compound **4a** in DMSO-d_6

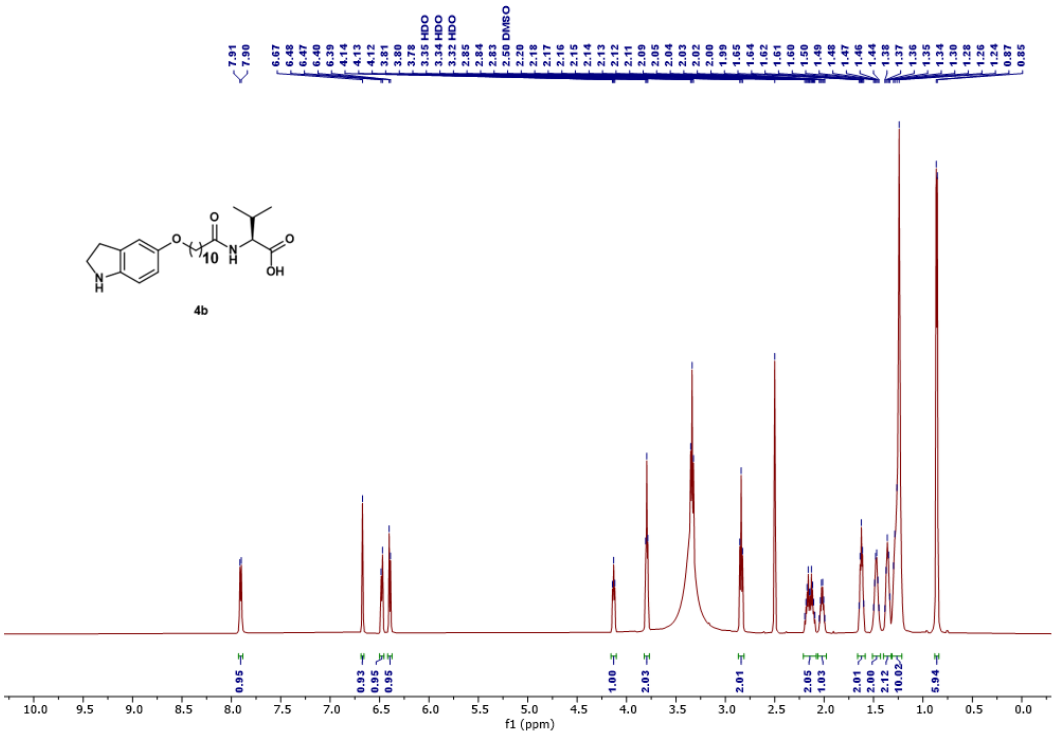

Supplementary Fig. 74 | ^{1}H NMR spectrum (600 MHz, 25 °C) of compound **4b** in DMSO-d_6

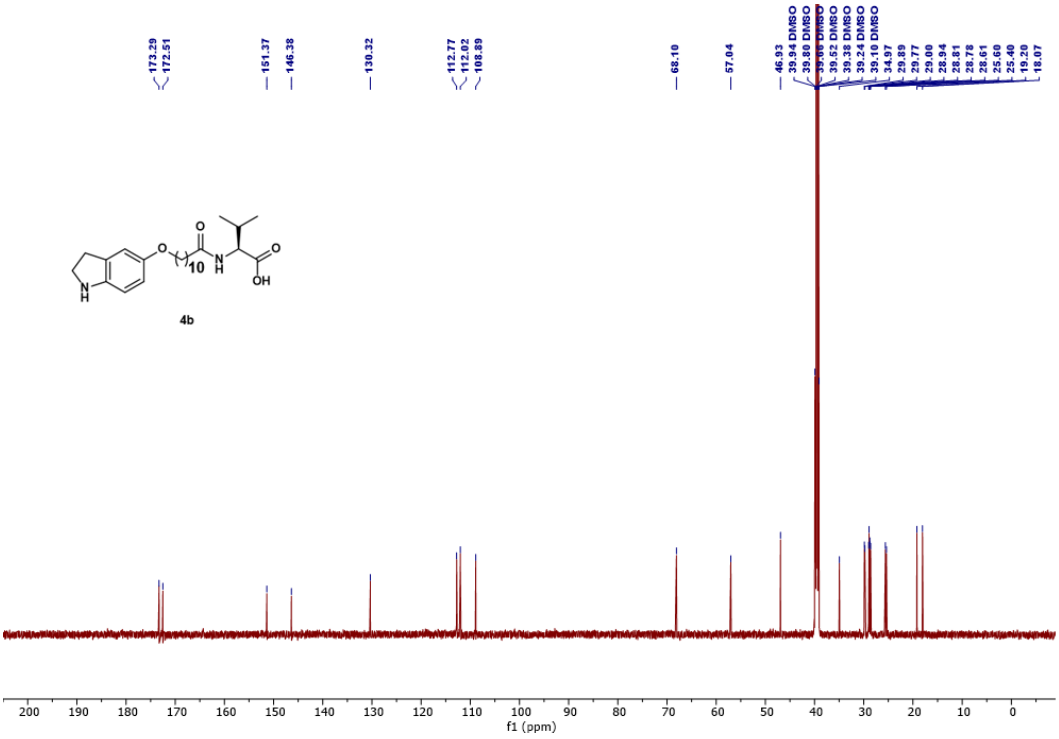

Supplementary Fig. 75 | ^{13}C NMR spectrum (151 MHz, 25 °C) of compound **4b** in DMSO-d_6

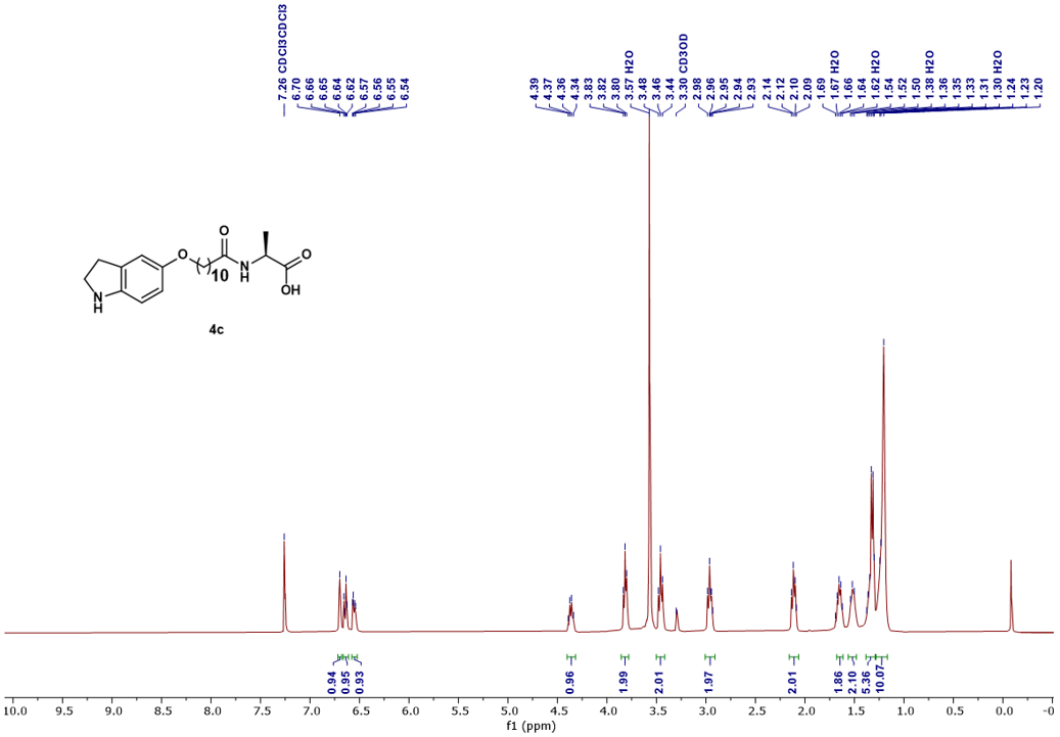

Supplementary Fig. 76 | ^{1}H NMR spectrum (400 MHz, 25 °C) of compound **4c** in 9 : 1 $CDCl_3$ with 0.03% v/v TMS: CD_3OD

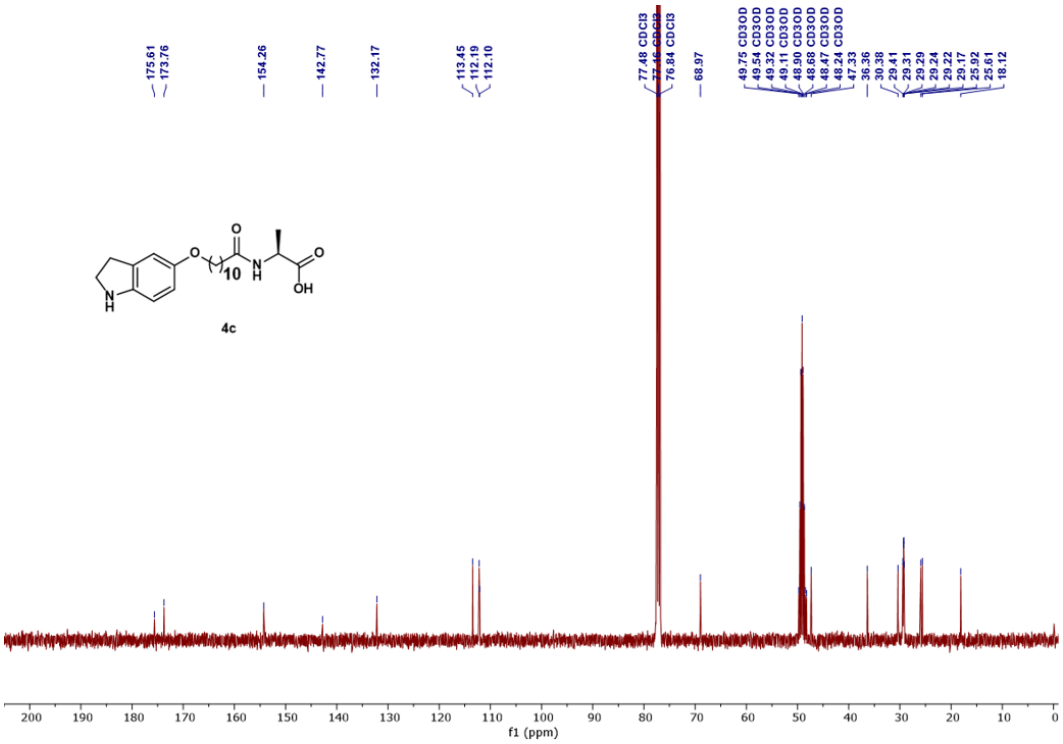

Supplementary Fig. 77 | ^{13}C NMR spectrum (101 MHz, 25 °C) of compound **4c** in 9 : 1 $CDCl_3$ with 0.03% v/v TMS: CD_3OD.

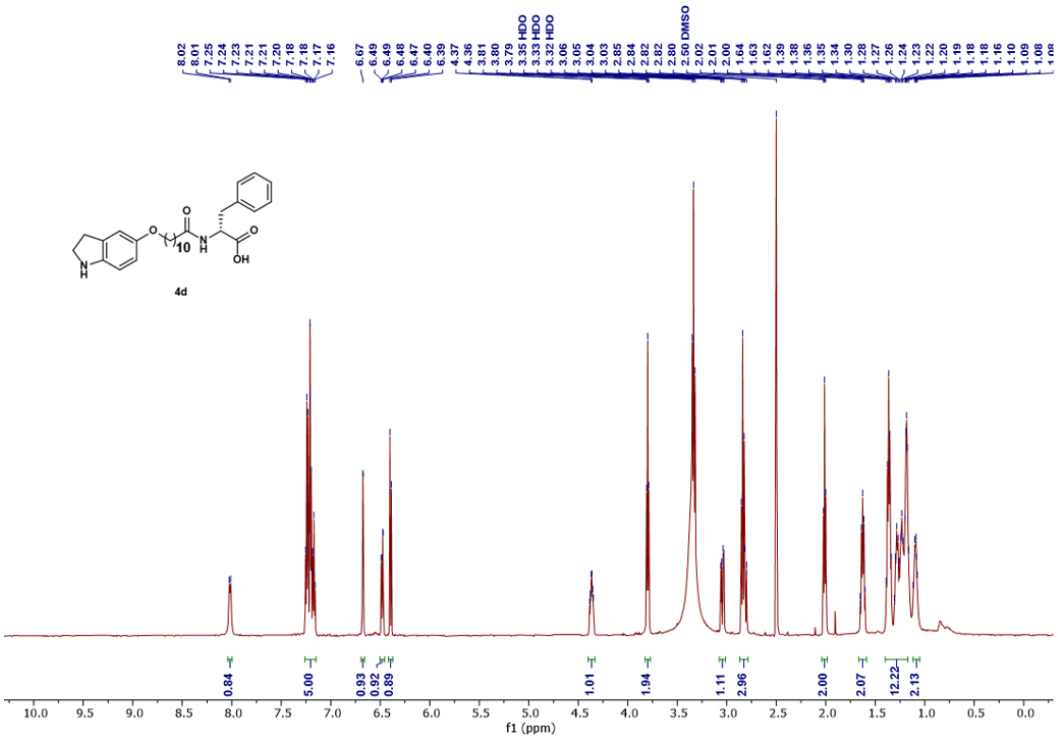

Supplementary Fig. 78 | ^{1}H NMR spectrum (600 MHz, 25 °C) of compound **4d** in DMSO-d_6

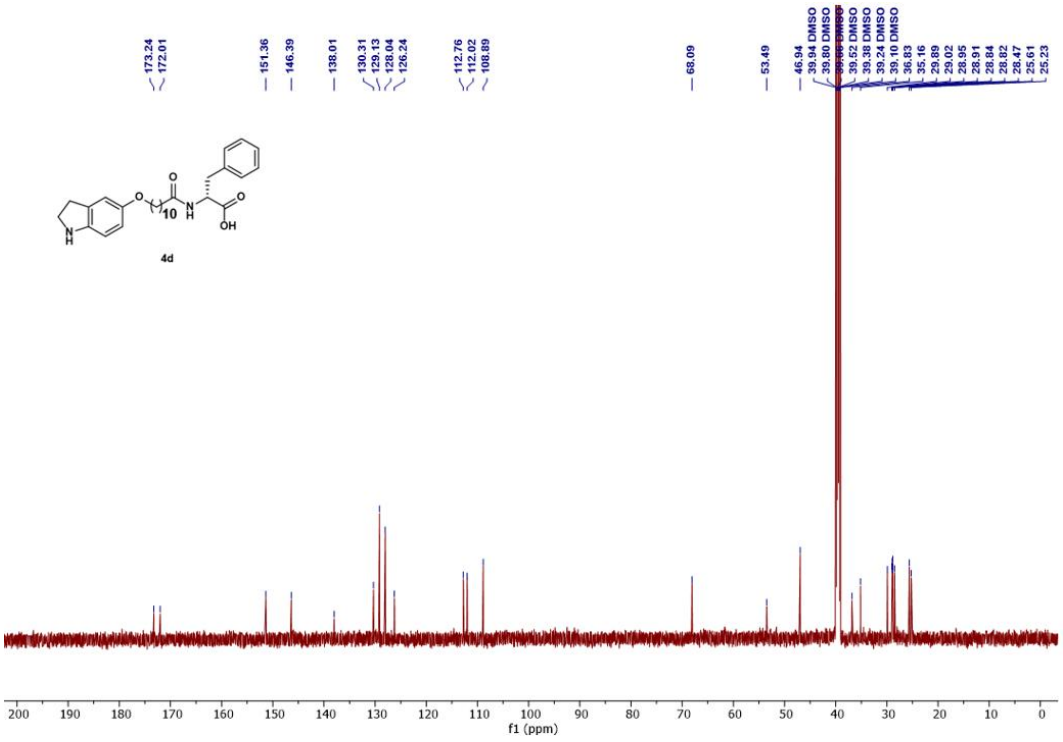

Supplementary Fig. 79 | ^{13}C NMR spectrum (151 MHz, 25 °C) of compound **4d** in DMSO-d_6

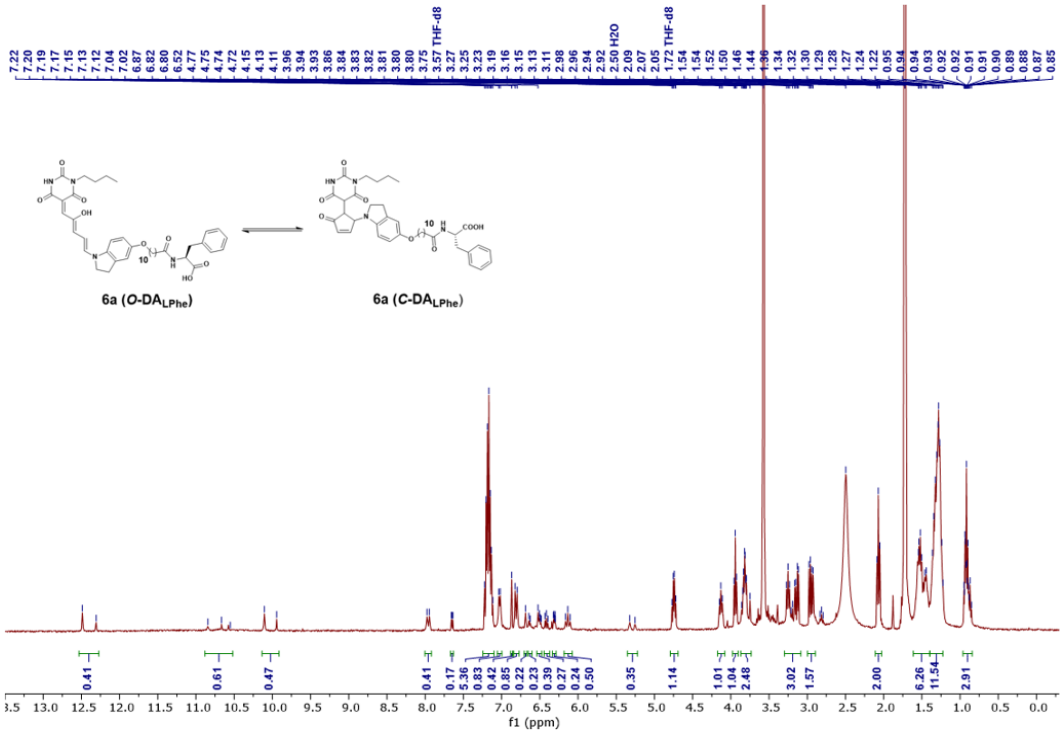

Supplementary Fig. 80 | ^{1}H NMR spectrum (400 MHz, 25 °C) of **compound 6a (DA$_{LPhe}$)** in THF-d_8.

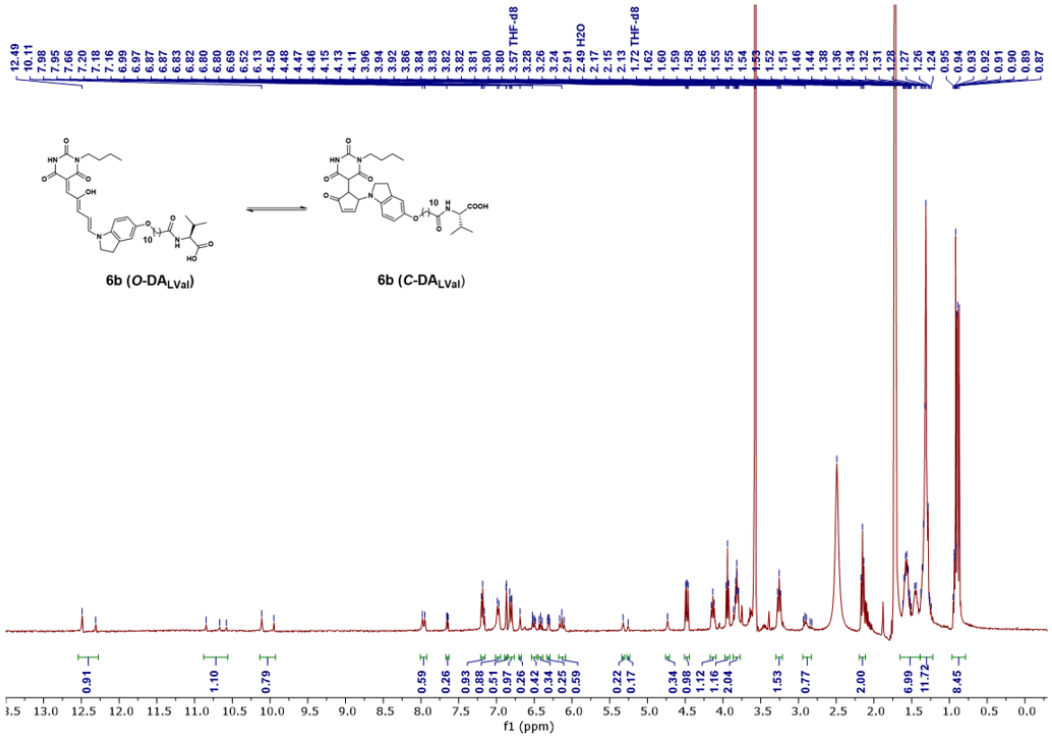

Supplementary Fig. 81 | ^{1}H NMR spectrum (400 MHz, 25 °C) of **compound 6b (DA$_{LVal}$)** in THF-d_8.

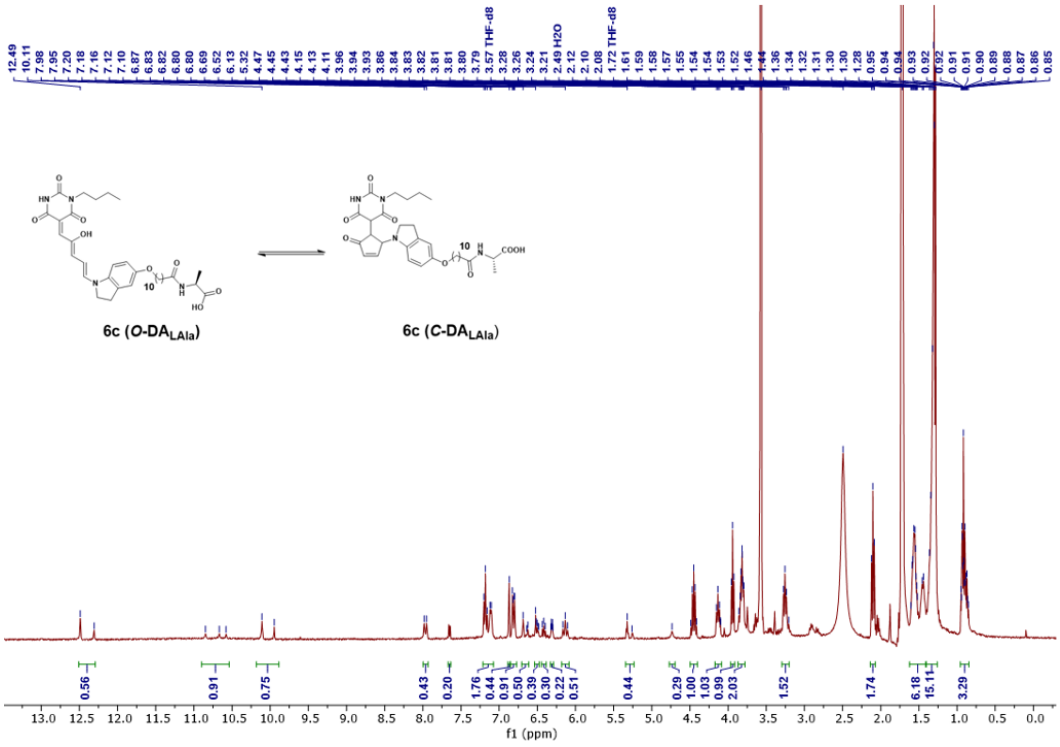

Supplementary Fig. 82 | ^{1}H NMR spectrum (400 MHz, 25 °C) of **compound 6c (DA$_{LAla}$)** in THF-d_8.

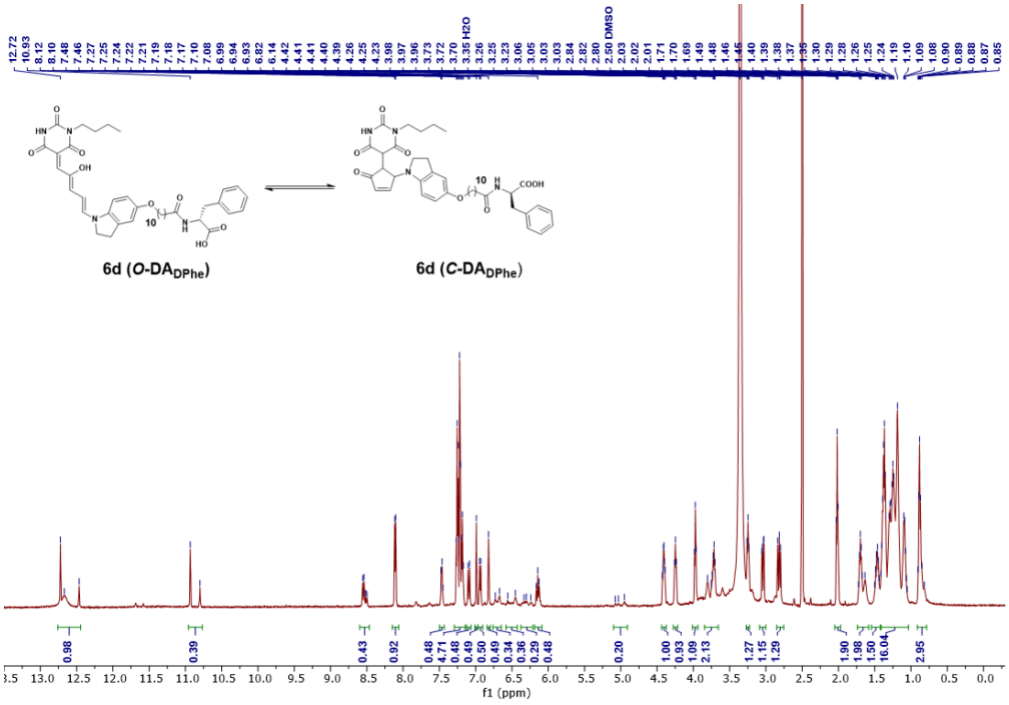

Supplementary Fig. 82 | ^{1}H NMR spectrum (400 MHz, 25 °C) of **compound 6d (DA$_{DPhe}$)** in DMSO-d_6.

5. References

1. Fulmer, G. R. *et al.* NMR Chemical Shifts of Trace Impurities: Common Laboratory Solvents, Organics, and Gases in Deuterated Solvents Relevant to the Organometallic Chemist. *Organometallics* **29**, 2176–2179 (2010).

2. Hung, K. L. *et al.* A Soft Robot Based on Charged Spiropyran Amphiphilic Supramolecular Nanoassembly for Macroscopic Actuation. *ACS Appl. Nano Mater.* **8**, 8876–8885 (2025).